EVALUATION OF EGM2008 BY MEANS OF GPS/LEVELLING IN UGANDA

BY:

DIANAH ROSE ABEHO

A thesis submitted to the school of Graduate studies of Addis Ababa University in partial fulfilment of the requirements for the Degree of Master of Science in Civil Engineering under Geodesy.

Addis Ababa, Ethiopia

April, 2013

Addis Ababa University

Institute of Technology

Department of Civil Engineering

The undersigned here by certify that they have read and recommend to the school of technology for acceptance a thesis entitled **"EVALUATION OF EGM2008 BY MEANS OF GPS/LEVELLING IN UGANDA"** by Dianah Rose Abeho in partial fulfilment of the requirements for the degree of Master of Science.

Date: 5th April, 2013

Supervisor/Advisor:

1. _____ _____ _____
   Signature Date

Co-Advisor:

1. _____ _____ _____

2. _____ _____ _____
   Signature Date

Examiner(s):

1. _____ _____ _____

2. _____ _____ _____

3. _____ _____ _____
   Signature Date

ACKNOWLEGMENT

I would like to thank several individuals who helped in different ways to make this research a success, not forgetting the Almighty God.

First and foremost I would like to thank my supervisor Dr. Roger Hipkin for his guidance and unfailing support all through the research work.

I thank my Co-Supervisor Dr. Tulu Besha Bedada for his unfailing support, timely advice and for sacrificing his time to make this research a success.

I sincerely thank Dr. Addisu Hunegnaw for providing assistance with GPS processing.

Dr. Elias Lewi for his advice and encouragement to complete the research and the study as well.

Mr. Ronald Ssengendo, for his unselfish support especially providing me with most of the GNSS observation data and for his endless advice and commitment towards the research.

I appreciate the Head of Department, Geomatics (MUK), Dr. Moses Musinguzi and all the staff members for all the support rendered to me and above all for giving me the ample time to complete this research in time.

I would also like to acknowledge the financial and academic support of Addis Ababa University and University of Edinburgh.

Last but not least to my family especially my husband Ian and daughter Kiersten for the unfailing support, love, encouragement and patience and my dad, James Bitaraabeho and mum Clarice Bitaraabeho for their inspiration all through my academic career. Thank you so much.

Table of Contents

LIST OF TABLES

LIST OF FIGURES

LIST OF ABBREVIATIONS

ArcGP	Arctic Gravity Project
CHAMP	CHAllenging Mini-satellite Payload
DNSC	Danish National Space Center
DORIS	Doppler Ranging Integrated on Satellite
DOS	Directorate of Overseas Surveys
DOT	Dynamic Ocean Topography
DTM	Digital Topographic Model
EGM	Earth Gravity Model
GGM	Global Geopotential Model
GNSS	Global Navigation Satellite System
GOCE	Gravity field and steady-state Ocean Circulation Explorer
GPS	Global Positioning System
GRACE	Gravity Recovery And Climate Experiment
IAG	International Association of Geodesy
IGFS	International Gravity Field Service
IGS	International GNSS Service
ITRF	International Terrestrial Reference Frame
ITRS	International Terrestrial Reference System
LSC	Least Squares Collocation
MSL	Mean Sea Level
MSS	Mean Sea Surface
NGA	National Geospatial-Intelligence Agency
NGS	National Geodetic Survey
NOAA	National Oceanic and Atmospheric Administration
PGM	Preliminary Gravitational Model
RTM	Residual Terrain Model
SIO	Scripps Institution of Oceanography
SLR	satellite Laser Ranging
SRTM	Shuttle Radar Topography Mission
SST	Satellite-to-Satellite Tracking
SWG	Special Working Group
VLBI	Very Long Baseline Interferometry
WGS	World Geodetic System

ABSTRACT

The global gravity model EGM2008 is evaluated in various regions of the country to assess if it is good enough for geodetic applications. The evaluation method involves comparison of geoid heights computed from the model with those computed at irregularly distributed GPS/levelling stations. For testing the model, a total of seven levelled benchmarks available in Uganda which belong to the New Khartoum datum are used. The spatial positions of these benchmarks were determined at mm accuracy, with respect to ITRF2008. The agreement between the EGM2008 geoid and the geoid undulation derived from GPS/levelling over the seven irregularly distributed benchmark points has a standard deviation of 0.255m, with a mean of -0.859m. The datum offset may be due the choice of Wo (potential of the geoid) and Uo (potential on the surface of the ellipsoid); using GRS80 for the gravitational reference system and WGS84 for the geometrical reference system; some possibly different tidal conventions; but, by using the same method of analysis for Ethiopia and Uganda, these absolute offset effects are eliminated when comparing the two so that the *computed difference [0.118 m]* in datum offset for the two states does tell us something about the differences in levelling datums. The standard deviation of 26 cm suggests that sparser, irregularly-distributed and inhomogenous gravity data for Uganda was used in the development of EGM2008 not ruling out errors in levelling since there is barely any documentation pertaining the accuracy of results obtained regarding the levelling network in Uganda.

.

1.0 INTRODUCTION

Most geodetic applications like determining the topographic heights of points on the globe require the geoid also referred to as mean sea level surface as the datum/reference surface. In this satellite era one is capable of obtaining a sufficiently accurate model of the gravity field over the surface of the earth. This is a great achievement in the fields of geodesy and geophysics since we can achieve heights with physical meaning without necessarily carrying out the tedious and time-consuming procedures of obtaining these levelled heights by levelling.

The release of the new Earth Gravitational Model EGM2008 by the US National Geospatial Intelligence Agency (Pavlis et al., 2008) is a big achievement in determination of the earth's gravity field. EGM2008 is a spherical harmonic model complete to degree and order of 2159, with additional spherical harmonic coefficients extending up to degree of 2190 and order 2159. This offers a spatial sampling resolution of approximately 9km for the recovery of gravity field functions over the entire globe (Kotsakis et al., 2008). EGM2008 incorporates 5x5 min gravity anomalies and altimetry-derived gravity anomalies and has benefited from the latest GRACE based satellite gravity field model (Pavlis et al., 2008).

For this model to be used for geodetic activities anywhere on the globe, there is need to quantify its accuracy using several validation data sets such as geoid heights through the combination of GPS and levelling heights, airborne and local surface gravity measurements, marine geoid heights from mean oceanographic surface topography models and altimetry observations among others (Kotsakis et al., 2008; Kılıçoğlu et al., 2008). For better assessment, however, these external data sets should be independent of the estimation procedures that were used in the development of the model.

This study focuses on assessing the accuracy of the EGM2008 model in various regions of the country using GPS/levelling over a network of 7 points that exhibit long wave length structures in the levelling heights. If this model best fits the study area, it could further be applied in determination of the geoid at both regional and national scales.

1.1 PROBLEM STATEMENT

In many surveying and engineering applications, orthometric heights are required. GPS derived heights refer to an ellipsoid and not to the geoid as orthometric heights. Ellipsoidal heights are less applicable in practical surveying, engineering, and geophysics as compared to orthometric heights which are often used. To have ellipsoidal heights converted to orthometric heights for application in geodetic activities, precise geoid heights are required. Several techniques can be used to determine these geoid heights. The most commonly used method for the determination of the

geoid is the combination of GPS data with levelling. Levelling is in general easy and practicable though it's a method that is uneconomic to apply and also becomes less accurate as the levelling distances become longer. With the use of a combination of the EGM2008 global gravity model to compute the geoid heights and dual frequency Global Positioning System receivers to obtain ellipsoidal heights with good accuracy, we can obtain orthometric heights which are useful in most geodetic activities. The orthometric heights obtained using the proposed method can only be trusted if the EGM2008 model has been assessed in the study area and proved to give high accuracy geoid heights.

1.2 AIMS AND OBJECTIVES

1.2.1 Major Objective

- To assess the accuracy of EGM2008 global gravity model in Uganda.

1.2.2 Specific Objectives

- To determine geoid heights based on EGM2008 global gravity model
- To determine geoid heights based on on GPS and leveled orthometric heights.
- To determine the residuals between the geoid heights based on EGM2008 global gravity model and geoid heights based on GPS and leveled orthometric heights.

2.0 LITERATURE REVIEW

2.1 HEIGHTING SYSTEMS

2.1.1 Orthometric heights

Orthometric heights (*H*) refer to an equipotential reference surface, e.g. the geoid. The orthometric height of a distinct point on the surface of the earth is the distance from that point to the geoid, measured along the plumb line normal to the geoid (Heister et al., 1999). Due to the fact that equipotential surfaces are not parallel, this plumb line is a curved line. Orthometric heights can be derived using various methods including spirit levelling or trigonometric levelling, global gravity models constituted from potential coefficients, use of vertical deflection obtained from astro-geodetic measurement and gravimetric measurement among others.

2.1.2 Ellipsoidal heights

Ellipsoidal heights (*h*) refer to a reference ellipsoid, e. g. the WGS84 ellipsoid. The height *h* of a point is defined as the distance from the ellipsoid measured along a normal to the reference ellipsoid. Ellipsoidal heights can be derived from geocentric Cartesian coordinates provided by GPS observations (Heister et al., 1999). The difference between orthometric heights and ellipsoidal heights is defined as the ***geoid height*** (*N*) see (Figure 1).

Ellipsoid, Geoid and Orthometric Heights

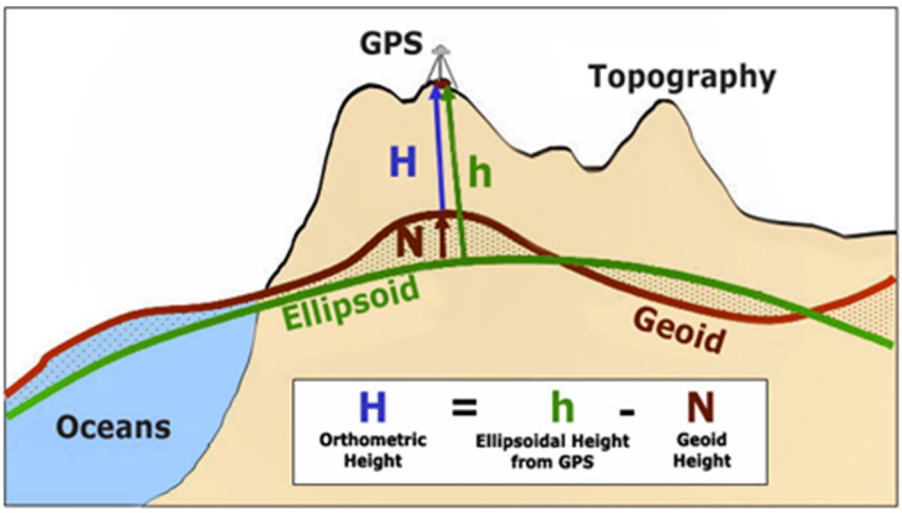

Figure 1*: Geoid, ellipsoidal and orthometric heights (www.nrcan.gc.ca)*

The basic relationship between geoid, ellipsoidal and orthometric heights is given by the following equation;

$$h = H + N \qquad (1)$$

Where *N* is the geoid height, *h* is the ellipsoidal height computed from GPS and *H* is the orthometric height computed from levelling (Figure 1).

2.2 METHODS OF DETERMINING ORTHOMETRIC HEIGHTS

2.2.1 Geometric levelling

Geometric levelling is the determination of the height differences by using a level and a vertical rod (Figure 2). Geometric levelling may at first appear as a very simple method and one that yields the best result. However, practical applications have shown that carrying out this method is very difficult on rough ground and is sensitive to regular or irregular model errors. Preventative measures must be taken to eliminate or reduce model errors stemming from instrumental and ambient conditions. They decrease the speed of survey, thus the cost of surveying rises (Banger, 1981; Niemeier, 1986; Ceylan,1988; Baykal, 1989).

The effects of such errors can be reduced by applying appropriate measurement methods including taking equal backward and forward observation range, round trip surveying, following BFFB (**b**ackward **f**orward **f**orward **b**ackward) or FBBF (**f**orward **b**ackward **b**ackward **f**orward) observation order, calibration in the laboratory and surveying additional parameters such as pressure, temperature and time at the survey moment (Baykal, 1989).

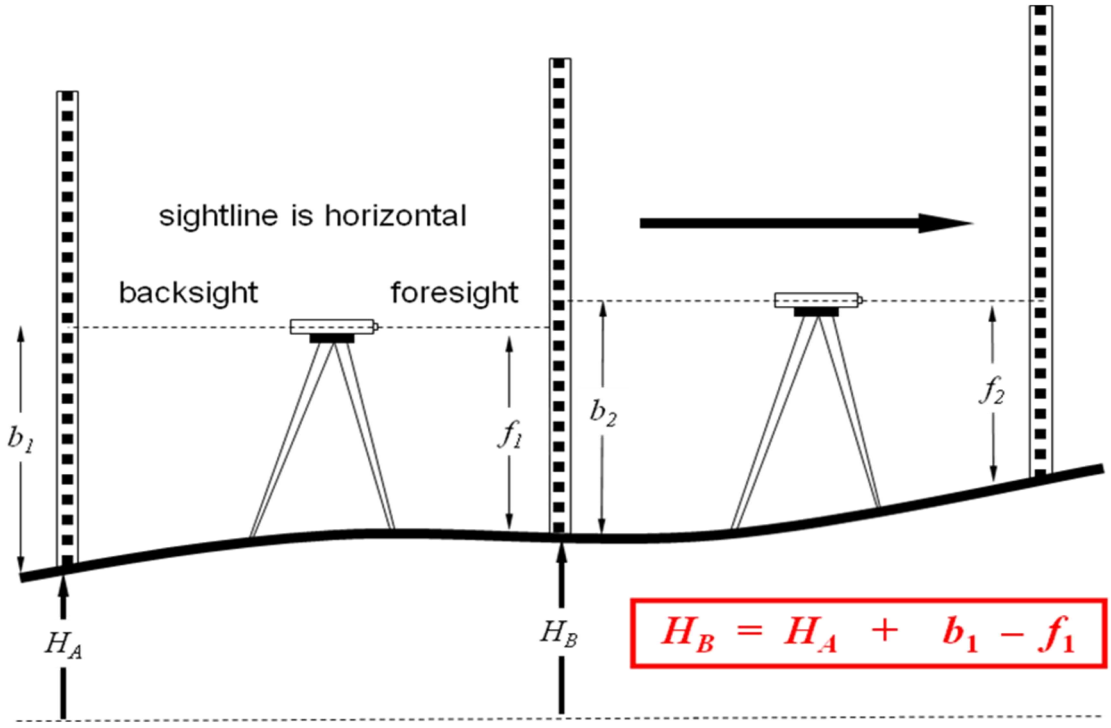

Figure 2 *The fundamental principal of geometric levelling*

Nowadays, motorized levelling has been done by establishing survey hardware on a land vehicle; and successful results have been obtained. The advantages of the motorized levelling may be summarized as follows; Improvement of 40-60% in production velocity, decrease in errors connected to time, observation rays are higher up thereby avoiding rays that graze the surface, thus decreasing refraction errors and More accuracy. The only disadvantage of this technique is that the cost of instrument and vehicles is very high and level points must be on the edge of the road (Niemeier, 1986; Becker, 1986).

2.2.2 Trigonometric levelling

In trigonometric levelling, the height differences are computed by using vertical angle and distance. According to the land, time and observing vertical angle, trigonometric levelling can be classified as follows (Rueger and Brunner, 1982; Kuntz and Schimitt, 1986; Aksoy, 1993):

a) Unidirectional trigonometric levelling
b) Leap-Frog (jumped) trigonometric levelling
c) Reciprocal trigonometric levelling

Applications of the motorized trigonometric levelling have been made by placing survey hardware of the trigonometric levelling on the land vehicle. Motorized trigonometric levelling has equal accuracy (≤ 2mm / km) and equal cost with motorized geometric levelling when the motorized trigonometric levelling is done according to following rules; Vertical angles are measured simultaneously from both ends of the ray path, ray distances are measured in both directions, observation ranges are short (~250-300 m), the instruments are calibrated, the survey is carried out by an experienced person. More than 27% speed of production has been reached with motorized trigonometric levelling. Therefore, the studies have shown that the motorized levelling may be alternative method to geometric levelling (Whalen, 1985; Chrzanowski v.d., 1985; Chrzanowski, 1989).

2.2.3 GPS/Levelling

GPS/Levelling is the most recent and advanced method that can be used in the determination of heights. Three-dimensional coordinates or coordinate differences can be obtained by GPS in the geocentric Cartesian coordinate system. The Cartesian coordinates are transformed to geodetic latitude (φ), geodetic longitude (λ), and ellipsoidal heights (h) according to selected reference ellipsoid, such as WGS84. The ellipsoidal heights obtained by GPS are not directly used for practical surveying. The ellipsoidal height has to be transformed to orthometric height, which is distance measured along the plumb line between the geoid and a point on the Earth's surface and taken positive upward from the geoid (National Geodetic Survey, 1986). The relationship between ellipsoidal height and orthometric height is shown in Figure 1. However geoid heights of all points have to be computed before computing orthometric heights.

Classicaly orthometric heights were computed from a combination of gravity measurements with height increments. Geometric levelling that sums the height increments, ignoring gravity, will give an apparent height difference that depends on the path taken and when carried out with very high precision, levelling around a closed loop will not close. A proper height system must explicitly determine the difference in potential (geopotential number) by summing the height increments multiplied by a measured gravity value.

$$c_p \quad = \quad W_0 - W_p \quad = \sum_0^p |\, g_i \,| \, \Delta H_i \tag{2}$$

Where;

Cp *is the geopotential number at a particular point (P)*

$\boldsymbol{W_o}$ *is the potential at the zero datum*

$\boldsymbol{W_p}$ *is the gravitational potential energy and depends only on where point* ***P*** *is, it doesn't depend on the route taken by the leveling.*

$\boldsymbol{g_i}$ *is the measured gravity at each respective station*

$\Delta\boldsymbol{H}$ *is the height increment at each respective station*

A geometrical conversion could be found by dividing this geopotential number by a constant gravity value (***g***),

$$H_P \quad = \quad \frac{c_P}{\overline{g}_P} \tag{3}$$

Where

$\overline{g}_P$ *is the average gravity along the plumb line*

Hp *is the orthometric height at point P*

Cp *is the geopotential number at P*

The logical difficulty with this approach is that it needs $\overline{g}_P$, an average gravity value inside the earth. In principle, we cannot know this value but ways of estimating it have been devised.

A better approach of determining orthometric height in the satellite era is the use of global geopetential models. Using GPS, an absolute height above a properly geocentric ellipsoid can be obtained and geopotential heights (from which orthometric height above sea level could be derived) can be obtained by inserting the coordinates given by the satellite positioning (h, φ, λ) into a global model of the Earth's potential.

2.3 GLOBAL GEOPOTENTIAL MODELS

There are essentially three classes of Global Geopotential Models (GGMs) according to Rapp (1997), Balmino et al. (1999), Featherstone (2002) and Rummel et al. (2002).

i. **Satellite-only GGMs**

These GGMs are derived solely from analysis of orbits of artificial Earth satellites and examples include;

- **GGM03S** (Tapley et al., 2007)
  This is a GRACE-only gravity model and is complete to degree and order 180.
- **GOCO01S** (Pail, R.*, et al.,* 2010*)*
  The satellite-only gravity field model GOCO01S is a combination solution based on 61 days of GOCE gravity gradient data, and 7 years of GRACE GPS and K-band range rate data, resolved up to degree/order 224 of a harmonic series expansion. The combination was performed consistently by addition of full normal equations and stochastic modeling ofGOCE and GRACE observations. The low to medium degrees of GOCO01S are primarily determined by GRACE, whereas the GOCE gradiometry measurements start to significantly contribute at degree 100. Beyond degree 150, the combined model is dominated by GOCE. The model has been validated against external global gravity models and regional GPS/leveling observations. This gravity model is beneficial for many applications in geophysics, oceanography, and geodesy.
- GOCO02S (Pail, R., 2011)
  GOCO02S is based on 8 months of GOCE data and it shows an improved performance mainly in the high degrees. As additional observation types also GPS satellite-to-satellite tracking (SST) data of GOCE and CHAMP, and satellite laser ranging (SLR) observations to 5 satellites are included.
- **GOCO03S** (Mayer-Gürr T. et al., 2012):
  GOCO03S contains more than 12 months of GOCE data and the same CHAMP, GOCE-orbit and SLR data as contained in GOCO02S.

ii. **Combined GGMs**

Combined GGMs are derived from a combination of satellite, altimetry, land, shiptrack and airborne gravity observation data. The additional information allows an increase of the maximum spherical harmonic degree of the GGMs. These gravity models include;

- **EGM96** (Lemione et al., 1998)
  This is a combined pre CHAMP gravity field model complete to degree and order 360. it was composed from various SLR and other satellite data and terrestrial gravity data from gravimetry and altimetry. EGM96 is the well known for runner of EGM2008.
- **GGM02C** (Tapley et al., 2005)
  This model is a combination of the coefficients of the GRACE-only model GGM02S with EGM96 and is complete to degree and order 200.

- **EIGEN-GLO4C** (Förste et al., 2008a)

  This combined gravity field model released in 2006 is complete to degree and order 360. The satellite part of EIGEN-GLO4C is based on GRACE and LAGEOS data.

- **EIGEN-5C and -5S** (Förste et al., 2008b)

  The combined gravity field model EIGEN-5C is an upgrade of EIGEN-GL04C and has a maximum degree/order of 360. The model is again a combination of GRACE and LAGEOS mission data of a maximum degree/order 150 (=EIGEN-5S) plus 0.5 x 0.5 degrees gravimetry and altimetry surface data.

- **EGM2008** (Pavlis et al., 2008)

  This is a combined model complete to degree and order 2160 with some additional coefficients up to degree and order 2190. This model represents a milestone in the development of global gravity field models and will be evaluated to identify its performance.

iii. **Tailored GGMs**

Tailored GGMs adjust (and often extended to higher degrees) a satellite-only or combined GGM using gravity data that may not necessarily have been used before (Wenzel, 1998a, 1998b). An example of a tailored GGM is GPM98C.

2.3.2 The Earth Gravity Model 2008

2.3.2.1 Design Rationale and Execution (Pavlis et al., 2012)

An additional consideration, pertinent to the design of the EGM2008 solution, involved the poor overall quality of the available marine (non-altimetric) gravity anomalies. Pavlis (1998a) compared the 1° area-mean gravity anomalies used in the development of **EGM96**, to the satellite-only solution **EGM96S**, and demonstrated that over the ocean areas, these non altimetric values were contaminated by significant long wavelength systematic errors. The main reason for using such marine data in EGM96 was to aid the satellite-only solution **EGM96S** in achieving the separation between the geoid and Dynamic Ocean Topography (DOT) signals contained within the altimeter range measurements. Nowadays, though, given the very high accuracy of the long wavelength part of the available GRACE-only models, it is questionable whether these marine gravity anomalies could have any such positive impact, in an ocean-wide sense. However, accurate marine gravity data are still quite useful, especially over areas where the altimetry-derived gravity anomalies are either unavailable or inaccurate. Therefore, in EGM2008, their use was restricted to certain coastal areas, and to areas where significant ocean surface variability makes altimetry-derived gravity anomalies less reliable, while marine data of verifiable quality exist, such as the Kuroshio and Gulf Stream areas.

With the above considerations in mind, it became clear that a very high degree (2159) combination solution could now be developed, not as a composite solution anymore, but

rather using a single least squares adjustment estimation technique, according to the following iterative procedure:

Step 1: A Mean Sea Surface (MSS) and a GRACE-only gravitational model are used to derive a low degree and order spherical harmonic expansion of the DOT.

Step 2: Satellite altimeter data, along with the estimated DOT model, are used to estimate an ocean-wide set of free-air gravity anomalies.

Step 3: The altimetry-derived free-air gravity anomalies are merged with corresponding values over land, and are supplemented with some "fill-in" values over areas void of any gravity observations, to form a complete global 5 arc-minute equiangular grid of surface free-air gravity anomalies.

Step 4: The 5 arc-minute surface free-air gravity anomalies are continued analytically to the surface of an ellipsoid of revolution.

Step 5: The 5 arc-minute free-air gravity anomalies on the ellipsoid and their associated error estimates are input to a Block-Diagonal (BD) least squares estimator, which produces a "terrestrial" estimate of the gravitational potential coefficients, accompanied by a set of BD normal equations. The fact that a spherical harmonic expansion of the gravitational potential complete to degree and order 2159 involves approximately 4.7 million coefficients is what necessitates here the BD approximation of the normal equations.

Step 6: The GRACE-only normal equations' matrix is approximated so that it adheres to the same BD pattern that was used in the "terrestrial" gravity normal equations, by simply equating to zero the elements of the matrix that reside outside the diagonal blocks of interest. The two sets of BD normal equations are then combined and inverted to yield the potential coefficients of the combination solution and their associated error estimates.

Step 7: The MSS from Step 1 and the combination solution from Step 6 are used to estimate a new model of the DOT. Using this new DOT model, one returns to Step 2 and re-iterates the process.

Even though iterative, the procedure outlined above is quite straightforward and very economic with respect to its computational resource requirements. A shortcoming of the above procedure is that it does not permit the simultaneous estimation of the DOT model along with the gravitational potential coefficients. This shortcoming is offset by the fact that the procedure yields a combined gravitational model as the output of a single least squares adjustment, with an estimated error spectrum free of any discontinuities, and without the need to resort to composite gravitational solutions.

The development of EGM2008 involved essentially two iterations of the procedure outlined above. The timing of the preparation and availability of certain data sets required appropriate modifications to be made to the above procedure, so that the EGM2008 development project could progress without significant delays. During the course of the project, three sets of

Preliminary Gravitational Models were developed: **PGM2004** *(Pavlis et al., 2005)*, which served as a demonstration of the capability to perform such combination solutions to degree 2160 and indicated the quality of the results to be expected, **PGM2006** *(Pavlis et al., 2006a)*, and **PGM2007** (Pavlis et al., 2007a). Unlike PGM2004 and PGM2006, which remain internal to the project, one of the PGM2007 solutions was also released for evaluation to an independent **IAG/IGFS** Special Working Group.

2.3.2.2 Basic Relations (Pavlis et al., 2012)

Below is a brief discussion of the main concepts associated with Molodensky's theory approach which aims to determine the external gravity field of the Earth without any assumptions concerning the density of the masses above the geoid *(Heiskanen and Moritz, 1967)*. The physical topographic surface of the Earth and the telluroid are central to Molodensky's formulation. The former is the surface where gravity field measurements are made or to which they are reduced if they were made above that surface; the latter is a surface whose normal potential U at every point Q is equal to the actual gravity potential W at the corresponding surface point P, with the points P and Q being situated on the same line that is normal to the ellipsoidal *(Heiskanen and Moritz, 1967)*.

The Earth's external gravitational potential, V, at a point P defined by its geocentric distance (r), geocentric colatitudes (Θ) (defined as 90°-latitude), and longitude (ƛ) is given by:

$$V(r,\theta,\lambda) = \frac{GM}{r}\left[1 + \sum_{n=2}^{\infty}\left(\frac{a}{r}\right)^n \sum_{m=-n}^{n} \bar{C}_{nm}^{s}\, \bar{Y}_{nm}(\theta,\lambda)\right] \quad (4)$$

where GM is the geocentric gravitational constant and a is a scaling factor associated with the fully normalized, unitless, spherical harmonic coefficients $\bar{C}_{nm}^{s}$. The superscript "s" identifies the coefficients as being spherical. a is usually numerically equal to the equatorial radius of an adopted reference ellipsoid. Equation (4) refers to the permanent part of the gravity field, either ignoring or having corrected first for the variable part due to tides, changes in Earth rotation, etc. The fully normalized surface spherical harmonic functions are defined as (Heiskanen and Moritz, 1967):

$$\bar{Y}_{nm}(\theta,\lambda) = \bar{P}_{n|m|}(\cos\theta).\begin{Bmatrix}\cos m\lambda\\ \sin|m|\lambda\end{Bmatrix}\begin{matrix} if\ m \geq 0\\ if\ m < 0\end{matrix} \quad (5)$$

$\bar{P}_{n|m|}(\cos\theta)$ is the fully normalized associated *Legendre function* of the first kind, of degree n and order |m|. Geocentricity of the coordinate system used, forces the absence of first-degree terms in equation (4). We define the disturbing potential *T* as the difference between the actual gravity potential of the Earth and the "normal" gravity potential associated with a rotating equipotential ellipsoid of revolution. If the rotational speed of the reference ellipsoid is the same as the actual rotational speed of the Earth, so that actual

and normal centrifugal potentials cancel out, the spherical harmonic expansion of T is given by:

$$T(r,\theta,\lambda) = \frac{GM}{r}\sum_{n=2}^{\infty}\left(\frac{a}{r}\right)^n \sum_{m=-n}^{n} \bar{C}_{nm}^{s}\bar{Y}_{nm}(\theta.\lambda) \quad (6)$$

The zero degree term in equation (6) has been set to zero, forcing the equality of the actual mass of the Earth and the mass of the chosen reference ellipsoid. Furthermore, the even-degree zonal harmonic coefficients in equation (6) represent now the difference between the harmonic coefficients of the actual minus the normal gravitational potentials.

We define next the quantity Δg^c (Rapp and Pavlis, 1990) as:

$$\Delta g^c = -\frac{\partial T}{\partial r} - \frac{2}{r}T, \quad (7)$$

So that, from equation (6) we have:

$$\Delta g^c(r,\theta,\lambda) = \frac{GM}{r^2}\sum_{n=2}^{\infty}(n-1)\left(\frac{a}{r}\right)^n \sum_{m=-n}^{n} \bar{C}_{nm}^{s}\bar{Y}_{nm}(\theta,\lambda) \quad (8)$$

The quantity Δg^c is not directly observable. However, it can be estimated, based on the Molodensky surface free-air gravity anomaly Δg (Heiskanen and Moritz, 1967). Δg is defined to be the difference of the magnitude of the *actual gravity acceleration*, which is directly observable using scalar gravimetric techniques, at the surface point P, minus the magnitude of the *normal gravity acceleration* that can be computed at the corresponding telluroid point Q (Heiskanen and Moritz, 1967) i.e.,

$$\Delta g = |\vec{g}_p| - |\vec{\gamma}_Q| \quad (9)$$

Point values of Δg, at arbitrarily scattered locations, are the primary data obtained from terrestrial gravimetric surveys. One can use these data, together with detailed digital elevation information, to estimate area-mean values of gravity anomalies (denoted by Δg), over cells equiangular in latitude and longitude.

Colombo (1981) put forward very efficient numerical techniques that may be used to estimate a set of spherical harmonic coefficients, given a complete global set of data values, defined on an equiangular grid, over a surface of revolution e.g., an ellipsoid of revolution. It is therefore desirable, starting from the original Δg data, which may originate not only from *terrestrial gravity surveys*, but also from *airborne, marine* and *satellite altimetry-derived estimates,* to form a complete global set of area-mean values of the quantities Δg^c (denoted by $\overline{\Delta g}^c$). If then these $\overline{\Delta g}^c$ values could be continued analytically, from their surface of reference (the earth's topography), to the surface of an ellipsoid of revolution, then they could be used as input to the potential coefficient estimator, exploiting the efficiencies of Colombo's (1981) techniques. This procedure could yield a **"***terrestrial" estimate of the potential coefficients*. This estimate, accompanied by its error covariance information, could then be combined in a least squares sense with a corresponding *"satellite" estimate* (obtained in the present study from GRACE data), to determine the potential coefficients of the combined solution.

The general procedure outlined above involves the application of several *systematic corrections* to the original data, as Rapp and Pavlis (1990) discuss in detail. Of these, the *atmospheric correction*, and the correction accounting for the *second-order vertical gradient* of normal gravity, are applied most conveniently during the pre-processing of the point gravity anomaly data Δg. *Ellipsoidal corrections* on the other hand, can be applied conveniently to the area-mean values $\overline{\Delta g}$, using some preliminary estimate of the potential coefficients Pavlis (1988).

Finally, one may use some technique of *analytical downward continuation* (Moritz, 1980) to compute from $\overline{\Delta g}^c$, a corresponding fictitious quantity $\overline{\Delta g}^e$, defined to reside on the surface of the reference ellipsoid. $\overline{\Delta g}^e$ is defined such that, when analytically continued in the opposite (upward) direction, it should reproduce $\overline{\Delta g}^c$. Apart from this requirement, $\overline{\Delta g}^e$ possesses no physical meaning and certainly does not represent the gravity anomaly inside the topographic masses.

Let r_i^e be the geocentric distance to the center of a cell residing on the i-th (i = 0, … N-1) latitude belt ("row") and j-th (j = 0, … 2N-1) meridional sector ("column"), within a global equiangular grid composed of N rows by 2N columns of $\overline{\Delta g}_{ij}^e$ area-mean values, on the surface of the reference ellipsoid. For the small (5 arc-minute) equiangular cell size used in this study, the small and regular latitudinal variation of r^e within the cell can be safely ignored (Rapp and Pavlis, 1990) so that we may approximate:

$$\overline{(r\Delta g)}_{ij}^e \approx r_i^e . \overline{(\Delta g)}_{ij}^e \qquad (10)$$

The product $r_i^e . \overline{(\Delta g)}_{ij}^e$, defined over the surface of the reference ellipsoid, can be expanded in surface ellipsoidal harmonic functions (Heiskanen and Moritz, 1967), as:

$$r_i^e . \overline{(\Delta g)}_{ij}^e = \frac{1}{\Delta\sigma_i}\frac{GM}{a}\sum_{n=2}^{\infty}(n-1)\sum_{m=-n}^{n}\bar{C}_{nm}^e . I\bar{Y}_{nm}^{ij} \qquad (11)$$

With δ denoting the reduced co-latitude (Heiskanen and Moritz, 1967), the terms in equation (11) are defined as:

$$\Delta\sigma_i = \Delta\lambda\int_{\partial_i}^{\partial_{i+1}}\sin\delta d\delta = \Delta\lambda.(\cos\delta_i - \cos\delta_{i+1}) \qquad (12)$$

$$I\bar{Y}_{nm}^{ij} = \int_{\partial_i}^{\partial_{i+1}}\bar{P}_{n|m|}(\cos\delta)\sin\delta d\delta . \int_{\lambda_j}^{\lambda_{j+1}}\begin{Bmatrix}\cos m\lambda \\ \sin|m|\lambda\end{Bmatrix} d\lambda \begin{matrix} if\ m \geq 0 \\ if\ m < 0\end{matrix} \qquad (13)$$

The quantity $r^e\Delta g^e$ represents a harmonic function, and, under the approximation of equation (10), so does the quantity $r_i^e . \overline{(\Delta g)}_{ij}^e$. This allows one to relate the ellipsoidal harmonic coefficients $\bar{C}_{nm}^e$ of equation (11), to the corresponding spherical harmonic coefficients $\bar{C}_{nm}^s$ appearing in equations (6) and (8), using the exact transformations derived by Jekeli (1988) and implemented and verified by Gleason (1988).

Note that our $\bar{C}_{nm}^s$ and $\bar{C}_{nm}^e$ coefficients are related to the corresponding $\bar{g}_{n,m}^s$and $\bar{\bar{g}}_{n,m}^e$coefficients of Gleason (1988) by:

$$\begin{Bmatrix}\bar{g}^{s}_{n,m}\\ \bar{\bar{g}}^{e}_{n,m}\end{Bmatrix} = \frac{GM}{a^2}(n-1).\begin{Bmatrix}\bar{C}^{s}_{nm}\\ \bar{C}^{e}_{nm}\end{Bmatrix} \quad (14)$$

The transformation from spherical to ellipsoidal harmonic coefficients is given in (Gleason, 1988, equation 2.8):

$$\bar{\bar{g}}^{e}_{n,m} = \bar{S}_{n|m|}\left(\frac{b}{E}\right).\sum_{k=0}^{s'} \lambda_{n,m,k}.\bar{g}^{s}_{n-2k,m} \quad (15)$$

and the transformation from ellipsoidal to spherical harmonic coefficients is given in (Gleason, 1988, equation 2.10):

$$\bar{g}^{s}_{n,m} = \sum_{k=0}^{s'} \frac{1}{\bar{S}_{n-2k,|m|}\left(\frac{b}{E}\right)}.L_{n,m,k}.\bar{\bar{g}}^{e}_{n-2k,m} \quad (16)$$

b is the semi-minor axis and E the linear eccentricity of the adopted reference ellipsoid (Heiskanen and Moritz, 1967) and the definition of the other terms appearing in equations (15) and (16) can be found in the work of Gleason (1988). It is important to note that both transformations are linear, and they both relate coefficients of the same type, order, and parity of n-m. Importantly, equations (15) and (16) imply that both transformations preserve the maximum order but not the maximum degree of a set of coefficients. As Jekeli (1988) has pointed out, a finite number of spherical harmonic coefficients generate an infinite number of ellipsoidal harmonic coefficients and vice versa. The additional coefficients, of degree higher than the highest degree within the series being transformed, are linear combinations of lower degree terms. These "extra" terms may be negligible for expansions up to degree 360 or so, but become important for expansions up to degree 2159, as Holmes and Pavlis (2007) have demonstrated.

Considering equation (14), the transformation (15) can be written in vector-matrix form as:

$$[\bar{C}^{e}_{m}] = T^{se}_{m}.[\bar{C}^{s}_{m}] \quad (17)$$

Where T^{se}_{m} is the transformation matrix applicable to order m, whose elements are computed based on equation (15). Let T^{se} be the combined transformation matrix, composed of the T^{se}_{m} sub-matrices, for all orders within a set of spherical harmonic coefficients $\bar{C}^{s}$, whose error covariance matrix is$\sum_{\bar{C}^{s}}$. Then the computation of the corresponding ellipsoidal harmonic coefficients, using the transformation of equation (15), can be written in the form:

$$[\bar{C}^{e}] = T^{se}.[\bar{C}^{s}] \quad (18)$$

Error propagation implies that the error covariance matrix of $\bar{C}^{e}$ is given by:

$$\sum_{\bar{C}^{e}} = T^{se}.\sum_{\bar{C}^{s}}.(T^{se})^{T} \quad (19)$$

Where the superscript "T" denotes the transpose of a matrix. Similarly, the transformation from ellipsoidal to spherical harmonic coefficients can be written in the form:

$$[\bar{C}^{s}] = T^{es}.[\bar{C}^{e}] \quad (20)$$

and the corresponding error covariance propagation formula is:

$$\sum_{\bar{C}^{s}} = T^{es}.\sum_{\bar{C}^{e}}.(T^{se})^{T} \quad (21)$$

Where the elements of matrix T^{es} are computed from equations (14) and (16).

The formulation presented so far allows one to estimate a set of ellipsoidal harmonic coefficients $\bar{C}^e$ from a global set of area-mean free-air gravity anomalies $\overline{\Delta g}^e$ that have been analytically continued to the surface of the reference ellipsoid. The estimation of $\bar{C}^e$ is based on the (linear) mathematical model of equation (11), expressed as a finite series, truncated to some maximum degree N_{max} that is commensurate with the size of the equiangular cells forming the global grid (e.g., N_{max} = 2159 for 5 arc-minute equiangular cells), i.e.,

$$r_i^e.\overline{(\Delta g)}_{ij}^e = \frac{1}{\Delta\sigma_i}\frac{GM}{a}\sum_{n=2}^{Nmax}(n-1)\sum_{m=-n}^{n}\bar{C}_{nm}^e.I\bar{Y}_{nm}^{ij} \tag{22}$$

Based on equation (22), one forms a system of observation equations that can be written as:

$$v = A.\hat{x} - L_b \tag{23}$$

Where L_b is the vector of observations $\overline{\Delta g}^e$, v is the vector of corresponding residuals, A is the design matrix whose elements are formed based on equation (22), and $\hat{\boldsymbol{x}}$ represents the vector of estimated coefficients $\bar{C}^e$. To be specific, $\hat{x}$ represents estimated incremental changes to the coefficients. The actual coefficient values are obtained after the adjustment, by adding $\hat{x}$ to the reference coefficient values that were used within the adjustment. The least squares solution,$\hat{x}$, which satisfies the condition:

$$v^T P v = minimum \tag{24}$$

is given by (Uotila, 1986):

$$\left.\begin{matrix} \hat{x} = N^{-1}U & (a) \\ N = A^T P A & (b) \\ U = A^T P L_b & (c) \end{matrix}\right\} \tag{25}$$

Where P is the weight matrix associated with the observations $\overline{\Delta g}^e$. In this study, *P* was assumed to be diagonal, with each diagonal element equal to the reciprocal of the error variance of the corresponding gravity anomaly observation, i.e.:

$$P = \sigma_0^2\begin{pmatrix} \frac{1}{\sigma_1^2} & & 0 \\ & \ddots & \\ 0 & & \frac{1}{\sigma_k^2} \end{pmatrix} \tag{26}$$

Where K is the total number of observations, and σ_0^2 is the a priori variance of unit weight, taken equal to 1. For the complete global equiangular grid of 5 arc-minute area-mean gravity anomalies used here, K = 2160 x 4320 = 9331200. The assumption that the gravity anomaly errors are uncorrelated is made out of necessity, rather than desire. It is extremely difficult to estimate error correlations between the gravity anomalies with any degree of accuracy. It is also practically impossible to handle numerically an arbitrary fully occupied (symmetric) weight matrix of dimension 9331200. Even the estimation of realistic error variances for the gravity anomalies is a very challenging task.

With N_{max} = 2159, the expansion given in equation (22) involves exactly 4665596 unknown ellipsoidal harmonic coefficients. A weight matrix P, with elements of arbitrary value on the diagonal, would result, in general, in a fully occupied, symmetric, normal matrix *N* of dimension 4665596 x 4665596. The creation, storage, and inversion of such a matrix are impractical, if not altogether impossible, given the presently available computational capabilities. Therefore, the normal matrix *N* is approximated with its "Type 1" Block-Diagonal form (BD1), whereby nonzero off-diagonal elements occur only between coefficients of the same type, order, and parity of n-m, as it is discussed in detail by Pavlis (1998c)**.** This approximation requires also the careful "calibration" of the values of the weights used in P, so that excessive weight ratios are avoided (see also Pavlis, 1998d).
The residuals obtained from equation (23) represent merely a measure of "goodness of fit" of the truncated model (22) to the input data $\overline{\Delta g}^e$, i.e., they show how well the truncated series of ellipsoidal harmonics of equation (22) manages to reproduce the input data, but do not provide any information regarding the accuracy itself of the input data.

Two additional aspects of the above formulation are noteworthy:
(a) In equations (11) and (22) the summation starts from harmonic degree 2. However, there is no guarantee that real data will not possess any zero- and first-degree terms. These terms, meaningless as they may be, if left in the data and are not solved-for, could alias other low degree coefficients of the same order. Therefore, in this study, any zero- and first-degree terms present in the data were estimated and removed from them, before using the data to estimate the $\bar{C}^e$ coefficients.
(b) The properties of the transformations (15) and (16) discussed previously are such that both transformations preserve the BD1 block-diagonal pattern in normal and error covariance matrices of coefficient sets. This has important implications in the combination

2.3.2.3 Data Used in the Analysis (Pavlis et al., 2012)

The essential "ingredients" necessary for the estimation of the present high resolution global gravitational model are a solution based on *GRACE data*, accompanied by its complete error covariance matrix, and a complete *global set of 5 arc-minute area-mean free-air gravity anomalies,* see Figure 3*.*

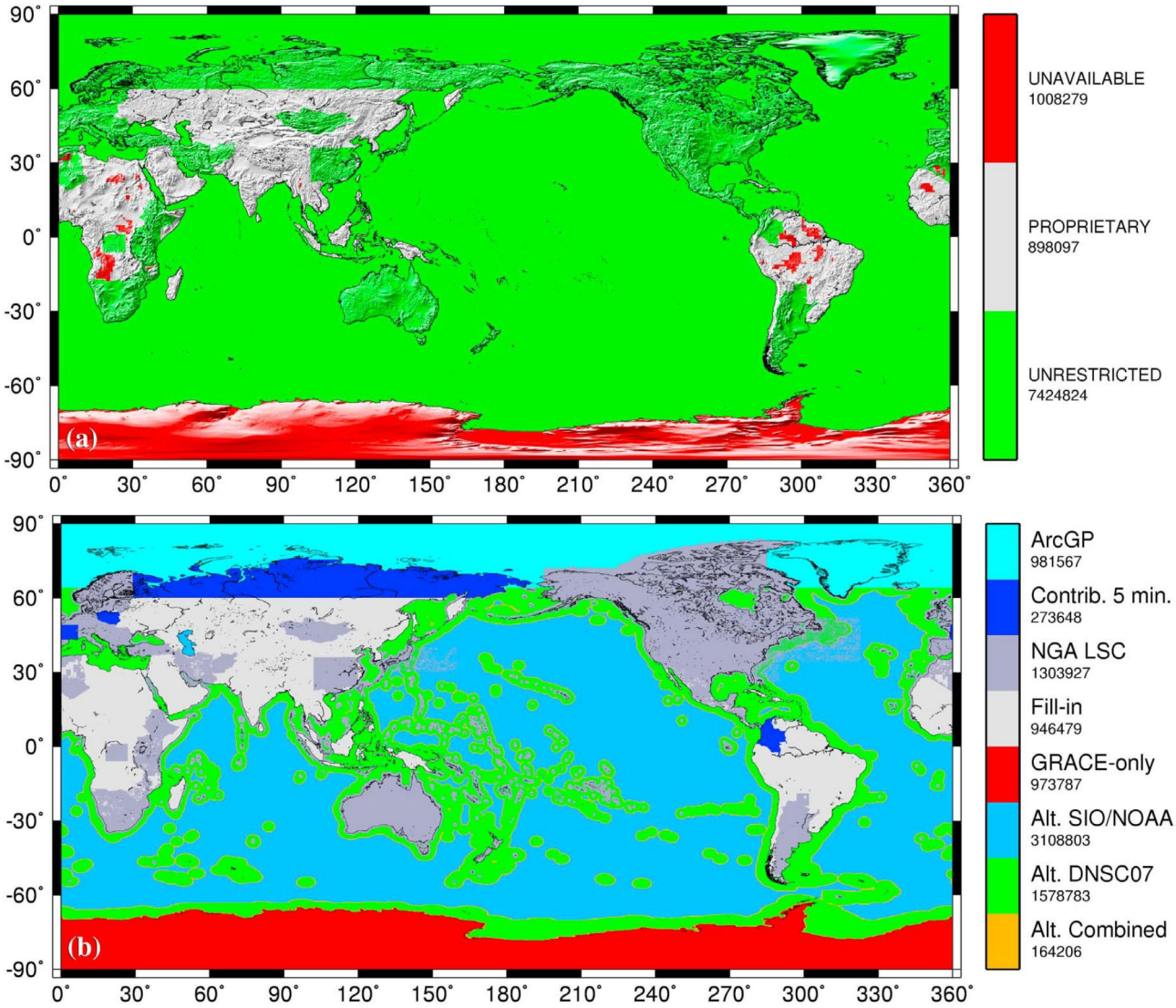

Figure 3: *Geographic display of some of the characteristics of the 5 arc-minute area-mean gravity anomalies in the merged file used to develop the EGM2008 model: (a) Data availability. (b) Data source identification* (Pavlis et al., 2012).

The estimation of these gravity anomalies, as well as other aspects of the solution, also require a very high resolution global *Digital Topographic Model* (DTM). The estimated gravity anomalies need to be *analytically downward continued* to the surface of the reference ellipsoid. Ideally, these gravity anomalies should have uniform and high accuracy, and should only contain spectral information associated with the solved-for harmonic coefficients. Since the 5 arc-minute equiangular grid of the gravity anomalies on the reference ellipsoid permits the unbiased estimation of a set of ellipsoidal harmonic coefficients, complete to degree and order 2159 (Colombo, 1981), in order to minimize aliasing effects it is desirable to filter out of the 5 arc-minute data any spectral contributions beyond ellipsoidal harmonic degree and order 2159 (Pavlis, 1988; Jekeli, 1996). In the

following sections we describe the data that were used to compile the essential "ingredients" necessary to develop the combination solution.

A. THE ITG-GRACE03S MODEL

The ITG-GRACE03S (Mayer-Gürr, 2007) satellite-only model that was used in the development of EGM2008 was computed at the Institute of Theoretical Geodesy of the University of Bonn in Germany. ITG-GRACE03S is based on GRACE Satellite-to-Satellite Tracking (SST) data acquired during the 57-month period from September 2002 to April 2007. No other data were used in its development, which followed the short-arc analysis approach described by Mayer-Gürr et al. (2007). ITG-GRACE03S is complete to spherical harmonic degree and order 180, and was made available accompanied by its fully occupied error covariance matrix. The model was developed without application of any a priori information or any other regularization constraint. Therefore, the model ($\hat{x}$) itself and its complete error covariance matrix ($\sum_x$) are sufficient to recreate exactly the normal equation system that produced it, recalling that the error covariance matrix is the inverse of the normal equation matrix, i.e., from:

$$\begin{Bmatrix} N = \sum_x^{-1} & (a) \\ U = N_{\hat{x}} & (b) \end{Bmatrix} \qquad (27)$$

B. THE DIGITAL TOPOGRAPHIC MODEL DTM2006.0

The pre-processing and analysis of the detailed surface gravity data necessary to support the development of an EGM to degree 2160, depends critically on the availability of accurate topographic data, at a resolution sufficiently higher than the 5 arc-minute resolution of the area-mean gravity anomalies that will be used eventually to develop the EGM. Factor (1998) discusses some of the uses of such topographic data within the context of a high resolution EGM development. These include the computation of Residual Terrain Model (RTM) effects (Forsberg, 1984), the computation of analytical continuation terms, the computation of Topographic/Isostatic gravitational models that may be used to "fill-in" areas void of other data, and the computation of models necessary to convert height anomalies to geoid undulations (Rapp, 1997). For these computations to be made consistently, it is necessary to first compile a high-resolution global DTM, whose data will support the computation of all these terrain-related quantities.

For EGM96 (Lemoine et al., 1998), which was complete to degree and order 360, a global digital topographic database (JGP95E) at 5 arc-minute resolution was considered sufficient. JGP95E was formed specifically to support the development of EGM96, by merging data from 29 individual sources, and, as acknowledged by its developers, left a lot to be desired in terms of accuracy and global consistency. Since that time, and thanks primarily to the Shuttle Radar Topography Mission (SRTM) (Werner, 2001), significant progress has been

made on the topographic mapping of the Earth from space. During approximately 11 days in 2000 (February 11–22), the SRTM collected data within latitudes 60°N and 56°S, thus covering approximately 80 percent of the total land area of the Earth with elevation data of high, and fairly uniform, accuracy. Rodriguez et al. (2005) discuss in detail the accuracy characteristics of the SRTM elevations. Comparisons with ground control points whose elevations were determined independently using kinematic GPS positioning, indicate that the 90 percent absolute error of the SRTM elevations ranges from ± 6 to ± 10 m, depending on the geographic area (Rodriguez et al., 2005).

In preparation for the development of the EGM2008 model, DTM2006.0 was compiled by overlying the SRTM data over the data of DTM2002 (Saleh and Pavlis, 2003). In addition to the SRTM data, DTM2006.0 contains ice elevations derived from ICESat laser altimeter data over Greenland (S. Ekholm, personal communication, 2005) and over Antarctica (J. P. DiMarzio, personal communication, 2005). Over Antarctica, data from the "BEDMAP" project (http://www.antarctica.ac.uk/aedc/bedmap/) were also used to define ice and water column thickness. Over the ocean, DTM2006.0 contains essentially the same information as DTM2002, which originates in the estimates of bathymetry (Smith and Sandwell, 1997) from altimetry data and ship depth soundings. DTM2006.0 was compiled in 30 arc-second resolution, providing height and depth information only, and in 2, 5, 30 and 60 arc-minute resolutions, where lake depth and ice thickness data are also included. DTM2006.0 is identical to DTM2002 in terms of database structure and information content. DTM2006.0 data was used to compute the following quantities:

(a) Fully normalized spherical harmonic coefficients of the elevations($\bar{H}_{nm}$). These are consistent with the model:

$$\bar{H}_{ij} = \bar{H}\left(\theta_i, \lambda_j\right) = \frac{1}{\Delta\sigma_i}\sum_{n=0}^{k}\sum_{m=-n}^{n}\bar{H}_{nm}.I\bar{Y}_{nm}^{ij} \qquad (28)$$

where $\bar{H}_{ij}$ represents the area-mean value of an elevation-related quantity, such as heights above and depths below Mean Sea Level (MSL), over a cell located on the i-th "row" and j-th "column" of the global equiangular grid. The terms $\Delta\sigma_i$ and $I\bar{Y}_{nm}^{ij}$ are defined exactly as in equations (12) and (13), but evaluated here using the geocentric co-latitude Θ, instead of the reduced co-latitude δ. The 2 arc-minute version of DTM2006.0 was used to evaluate a set of coefficients $\bar{H}_{nm}$ complete to degree and order K = 2700. These coefficients, up to degree and order 2160, were used to form the terms necessary to convert height anomalies to geoid undulations, as described by Rapp (1997). The same coefficients, to degree and order 360, we used to form the reference surface, with respect to which the RTM-implied gravity anomalies were computed.

(b) The 30 arc-second version of DTM2006.0 was used to evaluate the g_1 analytical continuation terms, over all land areas, on the same 30 arc-second grid. We then formed

global equiangular grids of the area-mean values of these terms in both 2 and 5 arc-minute resolutions, and analyzed harmonically the 2 arc-minute grid to create a set of ellipsoidal harmonic coefficients of these g_1 terms, complete to degree and order 2700.

(c) The 30 arc-second version of DTM2006.0 was used and computed on the same 30 arc-second grid extending over all of the Earth's land areas, including a 10 km margin protruding into the ocean, gravity anomalies implied by a Residual Terrain Model (RTM). This RTM was referenced to a topographic surface, created from the elevation harmonic coefficients described under (a) above, to degree and order 360. RTM-implied gravity anomalies Δg_{RTM} were computed as described in detail by Forsberg (1984). The 2 arc-minute area-mean values of these anomalies were then formed and supplemented the land data set with zero values for the cells that are located over ocean areas, excluding the margin mentioned above. This 2 arc-minute Δg_{RTM} grid was analysed harmonically to compute a set of ellipsoidal harmonic coefficients complete to degree and order 2700. The computation of the RTM-implied gravity anomalies globally and on a regular grid enables their spectral decomposition, and so is of critical importance both to the estimation of a band-limited set of 5 arc-minute mean anomalies from terrestrial gravity data, and to the computation of "fill-in" anomalies in areas covered with proprietary data.

(d) The formulation described by Pavlis and Rapp (1990) was used to determine spherical harmonic coefficients of the Topographic/Isostatic (T/I) potential implied by the Airy/Heiskanen isostatic hypothesis, with a constant 30 km depth of compensation. These coefficients were evaluated up to degree and order 2160, employing the DTM2006.0 database, in two ways:

(i) Using 5 arc-minute data, and,

(ii) Using 2 arc-minute data.

These coefficients were originally intended to be used in combination with the satellite-only model, to compute "fill-in" gravity anomalies. This was not done however, as opted instead for the use of "fill-in" gravity anomalies, free of any isostatic hypothesis.

Pavlis et al. (2007b) provide additional details about the DTM2006.0 database and its use towards the development and implementation of the EGM2008 model.

It should be emphasised here that a single DTM should be used consistently in all the processes related to the development and the subsequent use of an EGM. This DTM is in fact inextricably connected to the resulting EGM. For example, elevation errors will propagate into errors in the downward continuation of gravity anomalies from the topography to the ellipsoid. However, one expects these propagated errors to cancel out to a large extent, when the resulting EGM is used to compute quantities such as height anomalies or gravity anomalies back on the topography, as long as the same DTM is used consistently in both operations. Otherwise, the use of different elevation information in

these operations could create inconsistencies that may degrade the results. Therefore, the availability of a global DTM of the highest possible accuracy and resolution is an important prerequisite of any high resolution EGM development effort and use.

C. THE GRAVITY ANOMALIES DERIVED FROM SATELLITE ALTIMETRY

The altimetry-derived gravity anomalies cover approximately 70 percent of the globe, and so are crucial to the formation of a complete, global 5 arc-minute gravity anomaly grid that can support the determination of a marine geoid with long wavelength integrity and very high resolution. The global 5 arc-minute merged gravity anomaly files, which supported the development of several Preliminary Gravitational Models (PGM) during the course of the project, employed altimetry-derived gravity anomalies from a variety of sources, one of them computed at the Danish National Space Center (DNSC) – DNSC07, the other at Scripps Institution of Oceanography, in collaboration with the National Oceanic and Atmospheric Administration (SIO/NOAA) – SSv18.1.

The main difference between the estimation algorithms employed by DNSC and SIO/NOAA is the form in which the altimeter data enter the estimation of gravity anomalies. DNSC uses (residual) Sea Surface Heights (SSH), while SIO/NOAA use (residual) slopes of the SSH, determined from the numerical differentiation of neighbouring altimeter data. There are advantages and disadvantages associated with either of the two estimation techniques, as these were actually implemented by DNSC and SIO/NOAA respectively. In particular, for a given reference gravitational model whose resolution is always finite, the use of residual SSH is affected less by the lack of data on the side of land in near-coastal areas, as compared to the use of residual SSH slopes. The use of residual SSH slopes on the other hand, tends to produce gravity anomalies that are noticeably “richer” in high frequency content, as compared to the use of residual SSH. The difference between the results from the two estimation techniques are of course reduced as the common reference models used in both become more accurate and of higher resolution.

D. THE GRAVITY ANOMALIES ESTIMATED FROM TERRESTRIAL DATA

The estimation of the 5 arc-minute area-mean free-air surface gravity anomalies $\overline{\Delta g}_{ij}^{t}$ from the corresponding point values was performed using a LSC prediction algorithm (Moritz, 1980), in a “remove-compute-restore” fashion. LSC is a mathematical technique for determining the Earth’s figure and gravitational field by a combination of heterogeneous data of different kinds. Its formulation may be interpreted in very different ways: as the solution of a geophysical inverse problem, as a statistical estimation method combining least squares adjustment and least squares prediction, and as an analytical approximation to the Earth’s potential by means of harmonic functions (Moritz, 1978). LSC is a form of

linear regression – estimating stochastic quantities from other stochastic quantities by using their statistical correlations – that is formally identical to objective mapping. The implementation of LSC used the remove-compute-restore computational methodology that is well known to geodesists. Thereby, long wavelength trends are removed from the observations using some a priori known reference model(s), the LSC prediction is applied to the residuals after the removal of the values of the reference model(s) from the observations, and finally the effects of the reference model(s) are restored back to the estimated quantities. Moritz (1980) provides a comprehensive treatise of LSC and the remove-compute-restore computational methodology. The main elements of this formulation are:

$$\overline{\Delta g}_{ij}^{t} = C_{\overline{\Delta g}_{ij}^{t},\Delta g_k^t}.\left(C_{\Delta g_k^t,\Delta g_k^t} + V\right)^{-1}.L + r_{ij} \qquad (29)$$

Where $C_{\overline{\Delta g}_{ij}^{t},\Delta g_k^t}$ is the signal cross-covariance matrix between the area-mean value to be predicted and the point values of the observations Δg_k^t, and $C_{\Delta g_k^t,\Delta g_k^t}$ is the auto-covariance matrix of the observations involved in the prediction. *V* is the noise covariance matrix of these observations, which was taken in this study to be diagonal, and *L* is the vector of observations. From the observations, quantities that can be modelled have been removed, so that an element l_k of the vector *L* is given by:

$$l_k = x_k - y_p \qquad (30)$$

where:

$$x_k = \Delta g_k^t - \Delta g_k^t(SH) - \Delta g_k^t(RTM) \qquad (31)$$

and y_p is the mean value of x_k over the area involved in the prediction, so that the residual observations involved in the prediction are centered. $\Delta g_k^t(SH)$) and$\Delta g_k^t(RTM)$) are point values of the free-air gravity anomalies implied by the reference spherical harmonic model used and by the RTM computation. In our notation, “SH” abbreviates “Spherical Harmonics” and refers to the computational method used to evaluate these gravity anomalies. It does not represent a variable, to which these gravity anomalies depend, but rather a computational method. The same applies to our “RTM” notation. Finally, in equation (29), r_{ij} is given by:

$$r_{ij} = \overline{\Delta g}_{ij}^{t}(SH) + \overline{\Delta g}_{ij}^{t}(RTM) + y_p \qquad (32)$$

and represents the sum of the area-mean values of the reference terms that have to be “restored” to the predicted quantity $\overline{\Delta g}_{ij}^{t}$. In equations (31) and (32), proper care should be exercised, so that the reference gravitational model and the RTM effects neither overlap nor leave any “gaps” in terms of spectral content. This LSC prediction algorithm was used to estimate the terrestrial gravity anomalies that supported the PGM2004A, PGM2006A/B/C, and PGM2007A/B preliminary models. For the final EGM2008 model however, a modification to this algorithm was implemented, which results in predicted

gravity anomalies $\overline{\Delta g}_{ij}^{t}$ that are band-limited to a high degree of approximation. Consider the frequency content of the various terms appearing in equations (31) and (32). The point value of the surface free-air gravity anomaly Δg_k^t contains the full spectrum of the gravity field. The reference value $\Delta g_k^t(SH)$ and $\overline{\Delta g}_{ij}^{t}(SH)$ contain only the bandwidth of the reference model used in the estimation. Due to the use of a reference topographic surface created from an expansion to degree 360 of the topography , the point values $\Delta g_k^t(RTM)$, contain spectral power from degree ~360, up to a degree commensurate with the grid size of the DTM used in their computation, which, in this case, was 30 arc-seconds. The corresponding 5 arc-minute area-mean values $\overline{\Delta g}_{ij}^{t}(RTM)$, which are the result of averaging, are certainly not band-limited, and contain spectral power beyond degree 2159. A simple modification of the quantities used in the LSC algorithm discussed before, can provide much better control on the frequency content of the predicted mean anomalies. Specifically, we modify equations (31) and (32) as:

$$x_k = \Delta g_k^t - [\Delta g_k^t(SH, n = 2159) - \Delta g_k^t(RTM, n = 2159)\,] - \Delta g_k^t(RTM) \qquad (33)$$

and

$$r_{ij} = \overline{\Delta g}_{ij}^{t}(SH, n = 2159) + \mathrm{y_p} \qquad (34)$$

where we have assumed here that the reference gravitational model extends to degree 2159, in ellipsoidal harmonics. Use of equations (33) and (34), instead of (31) and (32), results in predicted gravity anomalies $\overline{\Delta g}_{ij}^{t}$ that are band-limited to a high degree of approximation. The key element that enables the implementation of this new approach is the availability of the RTM-implied Δg, globally and in the form of a regular grid. Without such a file, there can be no spectral decomposition of the RTM-implied Δg, which produces the coefficients necessary to synthesize the terms $\Delta g_k^t(RTM, n = 2159)$ with the required spectral content. In the implementation, the quantity within the brackets in equation (33), referring to the Earth's topography, was evaluated as point values on a global 30 arc-second grid. This grid was then used to interpolate the values to the locations of the point gravity data. The gravity anomaly degree variances c_n, is computed according to equation (35).

$$C_n = \left[\frac{GM}{a^2}(n-1)\right]^2 \sum_{m=-n}^{n} (\bar{C}_{nm}^{e})^2 \qquad (35)$$

The LSC prediction algorithm implemented here also provides estimates of the error variances of the predicted $\overline{\Delta g}_{ij}^{t}$. These are given by:

$$\sigma^2_{\overline{\Delta g}_{ij}^{t}} = C_{\overline{\Delta g}_{ij}^{t},\overline{\Delta g}_{ij}^{t}} - C_{\overline{\Delta g}_{ij}^{t},\Delta g_k^t}.\left(C_{\Delta g_k^t,\Delta g_k^t} + V\right)^{-1}.C_{\Delta g_k^t,\overline{\Delta g}_{k}^{t}} \qquad (36)$$

These error variances do not necessarily account for systematic errors in the gravity data, and have to be modified carefully, in order to provide realistic measures of the errors associated with these data.

For the final iteration of the estimation of the 5 arc-minute gravity anomalies, which supported the development of EGM2008, the PGM2007B solution was used as reference gravitational model (to spherical harmonic degree 2190), consistent with the estimation of the altimetry-derived values.

E. Fill-in GRAVITY ANOMALIES USING RTM FORWARD MODELING

In terms of their availability, the gravity anomaly data that were necessary for the project divide the Earth into three distinct sub-divisions, as shown in Figure 3a.

(a) Areas where gravity anomaly data exist, and were made available for the computation of the 5 arc-minute area-mean values necessary for the project, without any restrictions. The majority of ocean areas fall in areas where the altimetry-derived gravity anomalies existed. These areas are colored green in Figure 3a.

(b) Areas where gravity anomaly data are either unavailable, or too sparse, or too inaccurate, to support the estimation of 5 arc-minute area-mean values of meaningful quality. These areas are colored red in Figure 3a.

(c) Areas where the gravity anomaly data available to this project were of proprietary nature. In agreement with the co-owners of these data, within this project, their use was only permitted at a resolution corresponding to 15 arc-minute area-mean values. The domain of these data covers approximately 42.9 per cent of the Earth's total land area, and is coloured grey in Figure 3a.

In order to compile a global gravity anomaly data set with as uniform spectral content as possible, capable of supporting the estimation of potential coefficients to degree 2159, the spectral content of the gravity anomalies in category (c) above, beyond degree 720 that corresponds to the 15 arc-minute resolution, and up to degree 2159, was supplemented with the gravitational information obtained from the global set of RTM-implied gravity anomalies. The specific details of the implementation of this approach are given by Pavlis et al. (2007b). This approach was tested and verified locally, over extended areas where high quality gravity anomaly data are available (USA, Australia), as Pavlis et al. (2007b) discuss in detail. In addition, the gravity anomaly degree variances obtained from the analysis of a global 5 arc-minute data set that included the proprietary data were compared with the degree variances obtained from the use of the RTM-implied gravity information. Pavlis et al. (2007b, Figure 5) demonstrate that the two spectra are in excellent agreement. Only after degree ~ 1650 the use of the RTM-implied gravity information provides a somewhat underpowered gravity anomaly spectrum. With this approach, the proprietary data issues were circumvented without degrading the gravitational solution significantly, at least in terms of the recovered power spectrum. An obvious shortcoming of our RTM based forward modelling approach is that it can only improve the modelling of short wavelength

gravitational signals (beyond degree 720), to the extent that these signals are generated by topographic masses.

Finally, there was need to provide an estimate for each of the 5 arc-minute area-mean gravity anomalies under (b) above. These cover approximately 12.0 percent of the Earth's land area, and are located in Africa, South America, and Antarctica. Over Africa and South America, the 5 arc-minute values were originally synthesised using the GGM02S coefficients (Tapley at al., 2005) for degrees 2 to 60, augmented with the EGM96 coefficients (Lemoine et al., 1998) for degrees 61 to 360, and further augmented with the coefficients from the analysis of the RTM-implied anomalies for degrees 361 to 2159. Over Antarctica, the 5 arc-minute values were synthesised using only the ITG-GRACE03S (Mayer-Gürr, 2007) model coefficients, up to degree and order 180.

F. THE 5 Arc-Minute GLOBAL MERGED GRAVITY ANOMALY FILE

The estimation of the $\bar{C}^e$ ellipsoidal harmonic coefficients implied by the "*terrestrial*" data up to degree and order 2159 requires a global, complete file of 5 arc-minute area-mean gravity anomalies $\overline{\Delta g}_{ij}^{t}$. Since this estimator does not allow for any gaps or overlapping duplicate data input, one has to select for each 5 arc-minute cell on the ellipsoid, the most accurate anomaly estimate out of multiple data that may be available for that cell (e.g., marine and altimetry-derived values). Rapp and Pavlis (1990) discuss such kind of data selection and merging algorithm. In the development of EGM2008, a similar algorithm was used. This process resulted in a complete global grid (9331200 values) of 5 arc-minute $\overline{\Delta g}_{ij}^{t}$, which were used in the model's estimation. Table 1 summarizes the overall statistics of this merged file.

Table 1: *Statistics of the 5 Arc-Minute Area-Mean Gravity Anomalies After Editing and Downward Continuation of the Merged File Used to Develop EGM2008 Model*[a] *(Pavlis et al., 2012).*

Data Source	Percent Area	Minimum	Maximum	RMS	RMS σ
ArcGP	3.0	-192.0	281.8	30.2	3.0
Altimetry	63.2	-361.8	351.1	28.4	3.0
Terrestrial	17.6	-351.9	868.4	41.2	2.8
Fill-in	16.2	-333.0	593.5	46.8	7.6
Non Fill-in	83.8	-361.8	868.4	31.6	2.9
All (ϕ,λ)	100.0	-361.8 19.4°,293.5°	868.4 10.8°,286.3°	34.5	4.1

[a]Unit is mGal. The latitudes and longitudes listed identify the location of the extreme values in the merged file.

It is interesting to note that the areas covered with the poorest quality gravity data, the "fill-in" values, are also characterized by the "roughest" gravity anomalies, with a ±46.8 mGal RMS gravity anomaly value, compared to ±34.5 mGal, which is the global RMS value of our present data. This should come as no surprise, since the areas occupied with "fill-in" data cover some of the most mountainous areas of the Earth, like the Himalaya and the Andes. The RMS values of the error standard deviations of the data given in Table 1 represent the error estimates obtained from the LSC estimator of equation (36), before applying any error "calibration." These noise-only error estimates many times are rather optimistic. Figure 3b displays geographically the source identification of the 5 arc-minute area-mean gravity anomalies in the merged file used to develop the EGM2008 model.

Some noteworthy aspects of this merged file include the extensive use of 5 arc-minute area-mean gravity anomalies from the Arctic Gravity Project (ArcGP) (Kenyon and Forsberg, 2008), and the avoidance of use of any Topographic/Isostatic mean anomalies (Pavlis and Rapp, 1990). Over Antarctica, the 5 arc-minute area-mean gravity anomalies were synthesized purely on the basis of the ITGGRACE03S (Mayer-Gürr, 2007) model. This makes the EGM2008 model completely free of any isostatic hypothesis, at the cost of producing a smoother field over Antarctica, since ITG-GRACE03S is complete only up to degree and order 180. Over parts of Siberia, as well as over France, Poland, and Colombia, the 5 arc-minute values used in the merged file were contributed to NGA by external organizations or individuals. The "splicing" of the SS v18.1 altimetry- derived anomalies from SIO/NOAA with the DNSC07 values is also shown in Figure 3b. Over the Gulf Stream and Kuroshio areas, where the increased sea surface variability makes the altimetry-derived anomalies less reliable, we made some use of marine gravity anomalies, after their quality was verified through comparisons with other independent marine gravity data.

2.3.2.3 Solution Development and Evaluation (Pavlis et al., 2012)

During the course of the development of EGM2008, several Preliminary Gravity Models (PGM) were developed in order to test various aspects of the solution and evaluate alternative modelling and estimation approaches. The progression of the PGM developments also paralleled the availability of improved satellite-only solutions from the GRACE mission, as well as improved versions of the terrestrial and the altimetry-derived gravity anomaly data. Three of these PGM development efforts constituted significant milestones for the project and the details of these PGM are given in next section.

2.3.2.3.1 Preliminary Solutions

a) PGM2004A

PGM2004A **(Pavlis et al., 2005)** was the first gravitational model ever developed that extended to degree 2160. PGM2004A used the GGM02S GRACE-only model (Tapley et al., 2005), which

extends to degree and order 160, and whose spherical harmonic coefficients were accompanied by their error estimates. A very preliminary version of the 5 arc-minute merged gravity anomaly file supported the development of PGM2004A. Among other shortcomings, PGM2004A was developed based on gravity anomalies that had not been downward continued. Nevertheless, as discussed by Pavlis et al. (2005), comparisons with TOPEX altimeter data, astrogeodetic deflections of the vertical, geoid undulations and/or height anomalies obtained from GPS positioning and spirit leveling, demonstrated clearly that PGM2004A performed quite well.

b) PGM2006A,B and C

After the successful development of PGM2004A, the effort focused on the compilation and verification of several data including; the compilation of the DTM2006.0 global topographic database, the computation of RTM implied gravity anomalies, globally and on a regular grid, and the computation of the g_1 analytical continuation terms. In parallel, the candidate Mean Sea Surface (MSS) data sets produced at DNSC were continuously evaluated. An updated global 5 arc-minute merged gravity anomaly file was compiled, where fill-in anomalies computed were incorprated. The estimation of the gravity anomalies within this file employed a refined LSC prediction approach near the coastlines, where the available land, marine, and altimetry-derived gravity data were combined. Using this global 5 arc-minute gravity anomaly file and the available g_1 analytical continuation terms, two combination solutions were created (Pavlis et al., 2006a): PGM2006A, where the gravity anomalies were not downward continued, and, PGM2006B, where the gravity anomalies were downward continued.

The solutions PGM2006A and B were evaluated, using various independent data (Pavlis et al., 2006a), as was also done with PGM2004A. It was reassuring to see that both 2006 solutions were performing considerably better than the 2004 solution, and furthermore that PGM2006B was outperforming PGM2006A.

With the help of the fifth version of the MSS model provided by DNSC, designated DNSC06E (O. B. Andersen, personal communication, 2006) and building upon the experience with PGM2006A, and B, the PGM2006C solution was developed paying special attention to the DOT that it implied. Over land areas, the differences between PGM2006B and PGM2006C are marginal.

c) PGM2007A and B

The development of PGM2007A and B constitutes the first of the two iterations of the general estimation approach discussed in section 2.3.2.1. The computation of these two solutions incorporated all the essential elements of the estimation approach.

In May 2007, the DNSC provided the eighth version of their MSS, which was designated DNSC07C (O. B. Andersen, personal communication, 2007). This version of the DNSC MSS had addressed several problems associated with the previous versions. The DNSC07C MSS was evaluated and found that it could be used to develop a preliminary DOT model. This DOT model,

along with the PGM, would form the reference models necessary for the re-iteration of the estimation of the altimetry-derived gravity anomalies.
In preparation for the PGM2007A and B solutions, an updated set of 5 arc-minute area-mean gravity anomalies was formed. This set used the PGM2006B solution as the reference model in the LSC estimation algorithm, in place of the EGM96 solution (Lemoine et al., 1998) that had been used in all previous gravity anomaly estimations. Over the areas occupied by proprietary data, the spectral content of the 5 arc-minute area-mean gravity anomalies from ellipsoidal harmonic degree 721 and up to degree 2159 was supplemented by the spectral information extracted from the RTM-implied gravity anomalies, as discussed in section 2.3.2.3 (E).

Evaluation of PGM2007A

By the end of October 2007, several members of the IAG/IGFS SWG, availed 19 reports from the evaluation of PGM2007A. The majority of these reports involved comparisons with locally available gravity anomaly data and with geoid undulations or height anomalies from GPS positioning and levelling data, as well as comparisons with local and regional high resolution geoid models. *Minkang Cheng* (Univ. of Texas, Center for Space Research – UT/CSR) reported orbit fit comparison results, using satellites tracked by Satellite Laser Ranging (SLR). These comparisons are particularly sensitive to long wavelength errors in the gravitational model. However, after the inclusion in combination solutions of the highly accurate long wavelength gravitational information from GRACE, acceptable results from these comparisons constitute a necessary but not sufficient condition for the long wavelength accuracy of the model.

After a careful study of the reports provided by the Special Working Group (SWG) including the results from the evaluation of PGM2007A an effort was made to address any comments indicating that the performance of the model could be improved, at least over those areas where data necessary to address such comments was readily available. Two specific cases where the information received from the SWG proved beneficial to the development of the final model involve the report received from *Jonas Ågren* (Swedish mapping, cadastre and registry authority) for the evaluation of PGM2007A over Sweden, and the report from *Heiner Denker* (Institut für Erdmessung, Hannover, Germany) who evaluated PGM2007A over Eurasia. The former indicated that some of the gravity anomaly data from the Arctic Gravity Project over Scandinavia, north of the 64°N parallel, could be improved; the latter revealed some problems over Eurasia, the most severe of which involved the data over Turkey. The data was carefully re-examined over these problematic areas and corrected these problems in the next, and final, re-iteration of the LSC estimation of gravity anomalies, which produced the data used in the final EGM2008 model.

2.3.2.3.2 Final EGM2008 Solution

In late October 2007, the ITGGRACE03S GRACE-only model was acquired (Mayer-Gürr, 2007), complete to degree and order 180, along with its complete error covariance matrix. By early February 2008, all the "ingredients" necessary for the development of the final model EGM2008 were available, including the latest 5 arc-minute area-mean terrestrial gravity anomalies obtained from the last re-iteration of our LSC estimation algorithm and the two sets of altimetry-derived gravity anomalies, DNSC07 and SS v18.1, which are combined as we discussed in section 2.3.2.3. (C). This data was combined to come up with a merged 5 arc-minute area-mean global gravity anomaly file by combining the terrestrial and altimetry-derived data files. The data within this merged file was carefully examined, paying special attention to smooth out any existing discontinuities over the boundaries between data from different sources. Ellipsoidal corrections were applied to the 5 arc-minute area-mean gravity anomalies of this merged file (Pavlis, 1988; Rapp and Pavlis, 1990) and the correction associated with the use of orthometric instead of normal heights in the numerical evaluation of the Molodensky freeair gravity anomalies (Pavlis, 1998a). PGM2007B solution was used as reference to evaluate these corrections. Finally, the 5 arc-minute gravity anomalies were analytically continued downward, from the Earth's topography where they refer, to the reference ellipsoid, using method that was used in the development of the PGM2007A and B solutions.

2.3.2.3.3 Evaluation of EGM2008 Using Independent Data

The residual gravity anomalies and the error spectra associated with a combination solution represent internal consistency indicators of the quality of a solution. Comparisons with data independent from the solution offer a verification and validation capability, necessary to assess the actual performance of a model. A single, global set of independent data with the spectral sensitivity and accuracy necessary to test the entire spectral bandwidth of the model and its complete global coverage does not exist. Even if it did, it would probably have been used for the estimation of a solution in the first place, thus eliminating its independence from the model being tested. Therefore, one is forced to use independent data of different spectral sensitivities and/or geographic extent, in an effort to evaluate a solution based on tests of complimentary spectral and/or geographic character (Pavlis et al., 1999).

A. Orbit Fit Tests

Table 2 shows the average RMS residual from 3-day orbit fits, spanning the year 2003, for six SLR-tracked spacecraft. The fits were performed without, as well as with, the adjustment of one cycle-per-revolution (1-cpr) empirical accelerations (Colombo, 1986, 1989), and are reported for EGM96 (Lemoine et al., 1998), GGM02C (Tapley et al., 2005), and the EGM2008 solution. The models that include GRACE information, GGM02C and EGM2008, show practically the same

performance in these tests, and an improvement over the pre-GRACE EGM96 solution. Additional details about these orbit fit tests are given by Cheng et al. (2009).

Table 2: *Average Laser Ranging Residual RMS From One Year (2003) of 3-Day Orbit Fits Without and With One Cycle-Per-Revolution (1-cpr) Empirical Accelerations Being Adjusted*[a] (Pavlis et al., 2012).

Satellite	EGM96		GGM02C		EGM2008	
	No 1-cpr	**1-cpr**	**No 1-cpr**	**1-cpr**	**No 1-cpr**	**1-cpr**
LAGEOS-1	1.5	1.05	1.5	0.96	1.5	0.97
LAGEOS-2	1.3	0.96	1.3	0.84	1.4	0.85
Ajisai	5.9	5.6	5.2	4.8	5.3	4.4
Starlette	5.1	3.7	3.5	1.8	4.8	1.8
Stella	9.0	6.5	3.1	2.2	3.0	1.6
BE-C	11.1	9.1	9.1	7.6	9.4	7.6

[a] Unit is cm.

Satisfactory results from the orbit fit tests shown in Table 2 represent a necessary but not sufficient condition for the quality of any GRACE-based model. The results from these tests are very similar for any GRACE-based model, due to the limited spectral sensitivity of these tests, in conjunction with the very high accuracy of the long wavelength gravitational information provided by the GRACE data (Cheng et al., 2009).

B. Comparisons With GPS/Levelling Data

A global database of GPS/Levelling (GPS/L) data has been maintained over years, generously contributed by various colleagues. These data remain independent from any of the existing gravitational models. Currently, the “thinned” version of the database contains a total of 12387 points, distributed over 52 countries or territories. The thinning of the points, which is applied after careful inspection of the geographic distribution of the original GPS/L data within each of the data sources, aims to avoid clusters of points located extremely close to each other. The thinning algorithm considers only the geographic location of the data, and does not discard any points based on comparisons with any gravitational model. The global distribution of the GPS/L stations is uneven, with the majority of the data located over *North America*, *Europe* and *Australia*, and considerably fewer points over *South America*, *Asia* and *Africa*. 4201 of our thinned data were located over Conterminous U.S. area (CONUS). These data originated from an update of the file documented by Milbert (1998) and were made available by the National Geodetic Survey in 1999. Within the database, some of the GPS/L data sources provide geoid undulations (N), while others provide height anomalies (ζ). This is accounted for in the comparisons, using Rapp’s (1997) formulation and the spherical harmonic coefficients from the analysis of the DTM2006.0 database in order to compute the height anomaly to geoid undulation conversion terms, to a spherical harmonic degree commensurate to the maximum degree of the model being tested.

Table 3 presents the results from GPS/Levelling data comparisons, using the entire compliment of the globally distributed sets of points. It includes the statistics of the differences between the GPS/L undulations and those from EGM96 (Lemoine et al., 1998) to degree 360, GGM02C (Tapley et al., 2005) up to degree 200 augmented with EGM96 from degree 201 to 360, EIGEN-GL04C (Förste et al.,2008) to degree 360, as well as EGM2008 to degree 360 and EGM2008 to degree 2190. The truncated to degree 360 version of EGM2008 outperforms its contemporary solutions GGM02C and EIGEN-GL04C. Using EGM2008 to its maximum degree 2190, results in $\pm$13.0 cm weighted standard deviation after removing a bias per data set, and $\pm$10.3 cm after removing a linear trend per data set. These results indicate that EGM2008 may have reached or even surpassed the $\pm$15 cm global RMS geoid undulation commission error goal set by NGA at the beginning of the project. Of course, we should note here that the distribution of GPS/Leveling data is confined to land areas only, and over these areas is certainly not uniform. In most cases, high quality GPS/Leveling data exist over the same areas covered with high quality gravity data.

The increased accuracy and resolution of EGM2008 as compared to other models, mandates special attention to the fact that the geoid undulations or height anomalies obtained from the GPS/Levelling data are not error free.

Table 3: *GPS/Levelling Comparisons Globally* (Pavlis et al., 2012).

Model (Nmax)	Bias Removed	Linear Trend Removed
	Weighted Standard Deviation (cm)	**Weighted Standard Deviation (cm)**
EGM96 (360)	30.3	27.0
GGM02C_EGM96 (360)	25.6	23.2
EIGEN-GLO4C (360)	26.2	23.5
EGM2008 (360)	23.0	20.9
EGM2008 (2190)	13.0	10.3

C. Comparisons With Astrogeodetic Deflections of the Vertical

Astrogeodetic deflections of the vertical are particularly useful for the evaluation of the high degree part of a gravitational model. Two sets of such independent data were available for evaluation. One consists of 3561 pairs of meridional and prime-vertical deflections (ξ, η) distributed over CONUS. This set is also discussed by Jekeli (1999). The other set consists of 1080 (ξ, η) pairs, scattered over Australia (W. E. Featherstone, personal communication, 2006). Using the specific procedures discussed in detail by Jekeli (1999), the independent astrogeodetic (ξ, η) data in these two sets

were compared to the corresponding gravimetric values computed by various models. The RMS differences ($\Delta\xi$, $\Delta\eta$) are shown in Table 4

Table 4: *RMS Differences Between Astrogeodetic and Gravimetric Deflections of the Vertical Over CONUS and Australia*[a] (Pavlis et al., 2012).

Model (Nmax)	CONUS 3561 Stations		Australia 1080 Stations	
	$\Delta\xi$	$\Delta\eta$	$\Delta\xi$	$\Delta\eta$
EGM96 (360)	2.80	3.22	1.91	2.23
GGM02C_EGM96 (360)	2.80	3.22	1.89	2.22
EIGEN-GLO4C (360)	2.81	3.20	1.92	2.23
EGM2008 (2190)	1.12	1.16	1.19	1.29
DEFLEC99 (1' ⟶ 10800)	0.91	0.92	-	-
AUSGeoid (2' ⟶ 5400)	-	-	1.31	1.37

[a]Unit is arc-second.

The results are practically equivalent for all models extending to degree 360. A significant reduction of the RMS differences by approximately a factor of three occurs when EGM2008 is extended to degree 2190. Up to that degree, the performance of EGM2008 is marginally inferior to that of the detailed DEFLEC99 model that has a 1 arc-minute resolution, and marginally superior to the performance of the 2 arc-minute resolution AUSGeoid98 model.

D. Comparisons With TOPEX Altimeter Data

Over a set of reference locations on the 10-day repeat ground track of the TOPEX/Poseidon altimeter satellite, temporally averaged values of the Sea Surface Heights (SSH) were formed, sampled at the rate of one-per-second, by "stacking" altimeter data over the 6-year period from 1993 to 1998. This mean track contains 517835 1 Hz SSH values. Over these locations the residual SSH was computed as:

$$\mathrm{rSSH} = \mathrm{SSH} - \mathrm{NMod} - \zeta\mathrm{Mod} \qquad (37)$$

Where N_{Mod} is the geoid undulation implied by a gravitational model and ζ_{Mod} is the Dynamic Ocean Topography implied by a DOT model. The DOT2007A model complete to degree and order 50, was used in all the comparisons whose results are summarized in Table 5. Also 494350 along-track residual SSH slope values were formed, by differencing consecutive residual SSH values and dividing these differences by the distance of the sub-satellite points. To avoid data gaps, no slopes were formed if the consecutive sub-satellite points were further than 8 km apart from each other. A 200m depth threshold was also applied, in order to avoid shallow water areas where tidal corrections may be less accurate. Inland and enclosed seas, such as the Caspian, Mediterranean, Black and Red Seas, and the Hudson Bay were excluded from this comparison.

Table 5: *Comparisons With TOPEX Altimeter Data From a Six-Year Mean Track Containing 517835 1 Hz SSH and 494350 Along-Track SSH Slopes* (Pavlis et al., 2012).

Model (Nmax)	Residual SSH (cm)		Residual Along-Track Slope (arc-second)	
	Max Absolute Value	Standard Deviation	Max Absolute Value	Standard Deviation
EGM96 (360)	334	20.0	30.0	1.96
GGM02C_EGM96 (360)	300	18.2	29.3	1.96
EIGEN-GLO4C (360)	288	19.2	29.7	1.98
EGM2008 (360)	307	16.0	28.5	1.90
EGM2008 (2190)	121	5.2	7.6	0.30

Table 5 shows the maximum absolute residual SSH and residual SSH slope, as well as the standard deviation of these quantities, for the same global models as those compared in the GPS/L tests. Up to degree 360, the EGM2008 solution clearly outperforms its contemporary models GGM02C and EIGEN-GL04C, both in terms of the residual SSH and the residual SSH slope comparisons. Expanding the EGM2008 solution to its maximum degree yields an improvement by a factor of approximately three in the standard deviation of *rSSH*, and a factor of 6.3 in the standard deviation of *rSSH* slopes, compared to its truncated to degree 360 version.

E. Dynamic Ocean Topography Comparisons

The DNSC08B MSS provided in 1, 2, and 5 arc-minute versions by DNSC was used to compare the DOT implied by EGM2008 and by its contemporary GRACE-based gravitational models GGM02C (Tapley et al., 2005) and EIGENGL04C (Förste et al., 2008). For this test, three sets of residual SSH were created by subtracting area-mean values of height anomalies computed from the three gravitational models over 2 arc-minute cells, from the 2 arc-minute version of the DNSC08B MSS. As before, GGM02C was augmented with the EGM96 coefficients from degree 201 to 360, and EIGEN-GL04C was used to degree 360. The height anomalies from all three models in the "Mean Tide" system were computed, to be consistent with the permanent tide system in which the DNSC08B MSS is expressed. The 2 arc-minute residual SSH values over 6 arc-minute and over 1° equiangular cells were averaged, without applying any other smoothing or filtering. These residual SSH represent also "direct" estimates of the DOT. Apart from the DOT signal, they are composed of errors present in the MSS, as well as errors of commission and of omission associated with each gravitational model used to define the geoid. The accuracy and resolution of the GRACE-based geoid information is the primary factor affecting the accuracy and resolution of the DOT that can be extracted from these residual SSH. The three DOT estimates obtained in this fashion are shown in Figure 4.

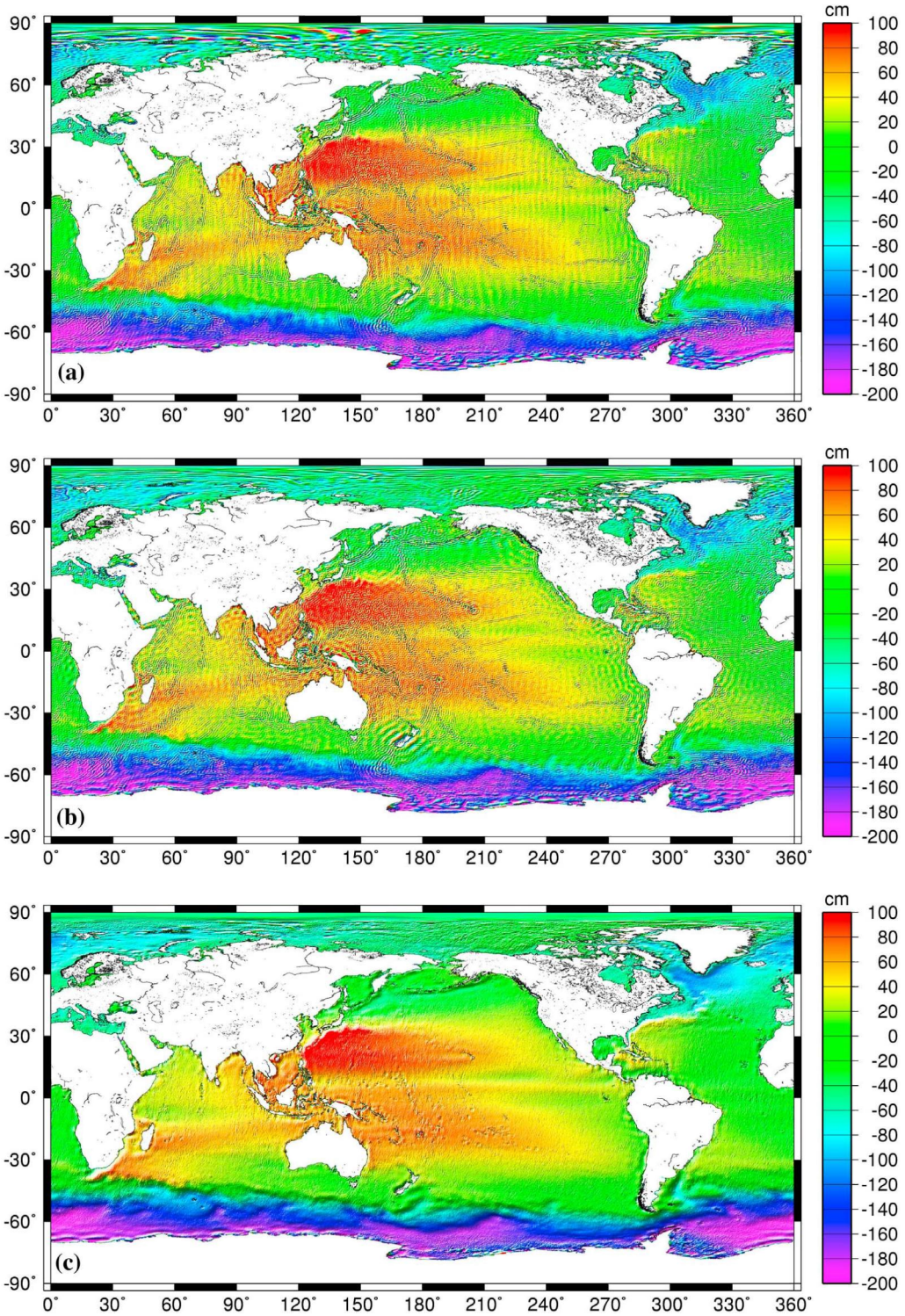

Figure 4: *Dynamic Ocean Topography (DOT) estimates averaged over 6 arc-minute equiangular cells, obtained by subtracting model-implied height anomalies from the DNSC08B Mean Sea Surface (MSS) model. (a) Using GGM02C to degree 200, augmented with EGM96 from degree 201 to 360. (b) Using EIGEN-GL04C to degree 360. (c) Using EGM2008 to degree 2190.*

Unit is cm (Pavlis et al., 2012).

The omission error associated with the two models that extend to degree 360 is visible in Figure 4, especially over trenches and sea mount chains, where these models fail to capture the large variations of the geoid, which are also present in the 6 arc-minute averages of the MSS. The DOT estimate based on GGM02C shows significant stripe artifacts. These are less pronounced in the estimate that is based on EIGEN-GL04C, which produces though some “ringing” artefacts that are most evident around the coast of New Zealand. The EGM2008 estimate of the DOT is largely free of the artefacts and shortcomings of the estimates based on the other two models. Over the 4247328 6 arc-minute cells displayed in Figure 4, the standard deviation of the residual SSH is $\pm$66.60 cm based on GGM02C, $\pm$66.58 cm based on EIGEN-GL04C, and $\pm$63.97 cm based on EGM2008.

The evaluation of EGM2008 performed by its developers as well as by the IAG/IGFS SWG both indicate that the model’s performance in orbit fits is comparable to any other GRACE-based solution. Over areas covered with high quality gravity data (e.g., USA, Europe, Australia), the discrepancies between geoid undulations computed from EGM2008 and those computed from independent GPS/ Leveling data are on the order of $\pm$5 to $\pm$10 cm. These results are comparable to, and in several cases better than, corresponding results obtained using regional detailed geoid models. Deflections of the vertical, derived from EGM2008 over USA and Australia are within $\pm$1.1 to $\pm$1.3 arc-seconds from corresponding values obtained from independent astronomical and geodetic observations. Compared to its predecessor, EGM96, the EGM2008 solution represents an improvement in resolution by a factor of six, and yields improvements in gravity modeling accuracy ranging from a factor of three to a factor of six, depending on the gravitational functional and the geographic area in question.

The EGM2008 solution is accompanied by a set of global 5 arc-minute grids that provide geographically specific estimates of its commission error, over the entire bandwidth of the model, in commonly used gravimetric quantities, such as gravity anomalies, height anomalies, and deflections of the vertical, being mindful, especially in the case of the deflections, of the significant but unaccounted omission error. This allows the model user to assign appropriate error estimates to the model’s quantities, without the need to propagate error covariance matrices of prohibitively large dimension. This represents a significant improvement over EGM96, whose geographically specific error estimates could be computed only up to degree and order 70.

The EGM2008 solution is accompanied by a Dynamic Ocean Topography model designated DOT2008A. This was developed based on the DNSC08B Mean Sea Surface and the EGM2008 geoid. DOT2008A is available in the form of spherical harmonic coefficients complete to degree and order 180, as well as in grid form.

Although the development of EGM2008 was the catalyst for the systematic re-evaluation of the gravity anomaly data involved in its development, significant margin for improvement remains in this area. This involves data that may be misidentified, e.g., with respect to terrain corrections, as we found the case to be in Turkey. Also, considerable effort is still required toward the acquisition of accurate gravity information over several areas of the Earth. Of these, Antarctica's landmass and surrounding coastal areas remain the least surveyed, and therefore most poorly modelled areas of the Earth's gravity field.

2.4 GLOBAL NAVIGATION SATELLITE SYSTEM

GNSS implies several existing satellite based positioning systems like GPS, GLONASS, Galileo and Compas.

2.4.1 Global Positioning System (Hofmann-Wellenhof et al., 2008)

The NAVSTAR Global Positioning System (GPS) is an all-weather, space-based navigation system developed by the U.S. Department of Defense (DoD) to satisfy the requirements for the military forces to accurately determine their position, velocity, and time in a common reference system, anywhere on or near the earth on a continuous basis (Wooden , 1985). Since the DoD is the initiator of GPS, the primary goals were military ones. But the US Congress, with guidance from the President, directed the DoD to promote its civil use. This was greatly accelerated by the production of a "portable" codeless GPS receiver for geodetic surveying that could measure short baselines to millimeter accuracy and long baselines to one part per million (ppm). GPS was conceived as a ranging system from known positions of satellites in space to unknown positions on land, at sea, in air and space. Effectively, the satellite signal is continually marked with its (own) transmission time so that when received the signal transit period can be measured with a synchronized receiver. The original objectives of GPS were the instantaneous determination of position and velocity (i.e., navigation), and the precise coordination of time (i.e., time transfer).

2.4.1.1 Coordinate system

The GPS terrestrial reference system is the World Geodetic System 1984 (WGS-84). This geocentric system was originally realized by the coordinates of about 1500 terrestrial sites which have been derived from Transit observations. Associated to this frame is a geocentric ellipsoid of revolution, originally defined by the four parameters: semi-major axis *a*, normalized second-degree zonal gravitational coefficient $\bar{C}_{2,0}$, truncated angular velocity of the earth ω_e, and earth's gravitational constant *μ*. This frame has been used for GPS since 1987. The gravitational coefficient $\bar{C}_{2,0}$ can be expressed by the flattening parameter *f* , which is defined by the semi-axes of the ellipsoid: f = (a - b)/a.

The comparison of the original WGS-84 and the international terrestrial reference frame (ITRF) revealed remarkable differences (Malys and Slater 1994):

1. The WGS-84 was established through Doppler observations from the Transit satellite system, while ITRF is based on SLR and VLBI observations. The accuracy of the Transit reference stations was estimated to be in the range of 1 to 2 meters, while the accuracy of the ITRF reference stations is at the centimeter level.

2. The numerical values for the original defining parameters differ from those in the ITRF. The only significant difference, however, was in the earth's gravitational constant $d\mu = \mu WGS - \mu ITRF = 0.582 * 10^8\ m^3\ s^{-2}$, which resulted in measurable differences in the satellite orbits.

Based on this information, the former Defense Mapping Agency (DMA) has proposed to replace the μ-value in the WGS-84 by the standard International Earth Rotation Service (IERS) value and to refine the coordinates of the GPS tracking stations. The revised WGS-84, valid since 1994, was given the designation WGS-84 (G730), where the number 730 denotes the GPS week number when DMA implemented the refined system (Bock 1996).

In 1996, the National Imagery and Mapping Agency (NIMA), the successor of DMA, implemented a revised version of the frame denoted as WGS-84 (G873). The frame is realized by monitor stations with refined coordinates. The associated ellipsoid is now defined by the four parameters which are slightly different from the respective ITRF values. The refined WGS-84 (G1150) frame was introduced in 2002. With respect to ITRF2005, the current WGS-84 frame shows unsignificant systematic differences in the order of 1 cm. Hence, both frames are virtually identical. Parameters of the WGS-84 ellipsoid are as follows: a = 6 378 137.0 m, f = 1/298.257 223 563, ω_e, = 7 292 $115 * 10^{-11}$ rad s^{-1} and μ = 3 986 004.418$*10^8$ m^3 s^{-2} (Merrigan et al., 2002).

2.4.1.2 Time System

The system time of GPS is related to the atomic time system and is referenced to coordinated universal time (UTC) as maintained by the US Naval Observatory (USNO). Nominally the GPS time has a constant offset of 19 seconds with TAI, the international atomic time, and was coincident with UTC at the GPS standard epoch January 6.d 0, 1980. TAI = GPS time + 19.000s
TAI and UTC differ by an integer number n of seconds. In January 2007, the integer value was n = 33 and, thus, GPS time is exactly 14 seconds ahead of UTC.

Starting at the GPS standard epoch, the system time of GPS is counted in terms of GPS weeks and seconds within the current week. GPS can be calculated using the relation;

WEEK = INT [(JD - 2 444 244.5)/7], where JD indicates the Julian Date and INT is an integer operator.

2.4.1.3 GPS signal structure

Each GPS satellite transmits a microwave radio signal composed of two carrier frequencies (or sine waves) modulated by two digital codes and a navigation message. The two carrier frequencies are generated at 1,575.42 MHz (referred to as the L1 carrier) and 1,227.60 MHz (referred to as the L2 carrier). The corresponding carrier wavelengths are approximately 19 cm and 24.4 cm, respectively, which result from the relation between the carrier frequency and the speed of light in space. All of the GPS satellites transmit the same L1 and L2 carrier frequencies. The code modulation, however, is different for each satellite, which significantly minimizes the signal interference. The two GPS codes are called coarse acquisition (or C/A-code) and precision (or P-code). Each code consists of a stream of binary digits, zeros and ones, known as bits or chips. The codes are commonly known as PRN codes because they look like random signals (i.e., they are noise-like signals). But in reality, the codes are generated using a mathematical algorithm. Presently, the C/A-code is modulated onto the L1 carrier only, while the P-code is modulated onto both the L1 and the L2 carriers. The chipping rate of the C/A-code is 1.023 Mbps and 10.23 Mbps for P-code.

The GPS navigation message is a data stream added to both the L1 and the L2 carriers as binary bi-phase modulation at a low rate of 50 kbps. It consists of 25 frames of 1,500 bits each, or 37,500 bits in total. This means that the transmission of the complete navigation message takes 750 seconds, or 12.5 minutes. The navigation message contains, along with other information, the coordinates of the GPS satellites as a function of time, the satellite health status, the satellite clock correction, the satellite almanac, and atmospheric data. Each satellite transmits its own navigation message with information on the other satellites, such as the approximate locationand health status.

2.4.1.4 Positioning Using GPS

If the distances from a point on the Earth (a GPS receiver) to three GPS satellites are known along with the satellite locations, then the location of the point (or receiver) can be determined by simply applying the well-known concept of resection. Each GPS satellite continuously transmits a microwave radio signal composed of two carriers, two codes, and a navigation message. When a GPS receiver is switched on, it will pick up the GPS signal through the receiver antenna. Once the receiver acquires the GPS signal, it will process it using its built-in software. The partial outcome of the signal processing consists of the distances to the GPS satellites through the digital codes (known as the pseudoranges) and the satellite coordinates through the navigation message.

Theoretically, only three distances to three simultaneously tracked satellites are needed. In this case, the receiver would be located at the intersection of three spheres; each has a radius of one receiver-satellite distance and is centered on that particular satellite. From the practical point of view, however, a fourth satellite is needed to account for the receiver clock offset.

2.4.1.5 Global Positioning System Services

For point positioning and timing, GPS provides two levels of service: the standard positioning service (SPS) with access for civilian users and the precise positioning service (PPS) with access for authorized users. The SPS is controlled by the JPO by applying selective availability and anti-spoofing to deny the full system accuracy to non-military users. GPS information services provide GPS status information, orbital and other data to the civilian users and the user may benefit from these different GPS information services.

2.4.1.6 Global Positioning System Errors and Biases

GPS pseudorange and carrier-phase measurements are both affected by several types of random errors and biases (systematic errors). These errors may be classified as those originating at the satellites, those originating at the receiver, and those that are due to signal propagation (atmospheric refraction).

The errors originating at the satellites include ephemeris, or orbital errors, satellite clock errors, and the effect of selective availability. The latter was intentionally implemented by the U.S. DoD to degrade the autonomous GPS accuracy for security reasons. It was, however, terminated at midnight (eastern daylight time) on May 1, 2000. The errors originating at the receiver include receiver clock errors, multipath error, receiver noise, and antenna phase center variations. The signal propagation errors include the delays of the GPS signal as it passes through the ionospheric and tropospheric layers of the atmosphere. In fact, it is only in a vacuum (free space) that the GPS signal travels, or propagates, at the speed of light. In addition to the effect of these errors, the accuracy of the computed GPS position is also affected by the geometric locations of the GPS satellites as seen by the receiver.

Some of these errors and biases can be eliminated or reduced through appropriate combinations of the GPS observables. For example, combining L1 and L2 observables removes, to a high degree of accuracy, the effect of the ionosphere. Mathematical modelling of these errors and biases is also possible. In this section we discuss the main GPS error sources and the ways of treating.

a) GPS ephemeris errors

Satellite positions as a function of time, which are included in the broadcast satellite navigation message, are predicted from previous GPS observations at the ground control stations. Typically, overlapping 4-hour GPS data spans are used by the operational control system to predict fresh satellite orbital elements for each 1-hour period. As might be expected, modelling the forces acting on the GPS satellites will not in general be perfect, which causes some errors in the estimated satellite positions, known as ephemeris errors. Nominally, an ephemeris error is usually in the order of 2m to 5m, and can reach up to 50m under selective availability. The range error due to the combined effect of the ephemeris and the satellite clock errors is of the order of 2.3 m. An ephemeris error for a particular satellite is identical to all GPS users worldwide. However, as different users see the same satellite at different view angles, the effect of the ephemeris error on the range measurement, and consequently on the computed position, is different. This means that combining (differencing) the measurements of two receivers simultaneously tracking a particular satellite cannot totally remove the ephemeris error. Users of short separations, however, will have an almost identical range error due to the ephemeris error, which can essentially be removed through differencing the observations.

b) Selective availability

GPS was originally designed so that real-time autonomous positioning and navigation with the civilian C/A code receivers would be less precise than military P-code receivers. Surprisingly, the obtained accuracy was almost the same from both receivers. To ensure national security, the U.S. DoD implemented the so-called selective availability (SA) on Block II GPS satellites to deny accurate real-time autonomous positioning to unauthorized users. SA was officially activated on March 25, 1990. SA introduces two types of errors; the first one, called delta error, results from dithering the satellite clock, and is common to all users worldwide. The second one, called epsilon error, is an additional slowly varying orbital error. With SA turned on, nominal horizontal and vertical errors can be up to 100m and 156m, respectively, at the 95% probability level. Using differential GPS (DGPS) would overcome the effect of the epsilon error. DGPS provides better accuracy than a standalone P-code receiver due to the elimination or the reduction of the common errors, including SA. Following extensive studies, the U.S. government discontinued SA on May 1, 2000, resulting in a much improved autonomous GPS accuracy. With the SA turned off, the nominal autonomous GPS horizontal and vertical accuracies would be in the order of 22m and 33m (95% of the time), respectively.

c) Satellite and receiver clock errors

Each GPS Block II and Block IIA satellite contains four atomic clocks, two cesium and two rubidium. The newer generation Block IIR satellites carry rubidium clocks only. One of the onboard clocks, primarily a cesium for Block II and IIA, is selected to provide the frequency and the timing

requirements for generating the GPS signals and the others are backups. The GPS satellite clocks, although highly accurate, are not perfect. Their stability is about 1 to 2 parts in 10 over a period of one day. This means that the satellite clock error is about 8.64 to 17.28 ns per day. The corresponding range error is 2.59 m to 5.18 m. Cesium clocks tend to behave better over a longer period of time compared with rubidium clocks. The performance of the satellite clocks is monitored by the ground control system. The amount of drift is calculated and transmitted as a part of the navigation message in the form of three coefficients of a second-degree polynomial.

Satellite clock errors cause additional errors to the GPS measurements. These errors are common to all users observing the same satellite and can be removed through differencing between the receivers. Applying the satellite clock correction in the navigation message can also correct the satellite clock errors. This, however, leaves an error of the order of several nanoseconds, which translates to a range error of a few meters (one nanosecond error is equivalent to a range error of about 30 cm).

GPS receivers, in contrast, use inexpensive crystal clocks, which are much less accurate than the satellite clocks. As such, the receiver clock error is much larger than that of the GPS satellite clock. It can, however, be removed through differencing between the satellites or it can be treated as an additional unknown parameter in the estimation process. Precise external clocks (usually cesium or rubidium) are used in some applications instead of the internal receiver clock. Although the external atomic clocks have superior performance compared with the internal receiver clocks, they cost between a few thousand dollars for the rubidium clocks to about $20,000 for the cesium clocks.

d) **Multipath error**

Multipath is a major error source for both the carrier-phase and pseudorange measurements. Multipath error occurs when the GPS signal arrives at the receiver antenna through different paths. These paths can be the direct line of sight signal and reflected signals from objects surrounding the receiver antenna. Multipath distorts the original signal through interference with the reflected signals at the GPS antenna. It affects both the carrier-phase and pseudorange measurements; however, its size is much larger in the pseudorange measurements. The size of the carrier-phase multipath can reach a maximum value of a quarter of a cycle (about 4.8 cm for the L1 carrier phase). The pseudorange multipath can theoretically reach several tens of meters for the C/A-code measurements. However, with new advances in receiver technology, actual pseudorange multipath is reduced dramatically. With these multipath-mitigation techniques, the pseudorange multipath error is reduced to several meters, even in a highly reflective environment.

A good general multipath model is still not available, mainly because of the variant satellite-reflector-antenna geometry. There are, however, several options to reduce the effect of multipath. The straightforward option is to select an observation site with no reflecting objects in the vicinity of the receiver antenna. Another option to reduce the effect of multipath is to use a chock ring antenna (a chock ring device is a ground plane that has several concentric metal hoops, which attenuate the reflected signals). As the GPS signal is right-handed circularly polarized while the reflected signal is left-handed, reducing the effect of multipath may also be achieved by using an antenna with a matching polarization to the GPS signal (i.e., right-handed). The disadvantage of this option, however, is that the polarization of the multipath signal becomes right-handed again if it is reflected twice.

e) **Antenna-phase-center variation**

A GPS antenna receives the incoming satellite signal and then converts its energy into an electric current, which can be handled by the GPS receiver. The point at which the GPS signal is received is called the antenna phase center. Generally, the antenna phase center does not coincide with the physical (geometrical) center of the antenna. It varies depending on the elevation and the azimuth of the GPS satellite as well as the intensity of the observed signal. As a result of this additional range error can be expected. The size of the error caused by the antenna-phase-center variation depends on the antenna type, and is typically in the order of a few centimeters. It is, however, difficult to model the antenna-phase-center variation and, therefore, care has to be taken when selecting the antenna type. For short baselines with the same types of antennas at each end, the phase center error can be canceled if the antennas are oriented in the same direction. Mixing different types of antennas or using different orientations will not cancel the error. Due to its rather small size, this error is neglected in most of the practical GPS applications.

f) Receiver measurement noise

The receiver measurement noise results from the limitations of the receiver's electronics. A good GPS system should have a minimum noise level. Generally, a GPS receiver performs a self-test when the user turns it on. However, for high-cost precise GPS systems, it might be important for the user to perform the system evaluation. Two tests can be performed for evaluating a GPS receiver (system): zero baseline and short baseline tests.

A zero baseline test is used to evaluate the receiver performance. The test involves using one antenna/preamplifier followed by a signal splitter that feeds two or more GPS receivers. Several receiver problems such as interchannel biases and cycle slips can be detected with this test. As one antenna is used, the baseline solution should be zero. In other words, any nonzero value is attributed to the receiver noise. Although the zero baseline test provides useful information on the receiver performance, it does not provide any information on the antenna/preamplifier noise. The contribution of the receiver measurement noise to the range error will depend very much on the

quality of the GPS receiver. Typical average value for range error due to the receiver measurement noise is of the order of 0.6 m.

To evaluate the actual field performance of a GPS system, it is necessary to include the antenna/preamplifier noise component. This can be done using short baselines of a few meters apart, observed on two consecutive days. In this case, the double difference residuals of one day would contain the system noise and the multipath effect. All other errors would cancel sufficiently. As the multipath signature repeats every sidereal day, differencing the double difference residuals between the two consecutive days eliminates the effect of multipath and leaves only the system noise.

g) **Ionospheric delay**

The ionosphere is a dispersive medium, which means it bends the GPS radio signal and changes its speed as it passes through the various ionospheric layers to reach a GPS receiver. Bending the GPS signal path causes a negligible range error, particularly if the satellite elevation angle is greater than 5°. It is the change in the propagation speed that causes a significant range error, and therefore should be accounted for. Due to the ionospheric effect, the receiver-satellite distance will be too short if measured by the carrier phase and too long if measured by the code, compared with the actual distance. The ionospheric delay is proportional to the number of free electrons along the GPS signal path, called the total electron content (TEC). The electron density level in the ionosphere varies with time and location. It is, however, highly correlated over relatively short distances, and therefore differencing the GPS observations between users of short separation can remove the major part of the ionospheric delay. Users with dual-frequency receivers can combine the L1 and L2 carrier-phase measurements to generate the ionosphere-free linear combination to remove the ionospheric delay.

h) **Tropospheric delay**

The tropospheric delay depends on the temperature, pressure, and humidity along the signal path through the troposphere. Signals from satellites at low elevation angles travel a longer path through the troposphere than those at higher elevation angles. Therefore, the tropospheric delay is minimized at the user's zenith and maximized near the horizon. Tropospheric delay results in values of about 2.3 m at zenith (satellite directly overhead), about 9.3 m for a 15° elevation angle, and about 20-28 m for a 5° elevation angle.

Tropospheric delay is broken into two components, dry and wet. The dry component represents about 90% of the delay and can be predicted to a high degree of accuracy using mathematical models. The wet component of the tropospheric delay depends on the water vapor along the GPS signal path. Unlike the dry component, the wet component is not easy to predict. Several mathematical models use surface meteorological measurements (atmospheric pressure,

temperature, and partial water vapor pressure) to compute the wet component. Unfortunately, however, the wet component is weakly correlated with surface meteorological data, which limits its prediction accuracy. It was found that using default meteorological data gives satisfactory results in most cases.

i) **Satellite geometry measures**

The various types of errors and biases discussed earlier directly affect the accuracy of the computed GPS position. Proper modeling of those errors and biases and/or appropriate combinations of the GPS observables will improve the positioning accuracy. However, these are not the only factors that affect the resulting GPS accuracy. The satellite geometry, which represents the geometric locations of the GPS satellites as seen by the receiver(s), plays a very important role in the total positioning accuracy. The better the satellite geometry strength, the better the obtained positioning accuracy. As such, the overall positioning accuracy of GPS is measured by the combined effect of the unmodeled measurement errors and the effect of the satellite geometry. Good satellite geometry is obtained when the satellites are spread out in the sky. In general, the more spread out the satellites are in the sky, the better the satellite geometry, and vice versa.

j) **GPS mission planning**

Even under the full constellation of 24 GPS satellites, there exist some periods of time where only four satellites are visible above a particular elevation angle, which may not be enough for some GPS works. Such a satellite visibility problem is expected more at high latitudes because of the nature of the GPS constellation. This problem may also occur in some low- or mid-latitude areas for a particular period of time. For example, in urban and forested areas, the receiver's sky window is reduced as a result of the obstruction caused by the high-rise buildings and the trees. Because the satellite geometry changes over time, the satellite visibility problem may be overcome by selecting a suitable observation time, which ensures a minimum number of visible satellites and good geometry. To help users in identifying the best observation periods, GPS manufacturers have developed mission-planning software packages, which predict the satellite visibility and geometry at any given location.

2.4.3 GLONASS (Hofmann-Wellenhof et al., 2008)

The Global Navigation Satellite System (GLONASS) is the Russian counter part to GPS and is operated by the Russian military. GLONASS differs from GPS in terms of the control segment, the space segment, and the signal structure. As defined in the GLONASS interface control document released by the Coordination Scientific Information Center (2002), the purpose of GLONASS is to provide an "unlimited number of air, marine, and any other type of users with all weather three-dimensional positioning, velocity measuring and timing anywhere in the world or near-earth space" on a continuous basis. GLONASS is operated by the Russian military forces and it is a military

system. This was the reason that almost no detailed information was publicly released. Later, this information deficit changed. In May 1988, at a meeting of the Special Committee on Future Air Navigation Systems of the International Civil Aviation Organization (ICAO), a paper with technical details of GLONASS was presented and the USSR offered the world community free use of the GLONASS navigation signals (Feairheller and Clark 2006: p. 596, Bauer 2003: p. 243). This was the first step towards opening the system to others than Russian military users. In March 1995, the government of the Russian Federation released the Decree No. 237 entitled “On executing works in use of the GLONASS global navigation satellite system for the sake of civil users”, where the Ministry of Defense of the Russian Federation, the Russian Federal Space Agency, and the Ministry of Transport of the Russian Federation “are to provide deploying of the GLONASS global navigation satellite system and the beginning of its operation with its full complement in 1995 in order to service national civil and military users and foreign civil users according to the existing commitments”.

2.4.3.1 Coordinate System

The GLONASS terrestrial reference system is denoted as PE-90 (sometimes also PZ-90). The first abbreviation derives from “parameters of the Earth 1990” and the second from its respective translation into Russian “Parametry Zemli 1990”. As specified in Roβbach (2001), originally the Soviet Geodetic System 1985 (SGS-85) was employed, which was later changed to the Soviet Geodetic System 1990 (SGS-90) based on the same definition. For the sake of completeness, Roβbach (2001) mentions that for a short period the acronym SGS was changed from Soviet Geodetic System to Special Geodetic System.

As given in Coordination Scientific Information Center (2002: Sect. 3.3.4), the reference frame as background of the PE-90 system is defined in the following way: the origin is located at the center of the earth; the Z-axis points to the conventional terrestrial pole as recommended by the International Earth Rotation Service (IERS); the X-axis results from the intersection line of the equatorial plane with the plane represented by the Greenwich meridian; the Y-axis completes a right-handed coordinate frame. Thus, the realization of the PE-90 reference frame is a geocentric system. For the realization, 26 ground stations were established from observations to a geodetic satellite, Doppler measurements, laser ranging, satellite altimetry; also electronic and laser range measurements of GLONASS and Etalon satellites are included (Boucher and Altamimi 2001). Associated to the PE-90 is a geocentric ellipsoid of revolution which is completely determined by four parameters. As defined in Coordination Scientific Information Center (2002: p. 16), the parameters of the PE-90 ellipsoid are given as a = 6 378 136 m, f = 1/298.257 839 303, ω_e = 7 292 115*10^{-11} rad s^{-1} and μ = 3 986 004.4*10^{8} m^3 s^{-2}. Comparing the WGS-84 with the PE-90, Boucher and Altamimi (2001) show that there exist many realizations of 7-parameter transformations. Some of them have almost only zero-values for the transformation parameters, e.g., Roβbach et al.

(1996) reduce the transformation to a rotation about the Z-axis. Similarly, the Radio Technical Commission for Maritime (RTCM) Services recommends in its binary format RTCM-SC 104, version 2.3, which is an internationally accepted standard for the transmission of GPS and GLONASS correction data, a rotation angle about the Z-axis of ?0.343 arcseconds.

2.4.3.1 Time System

The time system is maintained by the GLONASS central synchronizer using a set of hydrogen masers (Roβbach 2001: p. 31). The GLONASS time is closely related to the UTC but has a constant offset of three hours reflecting the difference between Moscow time and Greenwich time. This relation implies leap seconds for the GLONASS time. Apart from the constant offset, the difference between GLONASS time and UTC shall be within 1 millisecond (Coordination Scientific Information Center 2002: Sect. 3.3.3) arising from the keeping of the time scales by different clocks. The navigation message contains the information on this difference.

2.4.4 Galileo (Hofmann-Wellenhof et al., 2008)

Galileo is the European contribution to the future GNSS.

2.4.4.1 Coordinate system

Galileo relies on a geocentric Cartesian reference frame as defined by the Galileo terrestrial reference frame (GTRF). GTRF will be related to the international terrestrial reference frame (ITRF), which has been established by the International Earth Rotation Service (IERS) (Hein and Pany 2002). The GTRF is specified to differ from the latest version of ITRF by no more than 3 centimeters . This will be ensured by the Galileo geodetic service provider (GGSP).

2.4.4.2 Time system

The Galileo system time (GST) is a continuous atomic time scale with a nominal constant offset (i.e., integer number of seconds) with respect to the international atomic time (TAI). With respect to the coordinated universal time (UTC), the modulo 1 second offset is variable due to the insertion of leap seconds (cf. Sect. 2.3.2). GST will be maintained by an ensemble of atomic frequency standards (AFS), where active hydrogen maser clocks will serve as the master clock (Hahn 2005). Galileo will use the steering correction parameters provided by an external time service provider in order to steer GST towards TAI. Therefore, the external time service provider will interface to the International Bureau of Weights and Measures (BIPM), which maintains UTC time.

3.0 RESEARCH DESIGN AND METHODS

3.1 STUDY AREA AND DATA SET

3.1.1 Study Area

The study area is Uganda, located in eastern part of Africa and on the north-western shores of lake Victoria, extending from 1° South to 4° North and 30° to 35° East defining a total area of 241,139 square kilometres. Figure 5 shows the topography of Uganda.

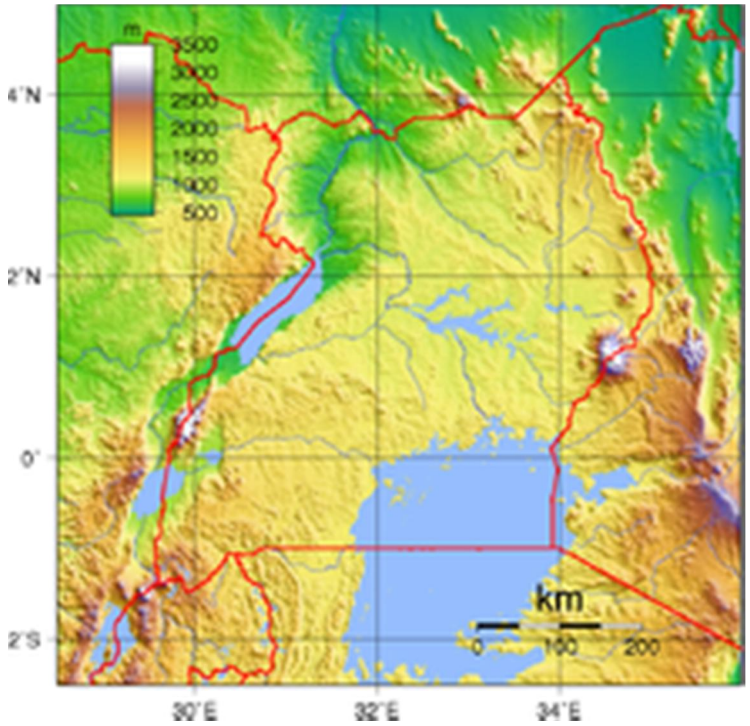

Figure 5: *T*opography of the Uganda ***(en.wikipedia.org)***

3.1.2 Data set

This study involves a network of 7 unevenly distributed fundamental benchmarks in Uganda, which were established by the Directorate of Overseas Surveys (DOS) for the Surveys and Mapping Department (SMD) in Entebbe, Uganda. These fundamental benchmarks refer to the Egyptian Benchmark BM 9029, itself related to MSL Alexandria. Figure 6 shows the distribution of the 7 benchmarks.

Figure 6: Geographical Distribution of the benchmark points in Uganda *(http://www.mapcruzin.com)*

3.1.2.1 Ellipsoidal heights

Ellipsoidal heights of the network points were determined by making GNSS static observations using dual frequency Trimble R7 GNSS and Trimble R7 receivers with respect to the IGS realisation of the ITRF 2008 reference frame. A GNSS campaign was undertaken starting 10th February to 18th February, 2012 and observations were made on the respective benchmarks for a minimum of 48 hours and a maximum of 144 hours (where we had receivers running through all the sessions) in three sessions as detailed below:

a) Session One

The network includes 4 stations namely *Jinja, Mbarara, Kasese* and *Mubende*. GNSS observations at these stations were taken for a period of 48 hours starting on 10th February to 12th February 2012.

b) Session Two

This network involves 4 stations namely *Jinja, Kiboga, Mbarara* and *Rhino Camp*. GNSS observations at these stations were taken for a period of 48 hours starting on 13th February to 15th February 2012.

c) Session Three

This network involves 4 stations namely *Jinja, Kampala, Mubende and Mbarara*. GNSS observations at these stations were taken for a period of 48 hours starting on 16th February to 18th

February 2012. Figure 7 clearly shows the network points included in each of the sessions described above.

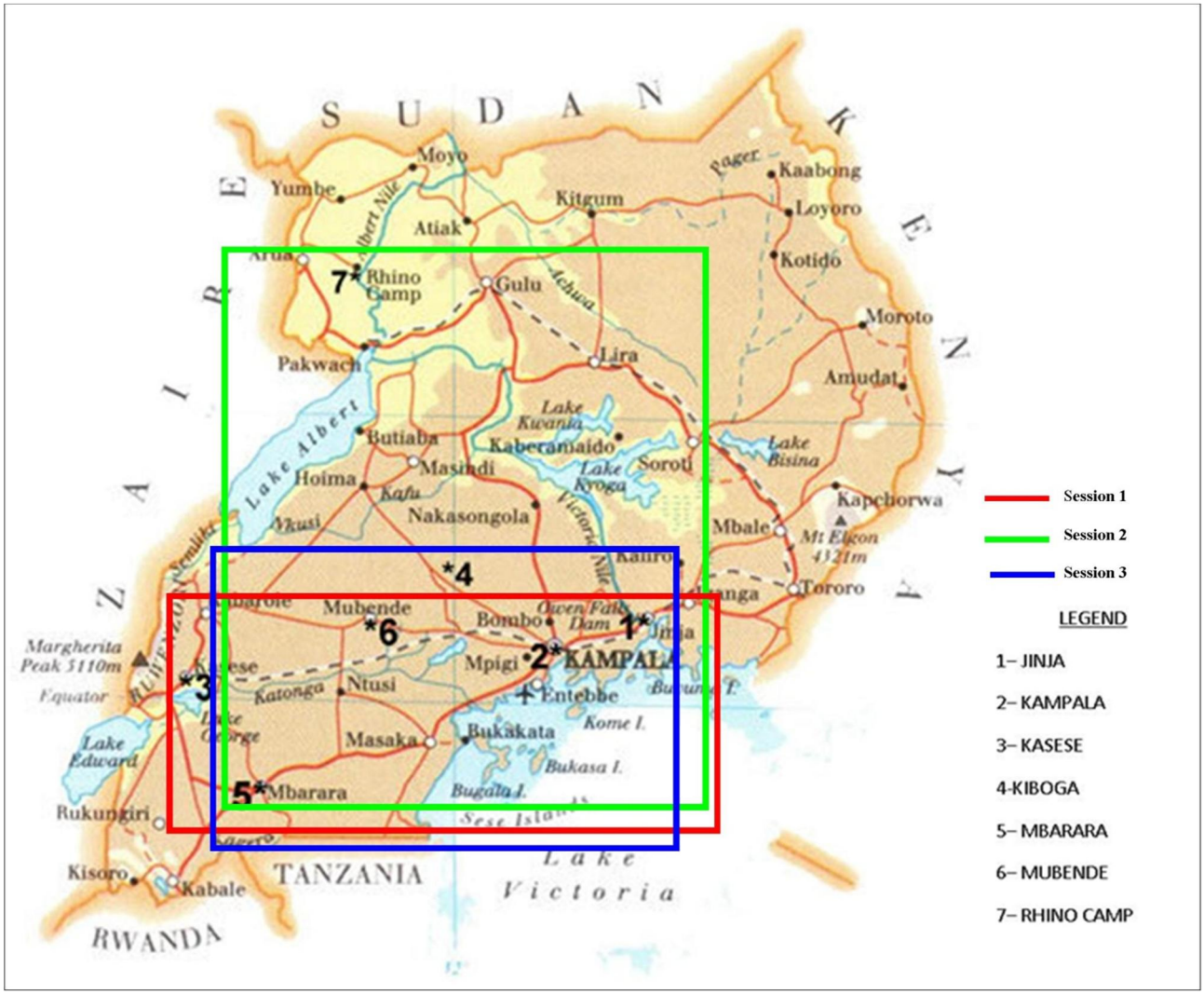

Figure 7: GPS/Levelling Network

After the field observations, the observation data was downloaded from the respective Trimble R7 GNSS in the TRIMBLE raw data format. The TRIMBLE rinex converter program was used to convert the raw data to RINEX (Receiver Independent Exchange) format and *teqc* program was used to splice the observation files for the receivers where observation data was saved in different files after every 6-12 hours and window the spliced data to produce rinex files for each respective Day of Year (DOY) for easy processing using the GAMIT GPS processing software.

3.1.2.2 Levelled Heights

The results of the precise leveling were obtained from the Surveys and Mapping Department in Entebbe together with their description cards which are attached in appendix A.

The levelled heights of the fundamental benchmarks in Uganda refer to the MSL at Alexandria.

Before the second world war, the Directorate of Overseas Surveys carried out precise differential levelling from the Kenyan coast to Uganda. As the reference sea level for this exercise was the Mombasa tide gauge, the datum was called MSL Mombasa. Another differential levelling came into Uganda all the way from Egypt (Alexandria) through Sudan. The reference sea level was obtained from the harbour of Alexandria, and new calculations for the altitude of all the benchmarks were carried out, in the so-called **New Khartoum datum** (the fundamental point of which is given at 363.082 meters above MSL at Alexandria) and consequently tied to the New MSL Alexandria datum. A block adjustment was carried out by the Survey Department using observation equation method, producing values referring to M.S.L. Alexandria with a standard error of 0.00115 foot [0.00035 m] per unit weight. The first order network was completed by 1970, but the second order network was done only in some limited areas of the country and around Lake Kyoga, before the start of the political turmoil. The difference between the new datum and the old one was calculated as -0.055 foot [0.01676 m] (MSL Mombassa is 0.01676 m lower than MSL Alexandria at the Khartoum gauge). Thus the altitudes in Uganda are based on only one connection to the Egyptian Benchmark BM 9029, itself related to MSL Alexandria.

4.0 RESULTS AND ANALYSIS

4.1 GPS PROCESSING

The Receiver INdependent EXhange (Rinex) data for each of the benchmark stations was processed using **GAMIT/GLOBK** software based on the realisation of the ITRF 2008 reference frame using IGS orbit product precise ephemeris. **GAMIT** is a collection of programs to process GPS phase data to estimate three-dimensional relative positions of ground stations and satellite orbits, atmospheric zenith delays, and earth orientation parameters (http://www-gpsg.mit.edu). To control processing, the software uses C-shell scripts which invoke the Fortran or C programs compiled in the respective directories. The software is designed to run under any UNIX operating system in this particular case, Ubuntu 12.04 was used. The maximum number of stations and atmospheric parameters allowed is determined by dimensions set at compile time and can be tailored to fit the requirements and capabilities of the analyst's computational environment.

GLOBK is a Kalman filter whose primary purpose is to combine various geodetic solutions such as GPS, VLBI, and SLR experiments. It accepts as data, or "quasi-observations" the estimates and covariance matrices for station coordinates, earth-orientation parameters, orbital parameters, and source positions generated from the analysis of the primary observations (http://www-gpsg.mit.edu). GLOBK was used to combine the individual sessions (days) of observations to obtain an estimate of station coordinates averaged over a 3-6 day experiment.

Using GAMIT the coordinates for each of the benchmark points on the respective days were computed to mm accuracy both in the North, East and Up (NEU) components with reference to WGS84 reference ellipsoid. All the coordinates were computed relative to three IGS network stations in; Addis Ababa (ADIS), South Africa (HARB) and GABON (NKLG). The stations were chosen based on proximity to the local network stations and stability based on the velocity solutions as presented in ITRF08. **GLOBK** was used to compute the average of the solutions obtained using GAMIT as well as plot the residuals in the NEU computed coordinates. These NEU residual plots showing the details of the normalised root mean square error (NRMS) as well as the weighted root mean square error (WRMS) are attached in ***appendix C*** and the extracted information is presented in Table 7.

Table 6 shows the computed geodetic coordinates (latitude, longitude and ellipsoidal height) of the benchmarks.

Table 6: *Geodetic coordinates for the benchmark points and their levelled heights*

Station	Latitude (DMS)	Longitude (DMS)	Ellipsoidal Height (m)	Levelled Height (m)
JINJA	0 25 08.69758	33 12 00.39103	1162.498	1176.064
71Y97 (Kampala)	0 20 17.73450	32 33 53.31548	1255.314	1267.942
KASESE	0 10 46.06511	30 04 37.67715	980.896	990.380
KIBOGA	0 54 52.41815	31 46 09.67010	1174.464	1187.649
MBARARA	-0 36 33.68073	30 39 12.62674	1448.208	1459.021
MUBENDE	0 33 43.59150	31 23 24.85620	1311.438	1324.002
RHINO CAMP	2 58 17.78812	31 23 43.05879	617.809	631.387

Table 7 presents the root mean square errors of the NEU coordinates extracted from the NEU residual plots after running GLOBK.

Table 7: *Root Mean Square Error of the Computed coordinates*

Station	Northings (mm)		Eastings (mm)		Up (mm)	
	NRMS	**WRMS**	**NRMS**	**WRMS**	**NRMS**	**WRMS**
JINJA	0.74	3.1	0.58	3.4	0.33	7.3
KAMPALA	0.73	2.4	0.10	0.4	0.22	3.2
KASESE	0.28	1.7	0.03	0.3	0.12	4.3
KIBOGA	0.41	1.3	0.07	0.3	0.40	5.6
MBARARA	1.02	2.6	0.60	1.8	0.41	4.1
MUBENDE	0.10	0.7	0.69	4.0	0.35	9.4
RHINO CAMP	0.10	0.3	0.47	1.6	0.84	9.5

4.2 EVALUATION PROCEDURE

4.2.1 GPS-based geiod heights

The geoid heights at the 7 points were computed according to equation (38) based on the computed ellipsoidal and known levelled heights.

$$N^{GPS/lev} = h - H \tag{38}$$

Where $N^{GPS/lev}$ is the geoid height determined by GPS/levelling. $N^{GPS/lev}$ provides the dataset upon which the evaluation tests are performed.

4.2.2 EGM2008-based geiod heights

The Synthesis FORTRAN program, Tg_Schmidt.f95 together with the coefficients of EGM2008 global gravity model adjusted to Schmidt semi-normalisation, was used to compute the anomalous

potential and gravity disturbance on a regular grid of latitude and longitude covering the whole region of Uganda and at nine levels with a vertical spacing of 500m on and above the ellipsoid. The Tg_Schmidt.f program was initially written by Dr Roger Hipkin in 1972 with updates added over the past 40 years. This programme uses basic formulae for the space domain spherical harmonic representations of the earth's potential or gravity. Using the interpolation and height comparison FORTRAN program, Tg_interp.f, together with the binary files output by Tg_Schmidt.f, values of the geoid height and thence orthometric height *H* are obtained at each of the surveyed stations.

With values of gravity disturbance and anomalous potential at equally-spaced levels on and above the ellipsoid given by Tg_Schmidt, the ellipsoidal heights *h* provided by GPS allows these quantities to be estimated both on the ellipsoid and on the ground surface, and continuously at all points in between. The latter can then give an average value for gravity disturbance between the ellipsoid and the ground surface. Normal gravity and the reference potential can be evaluated similarly using standard formulae. The combination of the gravity disturbance and normal gravity gives 'free-air gravity', *g**, that is subterranean gravity that ignores the attraction of the topographic masses but is analytically continuous with the external gravity field and the information used to construct EGM2008.

If we neglect the term in the square of anomalous gravity, the integrals relating distance and force to potential energy become;

$$\overline{g}^{*}\, h \;=\; \int_{h=0}^{h=h} g^{*}(h)dh \;=\; W(h) \;-\; W(0) \tag{39}$$

$$\overline{g}^{*}\, H \;=\; \int_{h=N}^{h=h} g^{*}(h)dh \;=\; W(h) \;-\; W(N) \tag{40}$$

Thus

$$h \;=\; H \;+\; \frac{W(0)-W(N)}{\overline{g}^{*}} \tag{41}$$

Note that $W(0)$ is the real Earth potential *on the ellipsoid* (h = 0), whereas W_o=62636854.19 m^2s^{-2} is the real Earth potential *at mean sea (Dayoub et al)*

An expansion of the real Earth potential at a small height Δh above the ellipsoid gives

$$W(\Delta h) \;=\; W(0) \;+\; \frac{\partial W(0)}{\partial h}\,\Delta h \;+\; \cdots \tag{42}$$

so, putting $\Delta h = N$,

$$\frac{W(0)-W(N)}{\overline{g}^*} \approx \frac{-\frac{\partial W(0)}{\partial h}N}{\overline{g}^*} \approx N \quad (43)$$

from which

$$h = H + N \quad (44)$$

The expression duplicates a classical result but does not indicate how *N* can be calculated from a program that calculates *T*.

$$N = \frac{W(0)-W(N)}{\overline{g}^*} = \frac{U(0)+T(0)-W(N)}{\overline{g}^*} = \frac{U_o - W_o + T(0)}{\overline{g}^*} \quad (45)$$

Thus *N*, the height of the levelling datum, essentially involves the value of the *anomalous potential on the ellipsoid* with a correction for difference in datum potentials.

The results of the two FORTRAN codes are presented in Table 8.Table 8 presents the geoid height values using two evaluation procedures described above and the geoid height differences. The geoid heights obtained from the FORTRAN program refers to the GRS80 reference system.

Table 8: *Geoid heights and Geoid height differences*

Station	$N^{EGM2008}$ (m)	$N^{GPS/lev}$ (m)	$N^{EGM2008}$ (m) - $N^{GPS/lev}$
JINJA	-14.269	-13.566	-0.703
71Y97 (Kampala)	-13.324	-12.628	-0.696
KASESE	-10.461	-9.484	-0.977
KIBOGA	-13.760	-13.185	-0.575
MBARARA	-11.854	-10.813	-1.041
MUBENDE	-13.237	-12.564	-0.673
RHINO CAMP	-14.930	-13.578	-1.352

Geoid heights obtained through a combination of GPS/levelling heights at the 7 GPS/levelling stations were compared against their respective values synthesized from EGM2008. Table 9 presents the validation results.

Table 9: *Statistics of the Geoid height differences*

Minimum (m)	Maximum (m)	Mean (m)	Standard Deviation (m)
-0.575	-1.352	-0.860	0.255

There exist biases (datum offset) of about 86 cm between the GPS-levelling derived geoid heights and the geoid heights determined using the gravity model EGM2008. The standard deviation of

0.255 m gives a measure of the level of agreement between the geoid (Mean Sea Level) and GPS-levelling.

The mean value may represent the difference between Uo (potential on the surface of the reference ellipsoid) in this case GRS80 used in the Tg_Schmidt.f95 Synthesis program and Wo (potential at MSL). Using the same method of analysis in Ethiopia, that is using Tg_Schmidt.f95 synthesis program and Tg_interp.f95 interpolation program taking GRS80 as the reference ellipsoid and Wo = Uo, the mean is -0.978 m and standard deviation is 0.039 m. Ruling out computational differences since the same methods of analysis were used in Uganda and Ethiopia, the difference in the standard deviations could be due to the quality of the gravity data input during the development of EGM2008. In Ethiopia, there is a complete and uniform coverage of high quality internally consistent airborne gravity compared to sparser, irregularly-distributed and inhomogenous gravity data for Uganda (see the Land Gravity Data Map in appendix B) according to the International Gravity Bureau.

The datum offset is more interesting. Note that the datum offset includes computational effects such as the choice of Wo and Uo; using GRS80 for the gravitational reference system and WGS84 for the geometrical reference system; some possibly different tidal conventions but, by using the same programme for Ethiopia and Uganda, these absolute offset effects are eliminated when comparing the two so that the computed *difference* [0.118 $\pm$ 0.255 m] in datum offset for the two states does tell you something about the differences in levelling datums. Because of the 25 cm uncertainty, the result is a rather imprecise way of connecting the levelling datums of the two countries but may still be better than nothing.

5.0 CONCLUSION AND RECOMMENDATIONS

Conclusion

The average standard deviation of the EGM2008 computed geoid heights compared with those computed from the combination of levelled and GPS-based geodetic heights at 7 stations reached the level of 0.*255* m. This discrepancy can partially be attributed to:

I. The observation errors in levelling. Since there is very little documentation presently available at the SMD about the historical aspects of the existing levelling network, there is limited information as well about the accuracy of the levelling results. All documents pertaining to observations and calculations were drafted by the Directorate of Overseas Surveys, and are now kept at the Ordnance Surveys, in Great Britain. Therefore it is not possible to ascertain if the misfit in the geoid heights is due to errors in levelling.

II. Limited gravity data available at the time of the development of EGM2008. According to the International Gravity Bureau, there are 3642 points with gravity data obtained in 1960's distributed though out Uganda, with more points in the North Eastern Region (see the Land Gravity Data Map in appendix B). Therefore discrepancies between the geoid heights as presented in Table 8 suggest that there is a possibility of having less gravity data in the Northern part of Uganda (RHINO CAMP) and South Western part of Uganda (MBARARA) since the discrepancy in the geoid heights deviates significantly from the geoid height discrepancy of the other 5 points. This however doesn't rule out the effect of topography since rough/undulating terrain as well as thick topographic cover has an effect on the accuracy of the geoid heights computed from the gravity model.

III. GPS positioning errors since all the errors affecting GPS observations can't be completely modelled out.

It is inconclusive whether the uneven distribution of the levelling benchmarks has any contribution to the discrepancy since a check on the levelled benchmarks wasn't carried out to rule out levelling errors at the first order benchmark points, therefore the 0.255 m discrepancy is greatly attributed to the poor and sparsely distributed gravity data set in Uganda.

Comparison with other parts of Africa

The standard deviation of 0.255 m between Ugandan geoids estimated by GPS/levelling and EGM2008 compare well with results from those other parts of Africa where EGM2008 relies on surface gravimetry for short wavelength information. In order of increasingly better gravity coverage available to EGM2008, Abd-Elmotaal (2009) finds a standard deviation of 2.1 m for Egypt, where the gravity coverage is very poor. For Algeria, where hydrocarbon exploration has

resulted in better gravity coverage, Benahmed Daho (2009) finds 0.21 m, while Merry (2009) finds 0.17 m for South Africa, where there is a long history of gravimetric and geodetic studies.

Thus, the results obtained in this test have shown the capability of determining orthometric heights acceptable for geodetic applications in Uganda and elsewhere in Africa using the new gravity model EGM2008, with modification using newly available gravity data in particular airborne gravity data and detailed topographic data in regions where terrain is rough.

Recommendation

I. I recommend that an airborne gravity survey be conducted over the whole country in order to have a dataset of similar qualities with systematic and uniform coverage since the existing gravity data points are unevenly distributed (and without accurate geodetic position attached) with more points in the North Eastern region. Therefore the is need for uniform quality gravity data set with accurate geodetic position to improve EGM2008. In places where there is evidently good and uniform coverage of gravity data such as Ethiopia where an Airborne gravity survey was carried out, the geoid height can be predicted using EGM2008 with a standard deviation of 0.039 m. The recommended flight line interval is 10 - 18 km, at an altitude of approximately 1.5 Km however this is dependent on the topography, in relatively flat areas it could go down to 1 km but in mountainous or rugged terrain 1.5 Km is recommended also for safety reasons to avoid collision. The along track resolution should be in the range 0.8 – 1.2 Km but also dependent on the ground speed. A ground speed of 240 Km/hr gives a sampling rate of 1 second. The accuracy should be between 2.0 and 3.0 mgals but this is also dependent on the technology used, the higher the accuracy the better.

II. I recommend that an independent check is done to verify the levelled heights assigned to the fundamental benchmarks in Uganda since there is no proper documentation to rule out any errors in the levelled heights. Levelled heights are susceptible to errors especially when long distances are involved, in the case of Uganda the levelling network was reference to mean sea level at Alexandria which relatively long distance from Uganda.

III. EGM2008 should be modified locally, where newer or higher resolution gravity data are available in Uganda without corrupting the long wavelength information.

IV. EGM2008 should be modified locally with detailed topographic data in regions where terrain is rougher. This could add more detail to gravity information.

REFERENCES

1. Abd-Elmotaal, H., (2009). “Evaluation of EGM2008 Geopotential model for Egypt”, pp 185-199 in *Newton’s Bulletin: External quality evaluation reports of EGM2008*, International Association of Geodesy/International Gravity Field Service.
2. Aksoy, A., Franke, P., Yalın, D., Bertold, W., 1993. “A Method for Precise Height Difference Determination Based on Trigonometric Leveling”. Prof.Dr.H.Wolf Geodesy Symposium, 3-5 November 1993, İstanbul, (in Turkish).
3. Balmino, G., F. Perosanz, R. Rummel, N. Sneeuw, H. Sunkel (1999). *CHAMP, GRACE and GOCE: mission concepts and simulations*, Bolletino di Geofisica Teorica e Applicata, vol 40, n. 3-4, 555-563.
4. Banger, G., 1981. Sources of Errors of Precise Levelling , I.U. Journal of Forest Faculty, Vol.31, No: 2, Page 194-207 (in Turkish).
5. Bauer M (2003): Vermessung und Ortung mit Satelliten – GPS und andere satellitengestutzte Navigationssysteme, 5th edition. Wichmann, Karlsruhe.
6. Baykal, O., 1989. Precise levelling technique, I.T.U. Notes of lesson in Graduate school (in Turkish).
7. Becker, J. M., 1986). The Experiences with New Levelling Techniques Ml and MTL, Symposium on Height Determination and Recent Vertical Crustal Movements in Western Europe, September 15-19, Hanover, Germany.
8. Benahmed Daho, S. (2009). “Evaluation of Earth Gravity Model EGM2008” in Algeria, pp. 172-184.
9. Boucher C, Altamimi Z (2001): ITRS, PZ-90 and WGS 84: current realizations and the related transformation parameters. Journal of Geodesy, 75(11): 613–619.
10. Ceylan, A., 1988. Important Systematic Errors of Precise Levelling, MSc. Thesis, Selcuk Univ., Konya, Turkey, (in Turkish).
11. Chrzanowski, A., 1989). Implement of Trigonometric Height Traversing in Geodetic levelling of height precision, Dept. of Surveying Engineering, Unv. of New Brunswick, Technical Report No:142, Canada.
12. Chrzanowski, A., Greening, T., Kornackı, W., Second, J., Vamosı, S. and Chen, Y.Q., 1985). Applications and Limitations of Precise Trigonometric Height Traversing, Proceedings of the third International Symposium on the North American Vertical Datum. Rockville, April, 21-26, pp. 81-93
13. Colombo, O. L. (1981), Numerical methods for harmonic analysis on the sphere, Rep. 310, Dept. of Geod. Sci. and Surv., Ohio State Univ., Columbus.
14. Colombo, O. L. (1986), Ephemeris errors of GPS satellites, Bull. Geod., 60, 64–84, doi:10.1007/BF02519355.

15. Colombo, O. L. (1989), The dynamics of Global Positioning System orbits and the determination of precise ephemerides, J. Geophys. Res., 94(B7), 9167–9182, doi:10.1029/JB094iB07p09167.
16. Factor, J. K. (1998), Introduction, in The Development of the Joint NASA GSFC and the National Imagery and Mapping Agency (NIMA) Geopotential Model EGM96, NASA Tech. Publ., TP-1998-206861, sect. 2.1, p. 2-1, NASA Goddard Space Flight Cent., Washington, D. C.
17. Feairheller S, Clark R (2006): Other satellite navigation systems. In: Kaplan ED, Hegarty CJ (eds): Understanding GPS.
18. Featherstone, W.E. (2002). *Expected contributions of dedicated satellite gravity field missions to regional geoid computations*, Journal of Geospatial Engineering, vol. 4,n.1, 2-19.
19. Forsberg, R. (1984), A study of terrain reductions, density anomalies and geophysical inversion methods in gravity field modeling, Rep. 355, Dept. of Geod. Sci. and Surv., Ohio State Univ., Columbus.
20. Förste C., Schmidt R., Stubenvoll R., Flechtner F., Meyer U., König R., Neumayer H., Biancale R.,Lemoine J.-M., Bruinsma S., Loyer S., Barthelmes F. and Esselborn S., (2008a), The GeoForschungs-Zentrum Potsdam/Groupe de Recherche de Geodesie Spatiale satellite-only and combined gravity field models: EIGEN-GL04S1 and EIGEN-GL04C. Journal of Geodesy, 82: 331 – 346,doi:10.1007/s0019000701838
21. Förste C., Flechtner F., Schmidt R., Stubenvoll R., Rothacher M., Kusche J., Neumayer K.-H.,Biancale R., Lemoine J.-M., Barthelmes F., Bruinsma S., Koenig R., Meyer U. (2008b), EIGENGL05C- A new global combined high-resolution GRACE-based gravity field model of the GFZGRGS cooperation, General Assembly European Geosciences Union (Vienna, Austria 2008), Geophysical Research Abstracts, Vol. 10, Abstract No. EGU2008-A-06944, 2008
22. Gleason, D. M. (1988), Comparing ellipsoidal corrections to the transformation between the geopotential's spherical and ellipsoidal spectrums, Manuscr. Geod., 13, 114–129.
23. Hein GW, Pany T (2002): Architecture and signal design of the European satellite navigation system Galileo – status December 2002. Journal of Global Positioning Systems, 1(2): 73–84.
24. Heiskanen, W. A., and H. Moritz (1967), Physical Geodesy, W.H. Freeman, San Francisco, Calif.
25. Heister H., Lang M., Merry C. L. and Rüther H., 1999. Determination of an Orthometric Height Profile in the Okavango Delta Using GPS Levelling. Proceedings of the FIG Working Week and Survey 1999, Sun City, South Africa, TS 20, B1-B10.
26. Hofmann-Wellenhof B, Lichtenegger H, Collins J (2008): GNSS Global Navigation Satellite Systems, Springer, Wien New York

27. Holmes, S. A., and N. K. Pavlis (2007), Some aspects of harmonic analysis of data gridded on the ellipsoid, in Gravity Field of the Earth: Proceedings of the 1st International Symposium of the International Gravity Field Service (IGFS), Special Issue 18, edited by A. Kiliçoglu and R. Forsberg, pp. 151–156, Gen. Command of Mapp., Ankara, Turkey.
28. Jekeli, C. (1988), The exact transformation between ellipsoidal and spherical harmonic expansions, Manuscr. Geod., 13, 106–113.
29. Jekeli, C. (1996), Spherical harmonic analysis, aliasing, and filtering, J. Geod., 70(4), 214–223, doi:10.1007/BF00873702.
30. Jekeli, C. (1999), An analysis of vertical deflections derived from high-degree spherical harmonic models, J. Geod., 73(1), 10–22, doi:10.1007/s001900050213.
31. Kenyon, S. C., and R. Forsberg (2008), New gravity field for the Arctic, Eos Trans. AGU, 89(32), 289–290, doi:10.1029/2008EO320002.
32. Kiliçoğlu, A., Direnç, A., Simav, M., Lenk, O., Aktuğ, B., Yildiz H., (2008), Evaluation of the EGM2008 gravity model, in *External Quality Evaluation Reports of EGM2008, Newton's Bull. 4*, Int. Assoc. of Geod. and the Int. Gravity Field Serv., Toulouse, France.
33. Kotsakis C, Katsambalos K, Ampatzidis D, Gianniou M (2008). Evaluation of EGM2008 in Greece using GPS and leveling heights. IAG International Symposium on Gravity, Geoid and Earth Observation, Chania, Greece.
34. Kuntz, E., and Schmitt, G., 1986. Precise Height Determination by Simultaneous Zenith Distances, The Symposium on Height Determination and Recent Vertical Crustal Movements in Western Europe, Hanover, Germany, September 15-19
35. Lemoine, F. G., S. C. Kenyon, J. K. Factor, R.G. Trimmer, N. K. Pavlis, D. S. Chinn, C. M. Cox, S.M. Klosko, S. B. Luthcke, M. H. Torrence, Y. M. Wang, R. G. Williamson, E. C. Pavlis, R. H. Rapp and T. R. Olson, 1998. The Development of the Joint NASA GSFC and NIMA Geopotential Model EGM96, NASA/TP-1998-206861, NASA Goddard Space Flight Center, Greenbelt, Maryland, 20771USA, July 1998.
36. Malys S, Slater J (1994): Maintenance and enhancement of the World Geodetic System 1984. In: Proceedings of ION GPS-94, 7th International Technical Meeting of the Satellite Division of the Institute of Navigation, Salt Lake City, Utah, September 20–23, part 1: 17–24.
37. Mayer-Gürr, T. (2007), ITG-Grace03s: The latest GRACE gravity field solution computed in Bonn, presented at the Joint International GSTM and SPP Symposium, Potsdam, Germany, 15–17 October.
38. Mayer-Gürr, T.; Rieser, D.; Hoeck, E.; Brockmann, J.M.; Schuh, W.D.; Krasbutter, I.; Kusche, J.; Maier, A.; Krauss, S.; Hausleitner, W.; Baur, O.; Jäggi, A.; Meyer, U.; Prange, L.; Pail, R.; Fecher, T.; Gruber, Th.: The new combined satellite only model GOCO03S; International Symposium on Gravity, Geoid and Height Systems GGHS 2012, Venice, 10.10.2012

39. Merrigan MJ, Swift ER, Wong RF, Saffel JT (2002): A refinement to the World Geodetic System 1984 reference frame. In: Proceedings of ION GPS 2002, 15th International Technical Meeting of the Satellite Division of the Institute of Navigation, Portland, Oregon, September 24–27: 1519–1529.
40. Merry, C. M. (2009) “EGM2008 evaluation for Africa”, pp 200-206 in *Newton’s Bulletin: External quality evaluation reports of EGM2008*, International Association of Geodesy/International Gravity Field Service.
41. Milbert, D. G. (1998), Documentation for the GPS Benchmark Data Set of 23-July-1998, Bull. 8, pp. 29–42, IGeS, Milan, Italy.
42. Moritz, H. (1978), Least-squares collocation, Rev. Geophys., 16(3), 421–430, doi:10.1029/RG016i003p00421.
43. Moritz, H. (1980), Advanced Physical Geodesy, Herbert Wichmann, Karlsruhe, Germany.
44. Niemeier, W., 1986. Observation Techniques For Height Determination and Their Relation to Usual Height System, The Symposium on Height Determination and Recent Vertical Crustal Movements in Western Europe, Hanover, Germany, September 15-19.
45. Pail, R.; Goiginger, H.; Schuh, W.-D.; Höck, E.; Brockmann, J. M.; Fecher, T.; Gruber, T.; Mayer-Gürr, T.; Kusche, J.; Jäggi, A.; Rieser, D.: Combined satellite gravity field model GOCO01S derived from GOCE and GRACE; Geophysical Research Letters, Vol. 37, EID L20314, American Geophysical Union, ISSN 0094-8276, DOI: 10.1029/2010GL044906, 2010.
46. Pail R., Goiginger H., Schuh W.D., Höck E., Brockmann J.M., Fecher T., Mayer-Gürr T., Kusche J., Jäggi A., Rieser D., Gruber T. (2011). Combination of GOCE data with complementary gravity field information (GOCO). Proceedings of 4th International GOCE User Workshop, München, 31.03.2011
47. Pavlis, N. K. (1988), Modeling and estimation of a low degree geopotential model from terrestrial gravity data, Rep. 386, Dept. of Geod. Sci. and Surv., Ohio State Univ., Columbus.
48. Pavlis, N. K. (1998a), Observed inconsistencies between satellite-only and surface gravity-only geopotential models, in Geodesy on the Move, IAG Symposia, vol. 119, edited by R. Forsberg, M. Feissel, and R. Dietrich, pp. 144–149, Springer, Berlin.
49. Pavlis, N. K. (1998c), The block-diagonal least-squares approach, in Development and preliminary investigation, in The Development of the Joint NASA GSFC and the National Imagery and Mapping Agency (NIMA) Geopotential Model EGM96, NASA Tech. Publ., TP-1998-206861, sect. 8.2.2, pp. 8-4–8-5, NASA Goddard Space Flight Cent., Washington, D. C.

50. Pavlis, N. K., C. M. Cox, E. C. Pavlis, and F. G. Lemoine (1999), Intercomparison and evaluation of some contemporary global geopotential models, Boll. Geofis. Teor. Appl., 40(3–4), 245–254.
51. Pavlis, N. K., S. A. Holmes, S. C. Kenyon, D. Schmidt, and R. Trimmer (2005), A preliminary gravitational model to degree 2160, in Gravity, Geoid and Space Missions, IAG Symposia, vol. 129, edited by C. Jekeli, L. Bastos, and J. Fernandes, pp. 18–23, Springer, Berlin.
52. Pavlis, N. K., S. A. Holmes, S. C. Kenyon, and J. K. Factor (2006a), Towards the next EGM: Progress in model development and evaluation, paper presented at the First International Symposium of the International Gravity Field Service, Istanbul, 28 August to 1 September, 2006.
53. Pavlis, N. K., S. A. Holmes, and O. B. Andersen (2006b), Dynamic ocean topography solutions based on a new mean sea surface model and a GRACE-based geoid model, Eos Trans. AGU, 87(52), Fall Meet. Suppl., Abstract G13C-08.
54. Pavlis, N. K., S. A. Holmes, S. C. Kenyon, and J. K. Factor (2007a), Earth gravitational model to degree 2160: Status and progress, paper presented at the XXIV General Assembly of the International Union of Geodesy and Geophysics, Perugia, Italy, 2–13 July.
55. Pavlis, N. K., J. K. Factor, and S. A. Holmes (2007b), Terrain-related gravimetric quantities computed for the next EGM, in Gravity Field of the Earth: Proceedings of the 1st International Symposium of the International Gravity Field Service (IGFS), Special Issue 18, edited by A. Kiliçoglu and R. Forsberg, pp. 318–323, Gen. Command of Mapp., Ankara, Turkey.
56. Pavlis NK, Holmes SA, Kenyon SC, Factor JK (2008). An Earth Gravitational Model to Degree 2160: EGM2008, General Assembly of the European Geosciences Union, Vienna, Austria.
57. Pavlis N. K., Holmes S. A., Kenyon S. C. and Factor J. K., 2012, The Development and Evaluation of the Earth Gravitational Model 2008 (EGM2008), J. Geophys. Res. 117, DOI:201210.1029/2011JB008916.
58. Rapp, R. H., and N. K. Pavlis (1990), The development and analysis of geopotential coefficient models to spherical harmonic degree 360, J. Geophys. Res., 95(B13), 21,885–21,911, doi:10.1029/JB095iB13p21885.
59. Rapp, R.H. (1997). *Past and future developments in geopotential modeling*, in: Forsberg, R., Feissl, M. and Dietrich, R. (Eds) Geodesy on the Move, Springer, Berlin, Germany, pp. 58-78.
60. Roβbach U (2001): Positioning and navigation using the Russian satellite system GLONASS. Schriftenreihe der Universitat der Bundeswehr Munchen, vol 71.

61. Roβbach U, Habrich H, Zarraoa N (1996): Transformation parameters between PZ-90 and WGS84. In: Proceedings of ION GPS-96, 9th International Technical Meeting of the Satellite Division of the Institute of Navigation, Kansas City, Missouri, September 17–20: 279–285.
62. Rodriguez, E., C. S. Morris, J. E. Belz, E. C. Chapin, J.M. Martin, W. Daffer, and S. Hensley (2005), An assessment of the SRTM topographic products, Tech. Rep. D-31639, Jet Propul. Lab., Pasadena, Calif.
63. Rueger, J.M., and Brunner, F.K., 1982. EDM Height Traversing Versus Geodetic Levelling, The Canadian Surveyor, 36, 69-81.
64. Rummel, R., G. Balmino, J. Johnhannessen, P. Visser, P. Woodworth (2002). *Dedicated gravity filds missions –principles and aims*, Journal of Geodynamics, vol. 33, n.1-2, pp.3-20.
65. Saleh, J., and N. K. Pavlis (2003), The development and evaluation of the global digital terrain model DTM2002, in Gravity and Geoid 2002: Proceedings of the 3rd Meeting of the IGGC, edited by I. N. Tziavos, pp. 207–212, Ziti, Thessaloniki, Greece.
66. Smith, W. H. F., and D. T. Sandwell (1997), Global sea floor topography from satellite altimetry and ship depth soundings, Science, 277, 1956–1962, doi:10.1126/science.277.5334.1956.
67. Tapley B., Ries J., Bettadpur S., Chambers D., Cheng M., Condi F., Gunter B., Kang Z., Nagel P.,Pastor R., Pekker T., Poole S., and Wang F., 2005. GGM02 – An Improved Earth Gravity Field Model from GRACE, Journal of Geodesy, 79: 467–478 doi:10.1007/s00190-005-0480-z.
68. Tapley B., Ries J., Bettadpur S., Chambers D., Cheng M., Condi F., and Poole S. (2007), The GGM03 Mean Earth Gravity Model from GRACE, Eos Trans. AGU 88(52), Fall Meet. Suppl. Abstract G42A-03, 2007.
69. Uotila, U. A. (1986), Notes on Adjustment Computations: Part I, Dept. of Geod. Sci. and Surv., Ohio State Univ., Columbus.
70. Wenzel, H.G., 1998a. Ultra-high degree geopotential model GPM93E97A to degree 1800 tailored to Europe, *Report 98:4*, Finnish Geodetic Institute, Masala, 71-80.
71. Wenzel, H.G., 1998b. Ultra-high degree geopotential models GPM98A, B and C to degree 1800, paper presented to the joint meeting of the International Gravity Commission and International Geoid Commission, Trieste, http://www.gik.unikarlsruhe.de/~wenzel/gpm98abc/gpm98abc.htm [coefficients available from http://www.gik.uni-karlsruhe.de/~wenzel/geopmods.htm]
72. Werner, M. (2001), Shuttle Radar Topography Mission (SRTM): Mission overview, Frequenz, 55(3–4), 75–79, doi:10.1515/FREQ.2001.55.3-4.75.
73. Whalen, C.T., 1985. Trigonometric Motorized Levelling at the National Geodetic Survey, Proceedings of the third international symposium on the north American vertical datum. Rockville, April, 21-26, pp. 65-80.

APPENDIX A

FBMJ1

Sited by _____ Date _____ Sorts UG 33

Built by _____ Date _____ Photo 084 085 (084)

Description by _____ Date _____ A 130 B 99

BM No. Jinja FBM

Ht. 3858.479

Ht. _____

< 72 > 156

KIRINYA ROAD

NILE AVENUE

Power Pole

Telephone Pole

Power Pole

Power Pole

photo point

BOYS QUARTERS

Concrete cover over Lower mark

Upper mark

House owned by African Grocer and presently occupied by Mr Peacock

Concrete Cover

Metal Cover

Lower Mark

N

USD Misc

SURVEY FORM 55

THE REPUBLIC OF UGANDA

DEPARTMENT OF SURVEYS AND MAPPING
GEODETIC CONTROL STATION
DESCRIPTION CARD

NAME OF STATION:		STATION NUMBER: KLY 97
DISTRICT: Kampala	COUNTY:	SUB-COUNTY: Makerere University
SHEET No.	AIR PHOTO No.	

CO-ORDINATES

UTM	N 30686.197 m	E 451400.209 m	HEIGHT 1260.842 m
WGS84	X	Y	H

STATION MARKED BY: Concrete block with Iron Pin

METHOD OF FIXATION: GPS
EQUIPMENT USED: WILD GPS System 200

Diagrams of location and Beacon showing observed rays, reference marks, etc. (See other side).

BUILT BY: SG

SURVEYOR: Jimmy Kawooya

DATE: July 1993

Description of point and method of approach
(With Location Sketch Map)

From Kampala take Rambo road up to Wandegeya round-about. Turn left and drive for 1.1 km up to Full Gospel Junction. Turn right and drive along the murram road for 1.28 km. Turn right and drive straight to the top of the hill to Makerere Primary School / Water tanks.

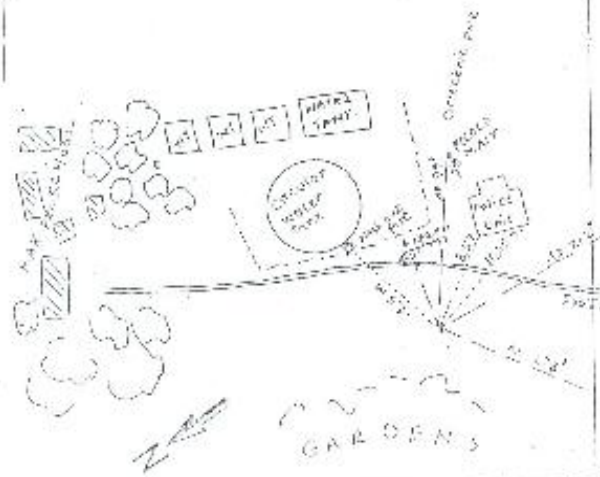

Diagram of Station Marker

Diagram of identification marks

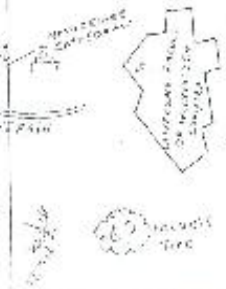

Sited by T.W. NEWMAN	Date 7 APRIL 65	Sortie NIL	BM No. F.B.M. KASESE
Built by W. ZABINIMA.	Date — —	Photo NIL	Ht. 3249·278'
Description by T.W. NEWMAN.	Date 22 APRIL 65.	A – B – C – D –	Surface Mark Ht. 3249·370'

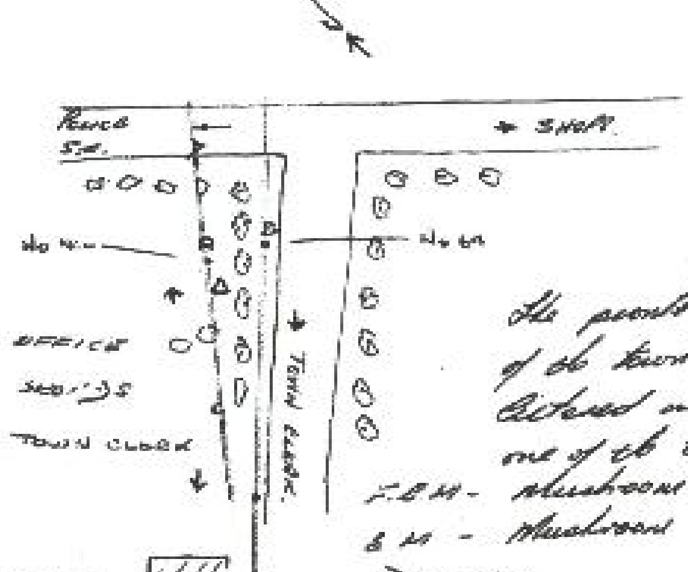

The F.B.M and surface mark are both cemented into live rock. FBM is a dolly and cement galvanised pipe with mushroom bolt as the mark. SM is a mushroom bolt cemented into the rock.

The points are situated in the eastern corner of the town offices grounds. These grounds are littered in rocks of various sizes, FBM being one of the largest.

F.B.M - Mushroom bolt in rock.
S.M - Mushroom bolt in rock.

Distance from 50/48
– 1 m approx.
Distance to 51/1
– 1 m approx.
1 Surface plate.

1:111

MEs to	FBM		SM	Distances to	F.B.M.	S.M.
A	45		97	A	6' 6"	31' 3"
B	93		101	B	42' 0"	58' 0"
C	238		387	C	—	—
Δ	37		90	Δ	69' 0"	73' 5"
SM.	301	FBM	121	SM.	17' 6"	—

Sited by	Date	Sortie	BM No. FBM F.3
Built by	Date	Photo	Ht. 3896·485'
			Surface Mark Ht. 3896·268'
Description by	Date	A B	C D

[illegible]

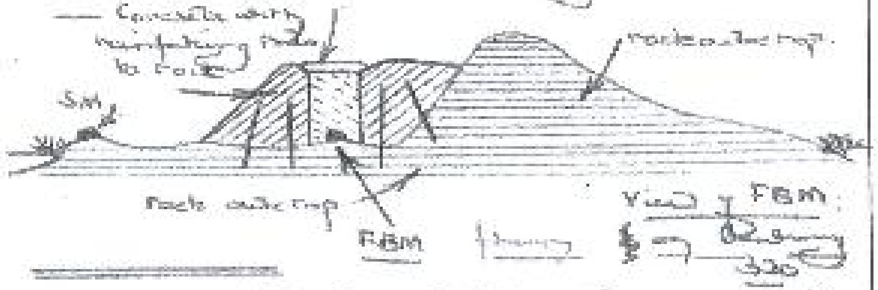

	Buried Mark bearing	Buried Mark dist	Surface Mark bearing	Surface Mark dist
BM	—	—	12°	3'9"
SM	192°	3'9"	—	—
A	336°	61'10"	337°	62'10"
B	16°	30'7"	15°	34'3"
C	91°	34'2"	89°	35'0"
Mango tree D	209°	57'4"	211°	53'9"
Top rock E	293°	20'2"	307°	21'6"
tree F	134°	33'5"	130°	31'7"

View from above

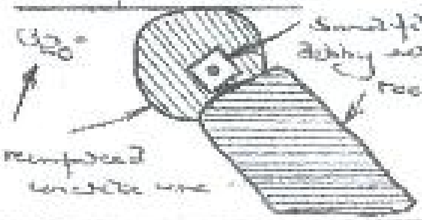

Sited by R. A. BARUA	Date 9/4/62	Sortie	BM No. F.B.M. MBARARA
Built by — " —	Date — " —	Photo	Ht. 4286·813'
			Surface Mark
Description by — " —	Date — " —	A B C D	Ht. 4285·416'

F. B. MARK MBARARA : MUSHROOM SHAPED BRASS BOLT CEMENTED INTO ROCK
BRASS BOLT AT WITNESS MARK
SITUATED ON ROCKY OUTCROP NEXT TO AGRIC OFFICERS (Phillips) HOUSE 0.25 ML from 35/40 at dist of 134' from Road
S. Pinnacle 315° 8/ 160

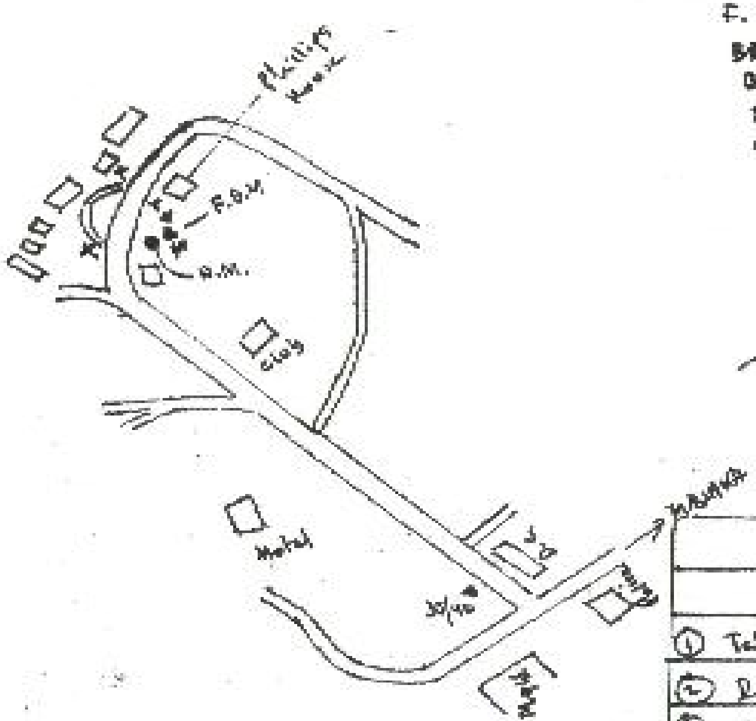

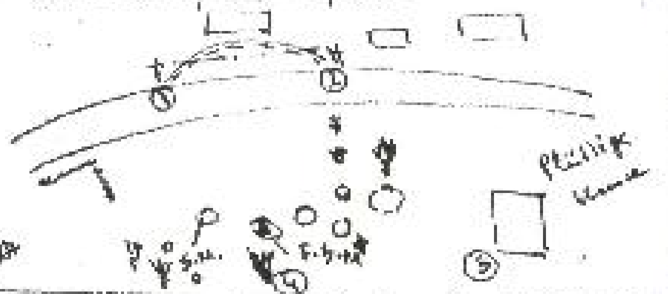

	F. B. M.		W. MARK	
	Brg	Dist	Brg	Dist
(1) Tel. Pole	280°	168'	281°	161'
(2) Double T. Pole	321°	165'	323°	163'
(3) House	64°	—	63°	—
(4) Tree	130°	31' 9"	118°	
From F.B.M.			243°	8' 6"
From S.M.	63°	8' 6"		

USD Misc 14 1000-3/62

1: New Khartoum Datum

Sited by R. G. Moffat. Date 20. Aug. 64. Sortie 31/UG/5.

Built by R. G. Moffat. Date 3. Sep. 64. Proco 047, (048).

Description by R. G. Moffat. Date 17. Apr. 65. A=137-0. B= 9:2 C = 123·2 D = 106·9 mm.

BM No. FBM, MUBENDE.
Ht. 4343·84 ft

Surface Mark
Ht. 4342·77 ft

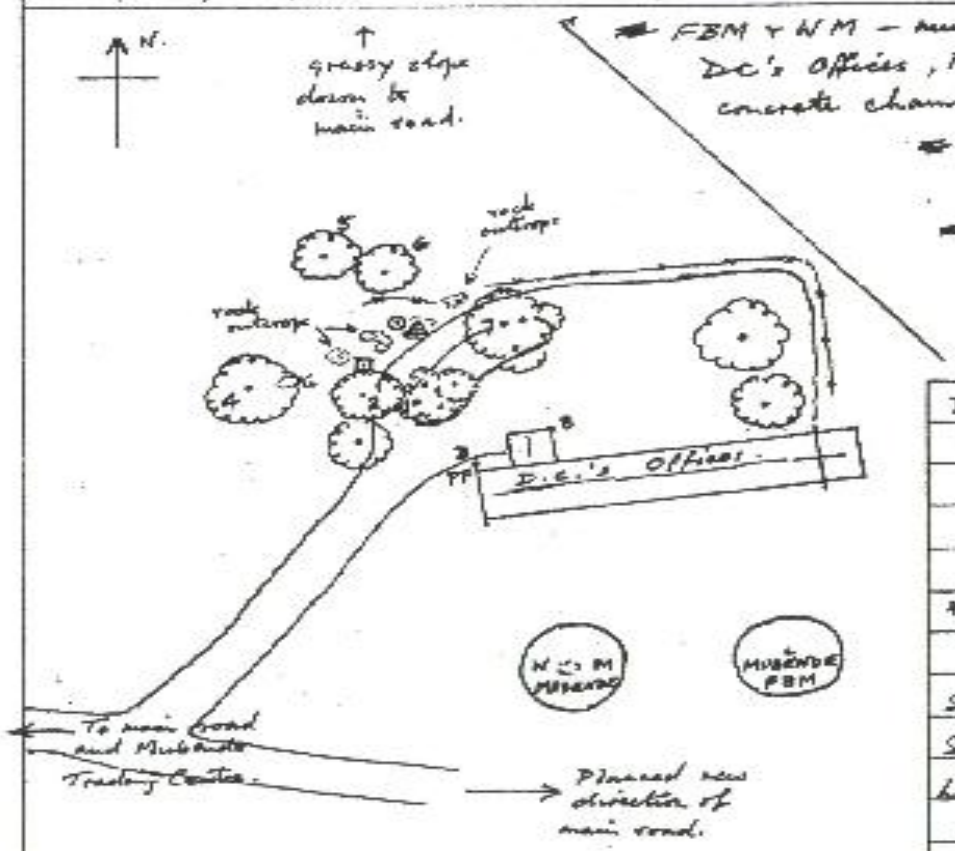

* FBM + WM – mushroom bolt in rock outside DC's Offices, Mubende. FBM surrounded by concrete chamber.

* Distances:- 40/80 · 0·65 mile.
41/1 · 0·9 "

* UTM. Co-ords:-
36N – UR – 218E – 625N.
(1:50,000 sheet 58/4).

Bearings magnetic – distances feet.						
* = P.P.		AM/FBM.		M/WM.		
	WM.	328°	26½.	–	–	
T.P.	1.	290°	7½.	31°	24·8.	
Tree.	2.	212°	37½.	180°	13¾.	
*Corner.	3.	162°	68.	139°	61½.	
Tree.	4.	247°	69.	256°	44½.	
Small tree.	5.	316°	49½.	345°	54½.	
Small tree.	6.	336°	29½.	10°	45½	
Large tree.	7.	85°	32½.	69°	56.	
Corner.	8.	134°	70.	113°	75½.	
Tree.	9.	158°	29½.	104°	34.	

OSD Misc 74 1006-360

Sited by P.S. Wadsworth Date 5th June 1968 Sortie 24/UG/3

Built by " Date " Photo 071

Described by " Date "

A 116·0 B 111·0 C 72·0 D 156·0

BM No. F.B.M. RHINO CAMP.
H: 2071·481

Surface Mark
H: 2072·408

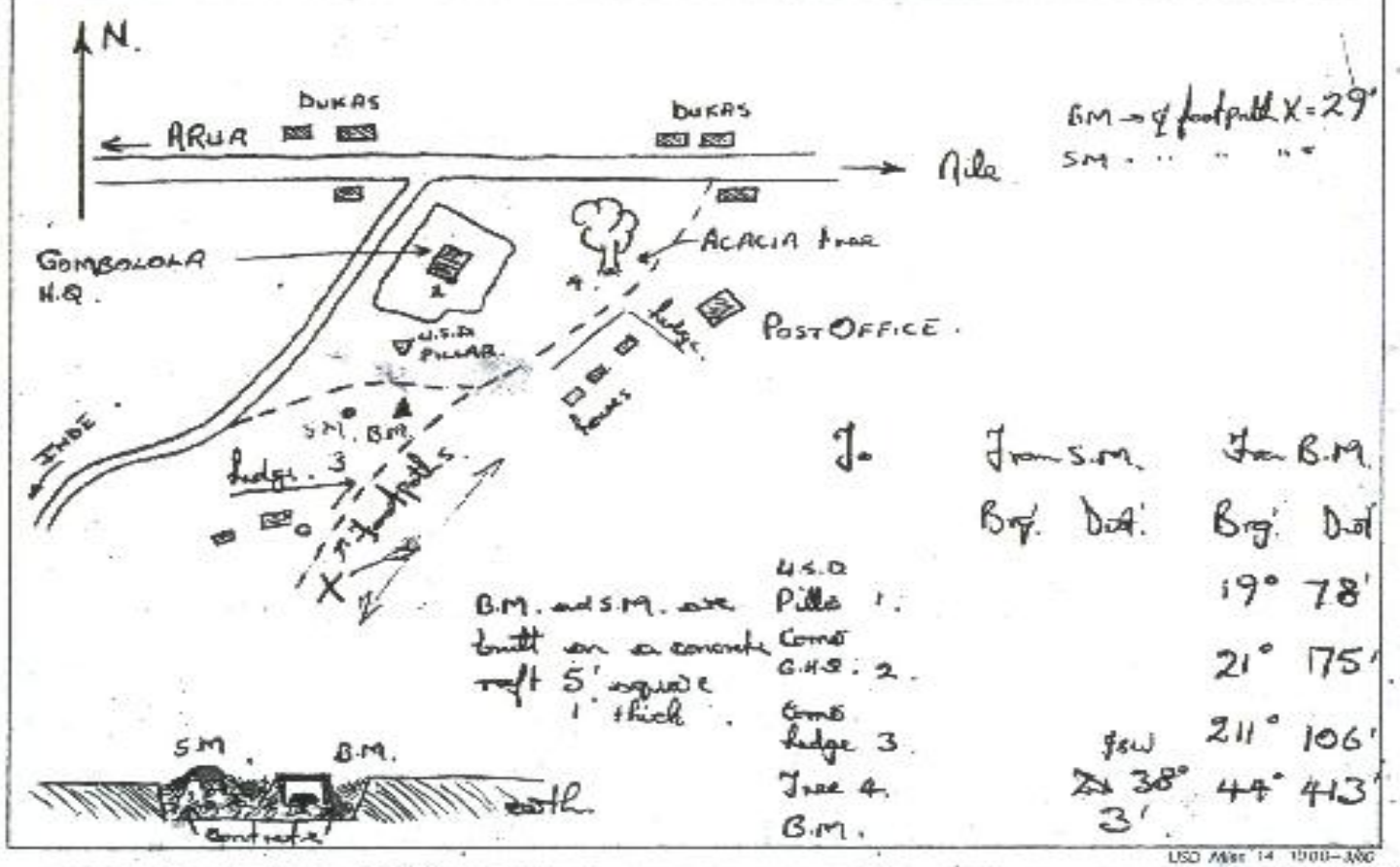

BM → ⊄ footpath X = 29°
SM " " " "

B.M. and S.M. are built on a concrete raft 5' square 1' thick.

To	From S.M. Brg.	Dist.	From B.M. Brg.	Dist.
U.S.D. Pillar 1.			19°	78'
Gomb G.H.Q. 2.			21°	175'
Gomb Ridge 3.			211°	106'
Tree 4.			38°	44° 413'
B.M.				3'

USD Misc 14 1000-3/60

APPENDIX B

Land Gravity data UGANDA (International Gravity Bureau)

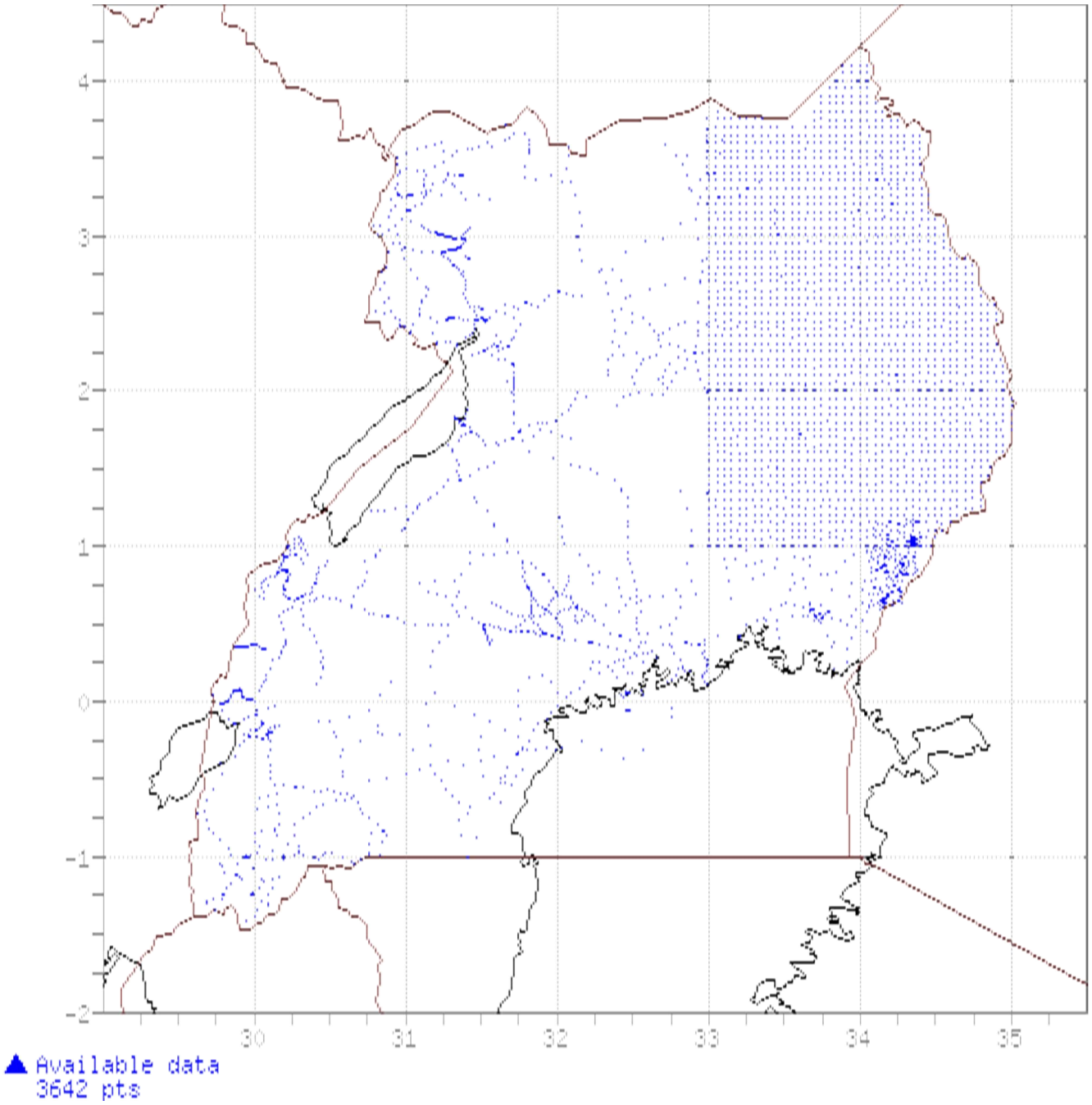

APPENDIX C

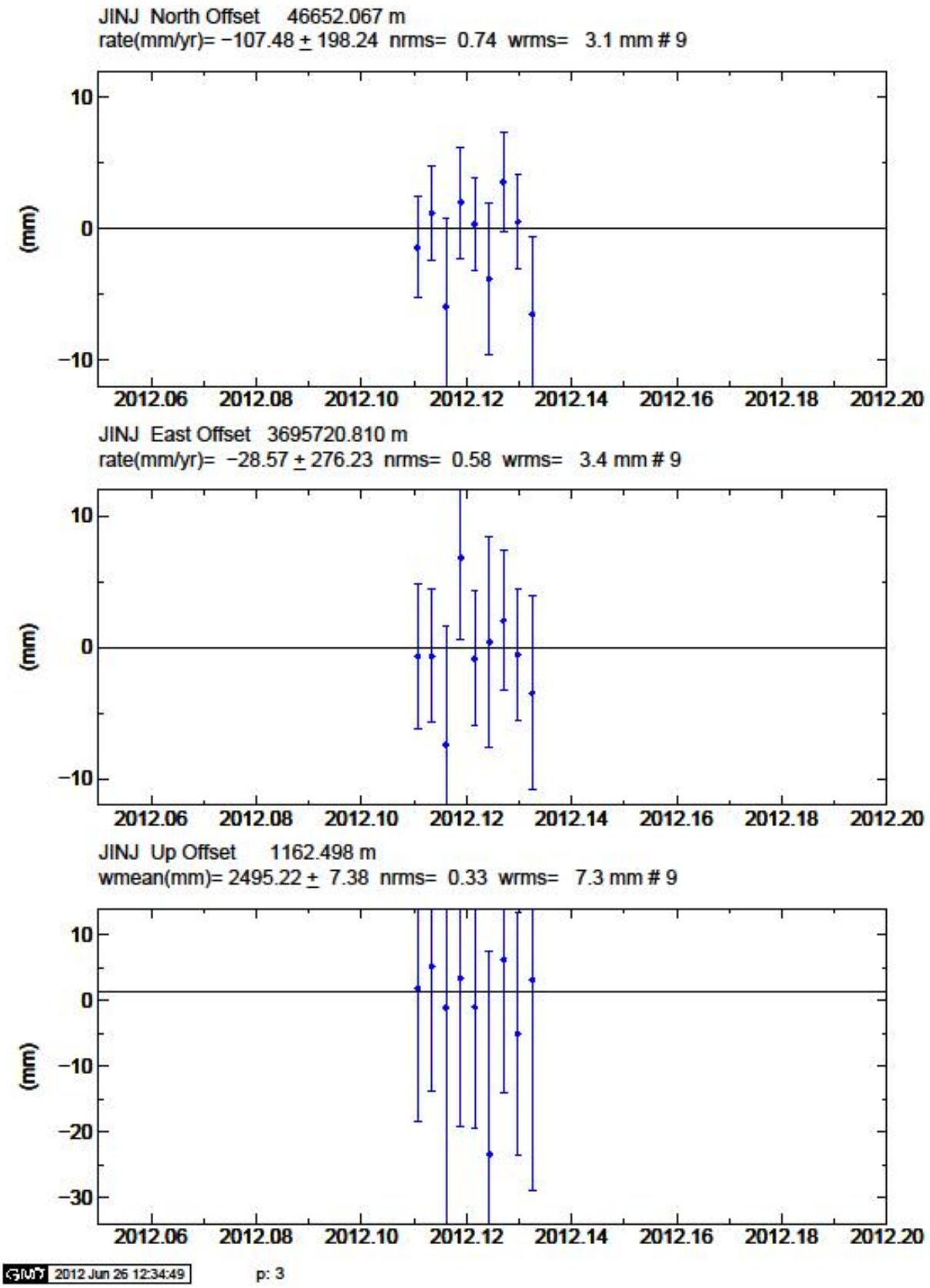
JINJ North Offset 46652.067 m
rate(mm/yr)= −107.48 ± 198.24 nrms= 0.74 wrms= 3.1 mm # 9
(mm)
10
0
−10
2012.06
2012.08
2012.10
2012.12
2012.14
2012.16
2012.18
2012.20
JINJ East Offset 3695720.810 m
rate(mm/yr)= −28.57 ± 276.23 nrms= 0.58 wrms= 3.4 mm # 9
(mm)
10
0
−10
2012.06
2012.08
2012.10
2012.12
2012.14
2012.16
2012.18
2012.20
JINJ Up Offset 1162.498 m
wmean(mm)= 2495.22 ± 7.38 nrms= 0.33 wrms= 7.3 mm # 9
(mm)
10
0
−10
−20
−30
2012.06
2012.08
2012.10
2012.12
2012.14
2012.16
2012.18
2012.20
GIMT 2012 Jun 26 12:34:49
p: 3

KAMP North Offset 37654.885 m
rate(mm/yr)= −1019.85 ± 957.90 nrms= 0.73 wrms= 2.4 mm # 3

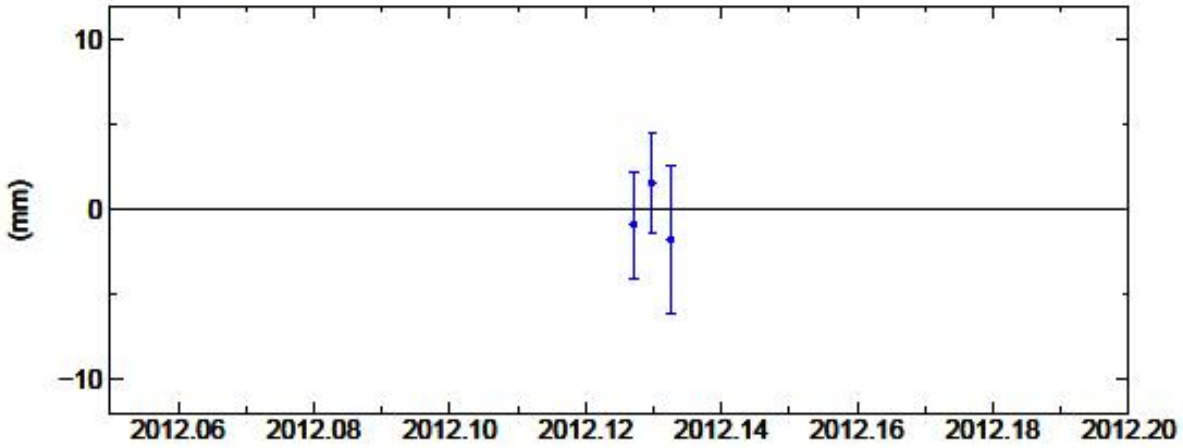

KAMP East Offset 3625035.034 m
rate(mm/yr)= 688.42 ± 1091.12 nrms= 0.10 wrms= 0.4 mm # 3

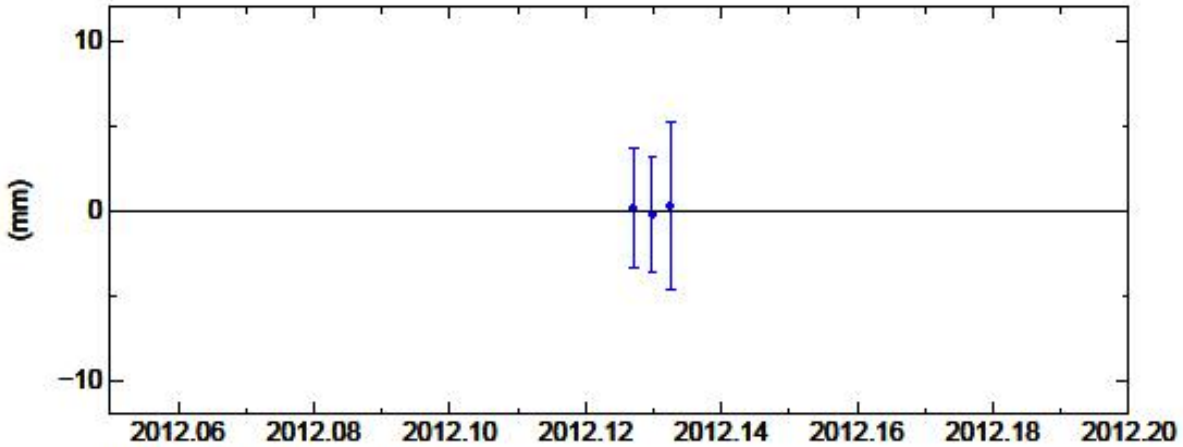

KAMP Up Offset 1255.313 m
wmean(mm)= 5313.86 ± 8.33 nrms= 0.22 wrms= 3.2 mm # 3

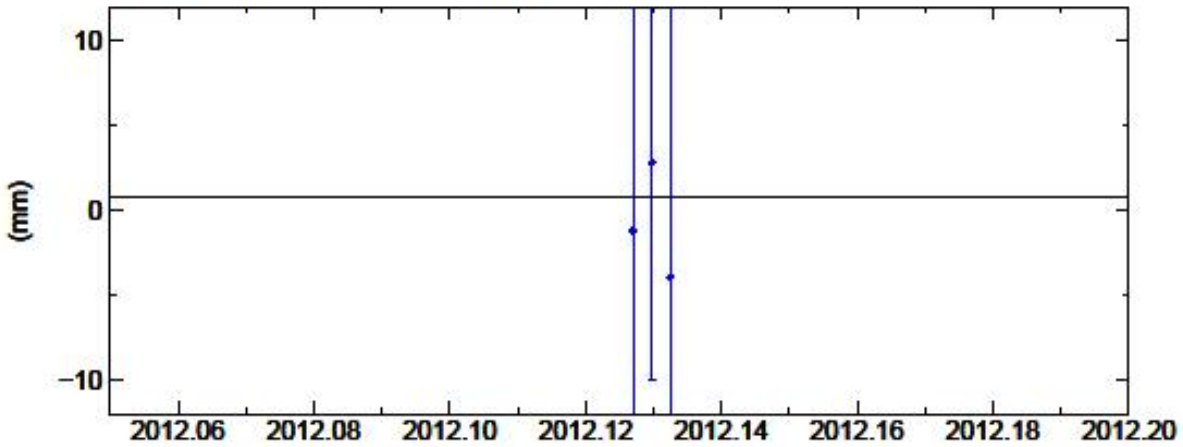

GMT 2012 Jun 25 16:51:09 p: 4

KASE North Offset 19977.677 m
rate(mm/yr)= −1.58 ± 1928.25 nrms= 0.28 wrms= 1.7 mm # 3

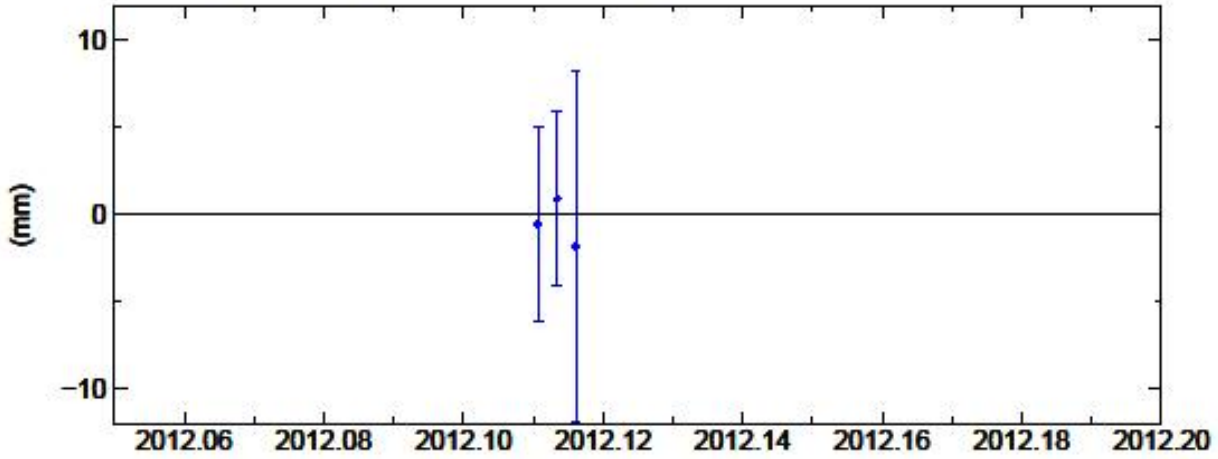

KASE East Offset 3348154.508 m
rate(mm/yr)= −486.22 ± 2361.53 nrms= 0.03 wrms= 0.3 mm # 3

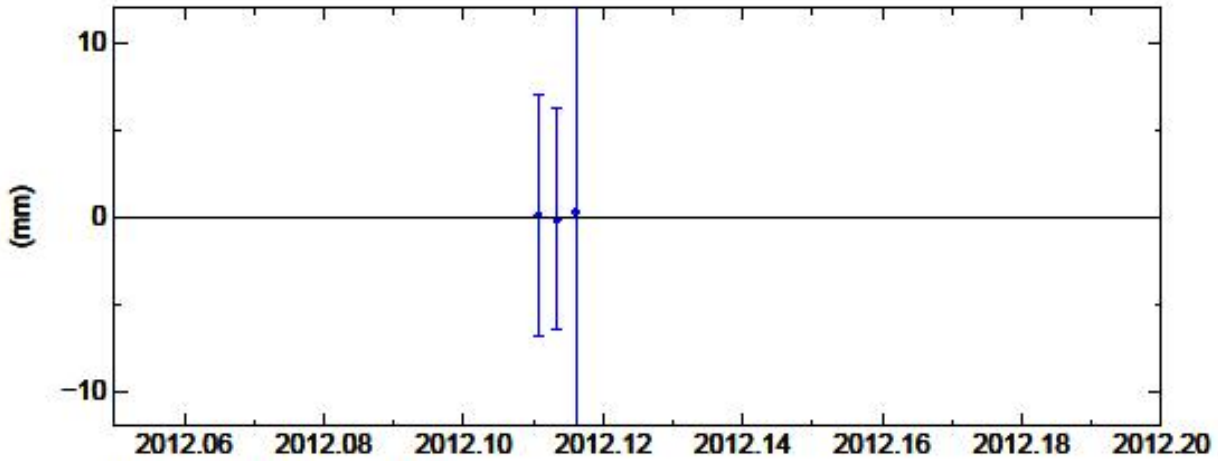

KASE Up Offset 980.897 m
wmean(mm)= 892.18 ± 19.85 nrms= 0.12 wrms= 4.3 mm # 3

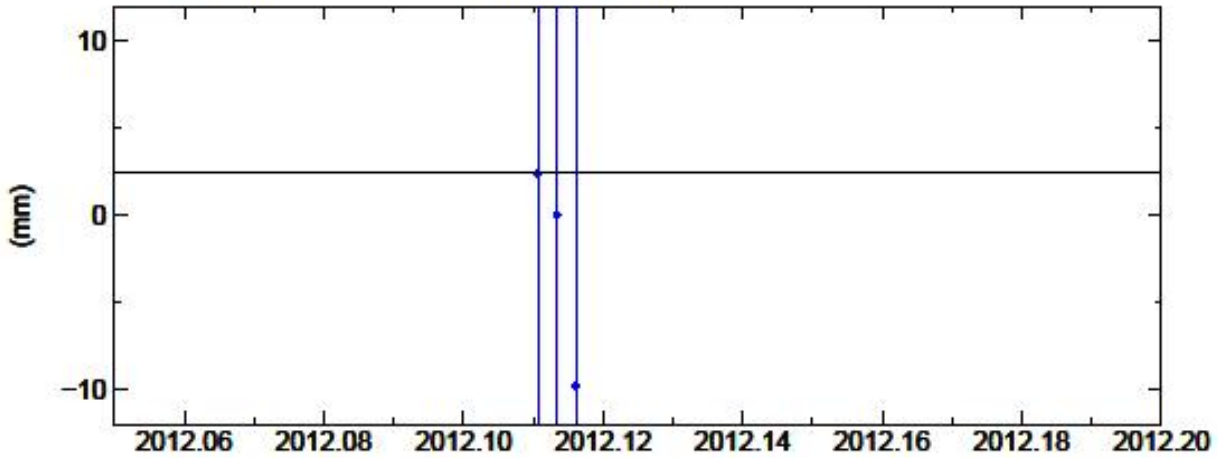

GMT 2012 Jun 25 17:39:27 p: 4

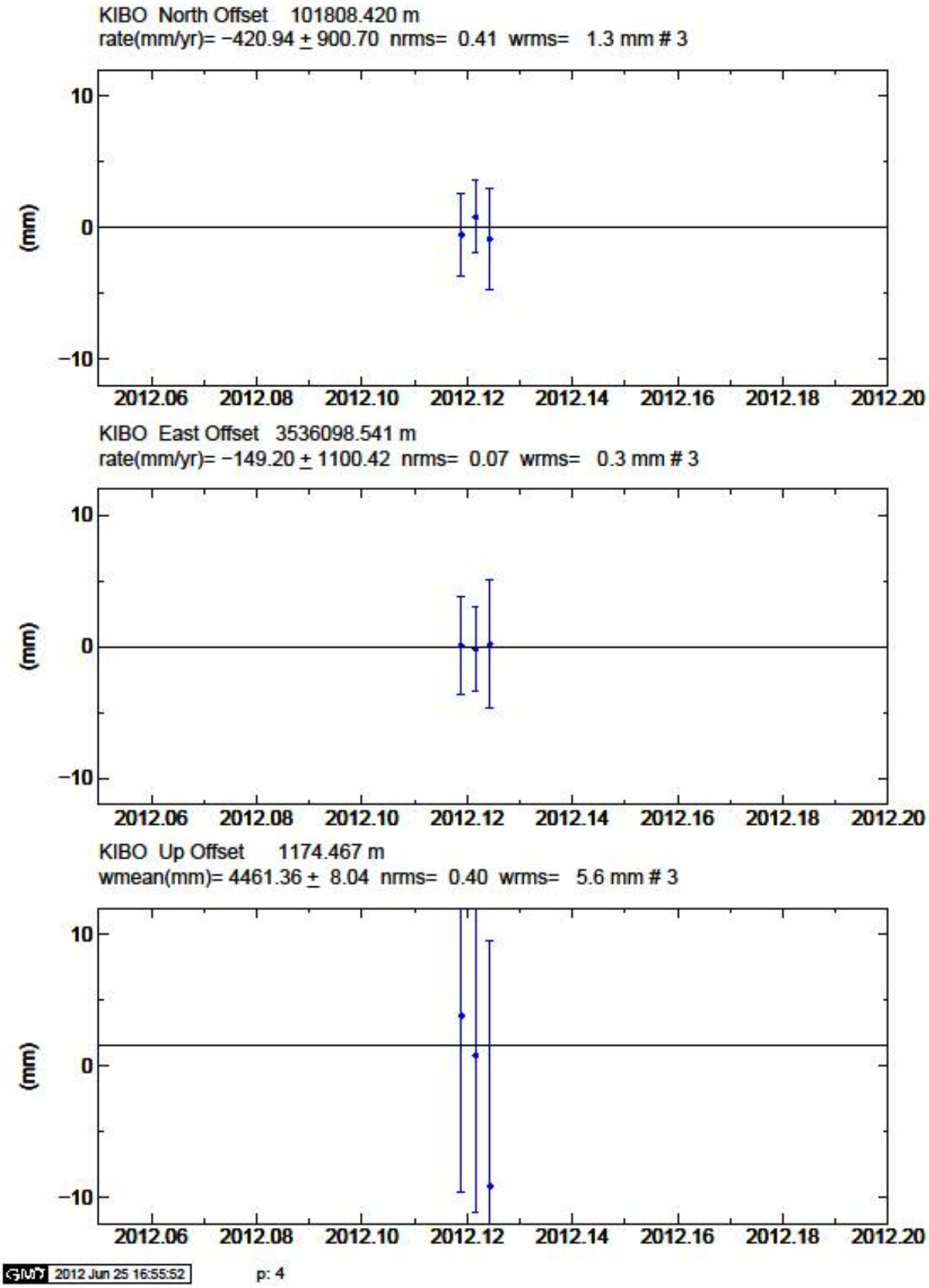
KIBO North Offset 101808.420 m
rate(mm/yr)= −420.94 ± 900.70 nrms= 0.41 wrms= 1.3 mm # 3
10
0
−10
(mm)
2012.06
2012.08
2012.10
2012.12
2012.14
2012.16
2012.18
2012.20
KIBO East Offset 3536098.541 m
rate(mm/yr)= −149.20 ± 1100.42 nrms= 0.07 wrms= 0.3 mm # 3
10
0
−10
(mm)
2012.06
2012.08
2012.10
2012.12
2012.14
2012.16
2012.18
2012.20
KIBO Up Offset 1174.467 m
wmean(mm)= 4461.36 ± 8.04 nrms= 0.40 wrms= 5.6 mm # 3
10
0
−10
(mm)
2012.06
2012.08
2012.10
2012.12
2012.14
2012.16
2012.18
2012.20
GMT 2012 Jun 25 16:55:52
p: 4

MBRA North Offset −67833.174 m
rate(mm/yr)= −242.38 ± 121.11 nrms= 1.02 wrms= 2.6 mm # 9

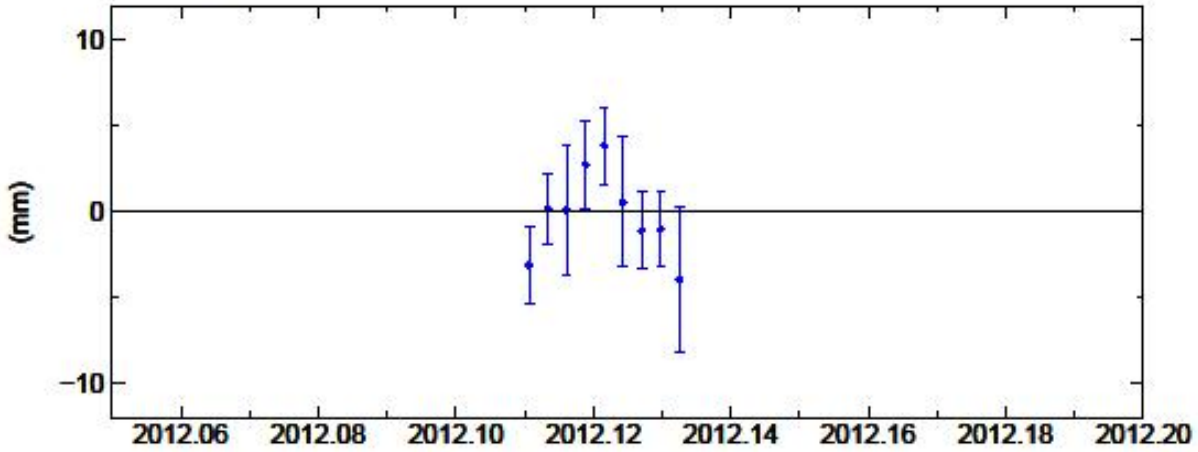

MBRA East Offset 3412139.193 m
rate(mm/yr)= −349.33 ± 137.90 nrms= 0.60 wrms= 1.8 mm # 9

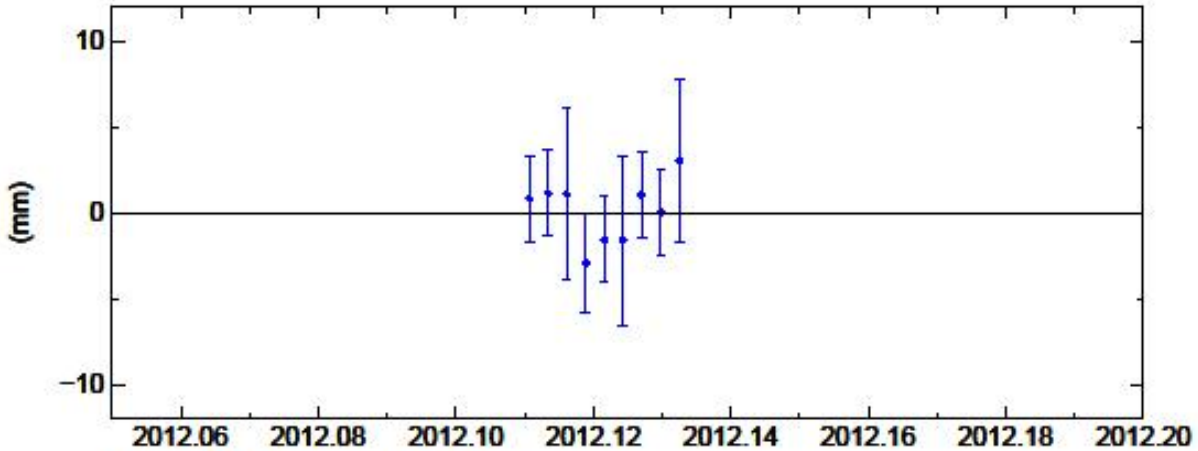

MBRA Up Offset 1448.212 m
wmean(mm)= 8204.78 ± 3.27 nrms= 0.41 wrms= 4.1 mm # 9

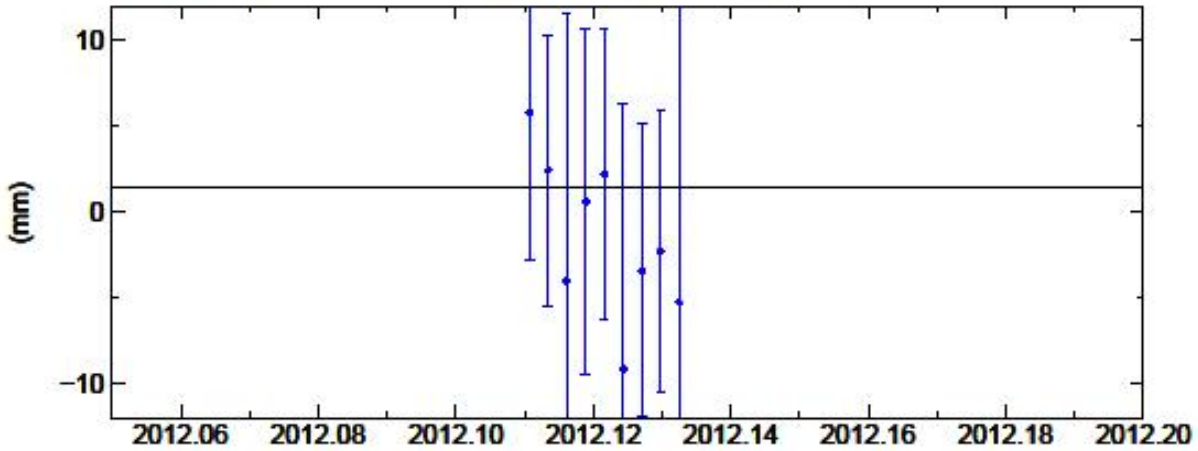

GIPSY 2012 Jun 26 12:34:49 p: 4

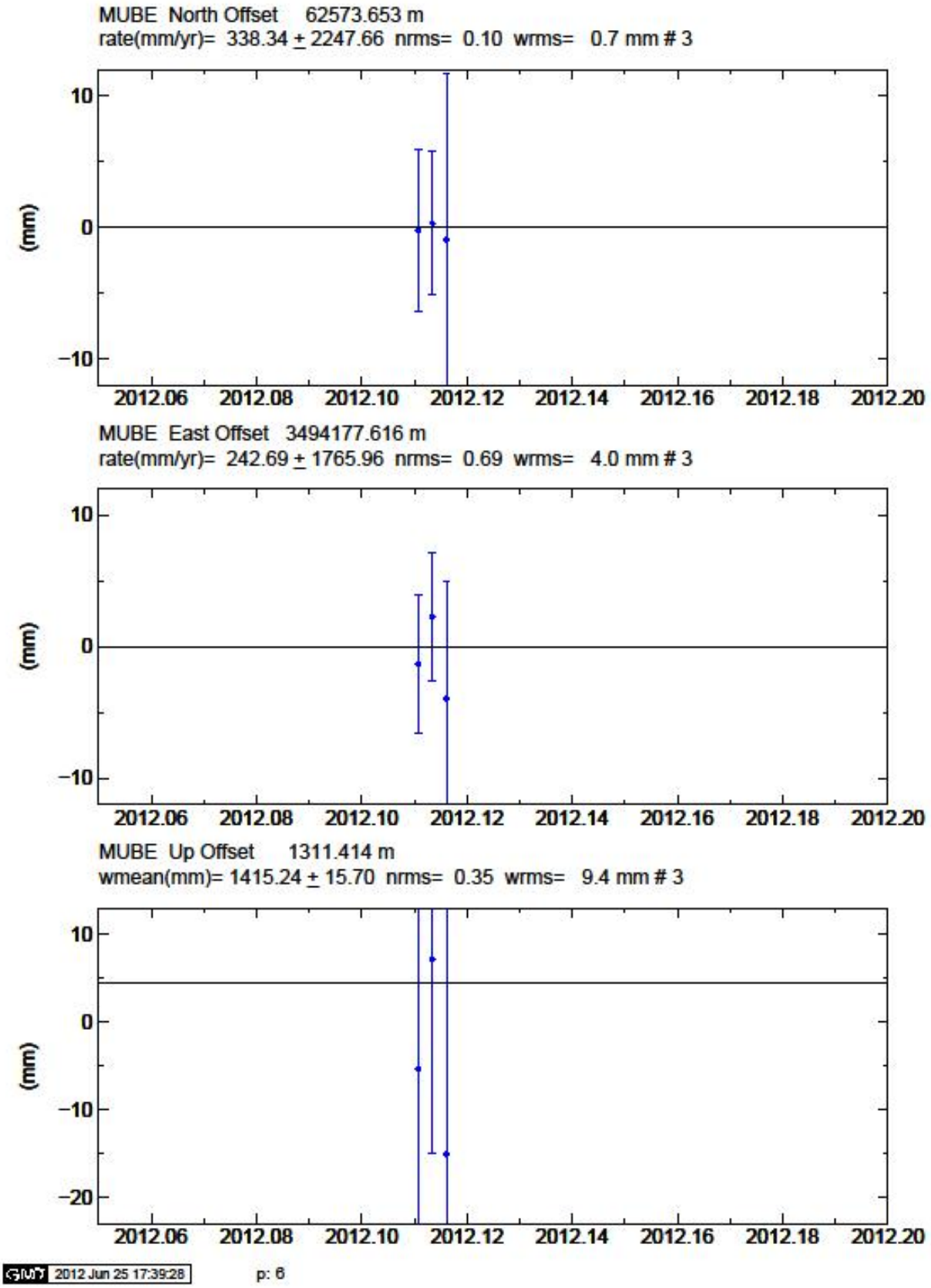
MUBE North Offset 62573.653 m
rate(mm/yr)= 338.34 ± 2247.66 nrms= 0.10 wrms= 0.7 mm # 3
10
0
−10
(mm)
2012.06
2012.08
2012.10
2012.12
2012.14
2012.16
2012.18
2012.20
MUBE East Offset 3494177.616 m
rate(mm/yr)= 242.69 ± 1765.96 nrms= 0.69 wrms= 4.0 mm # 3
10
0
−10
(mm)
2012.06
2012.08
2012.10
2012.12
2012.14
2012.16
2012.18
2012.20
MUBE Up Offset 1311.414 m
wmean(mm)= 1415.24 ± 15.70 nrms= 0.35 wrms= 9.4 mm # 3
10
0
−10
−20
(mm)
2012.06
2012.08
2012.10
2012.12
2012.14
2012.16
2012.18
2012.20
GMT 2012 Jun 25 17:39:28
p: 6

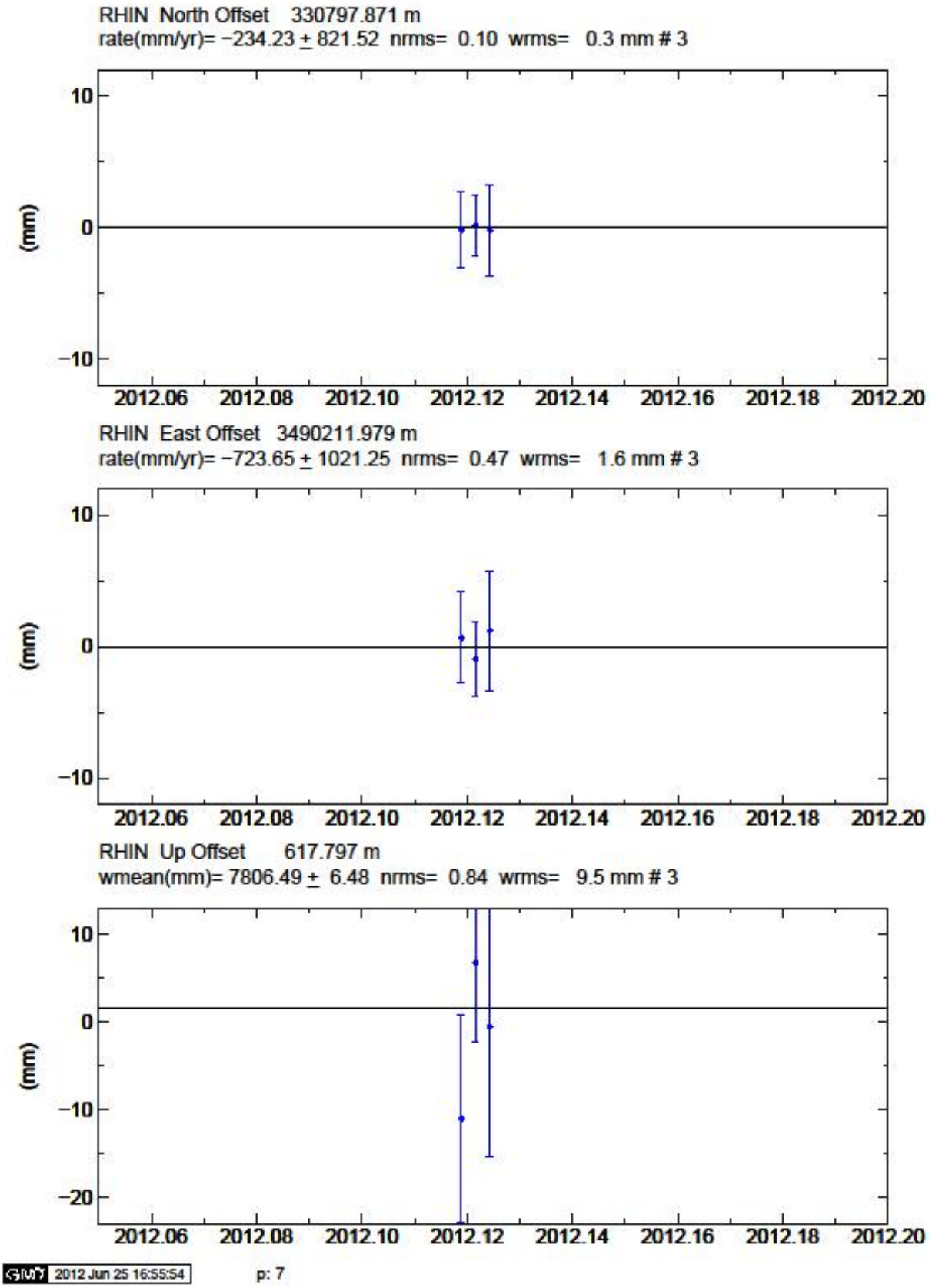
RHIN North Offset 330797.871 m
rate(mm/yr)= −234.23 ± 821.52 nrms= 0.10 wrms= 0.3 mm # 3
10
0
−10
(mm)
2012.06
2012.08
2012.10
2012.12
2012.14
2012.16
2012.18
2012.20
RHIN East Offset 3490211.979 m
rate(mm/yr)= −723.65 ± 1021.25 nrms= 0.47 wrms= 1.6 mm # 3
10
0
−10
(mm)
2012.06
2012.08
2012.10
2012.12
2012.14
2012.16
2012.18
2012.20
RHIN Up Offset 617.797 m
wmean(mm)= 7806.49 ± 6.48 nrms= 0.84 wrms= 9.5 mm # 3
10
0
−10
−20
(mm)
2012.06
2012.08
2012.10
2012.12
2012.14
2012.16
2012.18
2012.20
GMT 2012 Jun 25 16:55:54
p: 7

DECLARATION

I declare that this thesis is my own work and that it has not been submitted anywhere for any award and I have acknowledged other sources of information where used.

SUBMITTED BY:

Dianah Rose Abeho _____ _____

Signature Date

CONFIRMATION:

Dr. Roger Hipkin _____ _____

Advisor(s) Signature Date